Investigation of Kinetics of Nitroxide Mediated Radical Polymerization of Styrene with a Unimolecular Initiator

By

Mingxiao Zhou

A thesis

presented to University of Waterloo

in fulfillment of the

thesis requirement of the degree of

Master of Applied Science

in

Chemical Engineering

Waterloo, Ontario, Canada, 2009

I hereby declare that I am the sole author of this thesis. This is a true copy of the thesis, including any required final revisions, as accepted by my examiners. I understand that my thesis may be made electronically available to the public.

Mingxiao Zhou

Abstract

This thesis presents the results of a study on the kinetics of nitroxide-mediated radical polymerization of styrene with a unimolecular initiator. The primary objective was to obtain a more comprehensive understanding of how a unimolecular-initiating system controls the polymerization process and to clarify the effects of various reaction parameters.

Previous work in this field has met with some difficulties in the initiator synthesis, such as low yield and inconsistency of molecular weight. These problems were overcome by adjusting reaction conditions and procedures. Better yields of initiator with consistent molecular weight were produced by the improved methods.

Control of polymerization rate and polymer molecular weight in unimolecular nitroxide-mediated radical polymerization was studied by looking at the effects of the three main factors: initiator concentration, temperature, and the initiator molecular weight on polymerization rate, molecular weight and polydispersity. Results indicated that increasing the initiator concentration had no effect on polymerization rate at low conversion, but led to lower polymerization rate at high conversion; higher initiator concentration led to lower molecular weight of the resulting polymer. It was also found that temperature significantly increased the polymerization rate, yet had no effect on number-average molecular weight, M_n, at low conversion, while it caused a plateau at high conversion levels; there was no effect on weight-average molecular weight, M_w, through the whole conversion range. In addition, increasing initiator molecular weight was found to have no effect on either polymerization

rate or molecular weight.

The experimental molecular weights of the unimolecular system were compared to theoretical molecular weights based on ideal controlled radical polymerization (CRP). The results were found to be close to the theoretical values. This confirmed the advantages of the unimolecular system, namely, the degree of control over molecular weight was nearly ideal (for certain conditions); and molecular weights could thus be predicted by simply following general rules relating to CRP mechanisms.

Acknowledgements

A friend is one that knows you as you are,

understands where you have been,

accepts what you have become,

and still,

gently allows you to grow.

-- *William Shakespeare*

The completion of this work is based on the help of many people. First and foremost, I would like to express my deepest gratitude to my supervisor, Professor Neil McManus. You lightened me when I strayed on my journey in research. You helped me to build my confidence in my abilities, and taught me much regarding attitude and methodology for research and experimental hands-on skills. Without your unwavering guidance and support, this work would never have come to fruition.

I would also like to thank Professor Penlidis for his interest in the project. Having vast knowledge in the polymer field, Professor Penlidis provided much insight into the study. His constructive comments and suggestions were always appreciated.

Many thanks also go to my lab mates, Afsaneh Nabifar, who shared her precious research experience with me, and Joy Cheng, who taught me how to get involved into a different culture like an elder sister. Your companionship and friendship helped to make my work and my life more enjoyable. Additional thanks also go to Profs. Eduardo Vivaldo-Lima and L.

Lona for their expertise and collaboration in this work.

I would also like to thank the following institutions for their financial support of this project: Natural Sciences and Engineering Research Council of Canada; Inter-American Materials Collaboration; Canada Research Chair and the Department of Chemical Engineering at the University of Waterloo.

Lastly, I would like to thank my family for their support and encouragement throughout this endeavor.

Table of Contents

List of Figures

List of Tables

Chapter 1 Introduction

Radical polymerization (RP) is one of the most widely used processes for the commercial production of high-molecular-weight polymers. The versatility of radical polymerization is attributed to (i) the compatibility to a wide variety of monomers, including styrene, (methy)acrylates, (meth)acrylimides, acrylonitriles, dienes, etc.; (ii) tolerance of unprotected functionality in monomer and solvent (i.e., OH, NR_2, COOH, $CONR_2$, and SO_3H); and (iii) compatibility to a wide range of reaction conditions (i.e., bulk, solution, emulsion, miniemulsion, and suspension). However, conventional radical polymerization has notable limitations with respect to the degree of control over molecular weight distribution, end-functionality and macromolecular architecture. This deficiency has been compensated by the development of processes that provide living characteristics, the so-called "controlled radical polymerization (CRP)".

The success of CRP relies on the versatility of radical chemistry and the capability to control the polymerization like anionic polymerization; however, under reaction conditions requiring no solvent or rigorous experimental and purification techniques as for anionic polymerization. CRP can be used in the synthesis of well-defined homo-, gradient, di- or tri-block, star polymers and other more complex architectures. In addition, inorganic materials and natural products can be linked to synthetic polymers to form nanocomposites and copolymers tethered to surfaces. The application of CRP has penetrated a variety of fields, such as nano-technology (electronics, computer science), material technologies (compatibilizers, stabilizers, adhesives, dispersing agents, polymer toughening agents,

thermoplastic elastomers, hybrid materials, etc.), and bio-materials (bio-related polymers, drug delivery systems, etc.). The most recent developments in materials research are mainly devoted to end functionalization for nano-materials.

Nitroxide mediated radical polymerization (NMRP) is one of most attractive CRP techniques. It stands out of other CRP techniques by the relative simplicity of its mechanism, larger tolerance to many functional groups and easier purification of reagents. Based on different initiation strategies, NMRP can be divided in two types, unimolecular and bimolecular. In unimolecular NMRP, the radicals form from decomposition of an alkoxyamine at elevated temperature. In bimolecular NMRP, the radical initiation is from addition of a traditional initiator along with a stable nitroxide compound. To date, the organic chemistry and other kinetic/mechanistic aspects of NMRP are considered relatively well understood. However, many features of kinetics and mechanism remain to be unraveled. Thus a significant part of current research remains directed to this end.

Difficulties in synthesis of unimolecular initiators (i.e. low yield, inconsistent molecular weight) have been met in previous studies. This has discouraged an extensive study of unimolecular systems. The low yield, for example, leads to inadequate amounts of initiator available for an extensive kinetic program. Initiator had thus to be prepared in a variety of batches. This may bring about undesirable differences to initial initiator properties, and extensive study using such initiators may be complicated. Although many novel nitroxides and alkoxyamines with advanced functionality or structure have been developed to overcome the above mentioned deficiencies, the cost for synthesizing such materials is still a concern,

and further purification of product may be needed. Thus, it is worthy to develop a method that uses commercially available materials and simple procedures, yet can provide relatively high yield and consistent initiator properties (molecular weight, polydispersity).

Previous studies have indicated certain advantages of unimolecular systems over the corresponding bimolecular systems, such as better controlled molecular weight and lower polydispersity while keeping a comparable polymerization rate to a bimolecular system. Interestingly, some recent studies observed a distinct kinetic behavior, where the unimolecular system at high conversion had a relatively lower polymerization rate than that of a bimolecular system. Although there are a large number of publications devoted to explore the kinetics of NMRP, most of them conduct research at low conversion; discussions on high conversion are seldom provided. This is due to complex reaction factors present at high conversion. In NMRP of styrene, for example, the contribution of side reactions (i.e. termination, thermal self-initiation, decomposition of alkoxyamine) may be more significant at high conversion. The interpretation of the results, and control over the process, are thus more complicated at the high conversion range. However, a route toward higher molecular weight of polymer (driving monomer conversion to a sufficiently high level) has always been an important industrial concern. So investigation of NMRP process through the whole conversion range can provide more information on its mechanism, based on which we can develop methods to achieve better control over the process.

There is a reasonable understanding of a unimolecular system in terms of mechanism, and therefore a number of models have been developed. However, this theoretical understanding

has not been balanced by detailed experimental studies regarding the various reaction conditions. Proper selection of reaction conditions can provide the system with sufficient living nature, and reveal the relationship between reaction conditions and kinetic behavior, which can further be used to produce polymers with pre-determined properties.

Therefore, the objectives of the work carried out in this thesis were to:

1) Find optimal conditions to the extent possible to prepare initiator in sufficient quantity for extended kinetic studies;
2) Extend the understanding of advantages of a unimolecular system over a bimolecular system over the whole conversion range;
3) Investigate the effects of the main experimental factors in a unimolecular system.

In Chapter 2, a brief review of NMRP is given, including a brief historical perspective, and basic mechanisms and applications of CRP. Furthermore, the scope of components (monomer, nitroxides) in NMRP is described and the kinetic mechanisms of different initiating systems are discussed. The experimental techniques used to study the unimolecular NMRP are described in Chapter 3, and characterization methods are briefly discussed.

In Chapter 4, the experimental design and results from the experimental part are presented and discussed. The improved synthetic method for unimolecular initiator is described. Furthermore, the performance of unimolecular NMRP is compared to a bimolecular system. The effects of experimental factors (initiator concentration, temperature, and initiator molecular weight) on the kinetics of the unimolecular system are then investigated with respect to polymerization rate and molecular weight. In addition, the prediction of molecular

weights is discussed. Finally, concluding remarks and recommendations for further work are given in Chapter 5.

The thesis includes three appendices. Appendix A contains tables of the raw data collected for the figures of Chapter 4, whereas Appendix B contains complementary figures that were kept out of the main text for the sake of brevity. Appendix C contains a sample calculation of initiator concentration. Each chapter has its own reference section and all symbols used in the text are explained upon first use.

Chapter 2 Literature Review

2.1 Controlled radical polymerization (CRP)

2.1.1 Historical development of CRP

Until a little more than a decade ago, "controlled/living radical polymerization (CRP/LRP)" would have been a highly impossible concept. Simultaneous control over all aspects, including molecular weight distribution, end-functionality and macromolecular architecture, is impossible for regular radical polymerization (RP) due to its slow initiation, fast propagation and inevitable radical-radical termination (more details in section 2.1.2). The success of CRP is an integration of advances in synthetic organic chemistry, living ionic polymerization and conventional radical polymerization (Figure 2.1). Three main types of techniques have been developed over the years: 1) stable free radical polymerization (SFRP) with nitroxide-mediated radical polymerization (NMRP) as its most common example, 2) atom transfer radical polymerization (ATRP) and 3) reversible addition-fragmentation transfer (RAFT) polymerization.

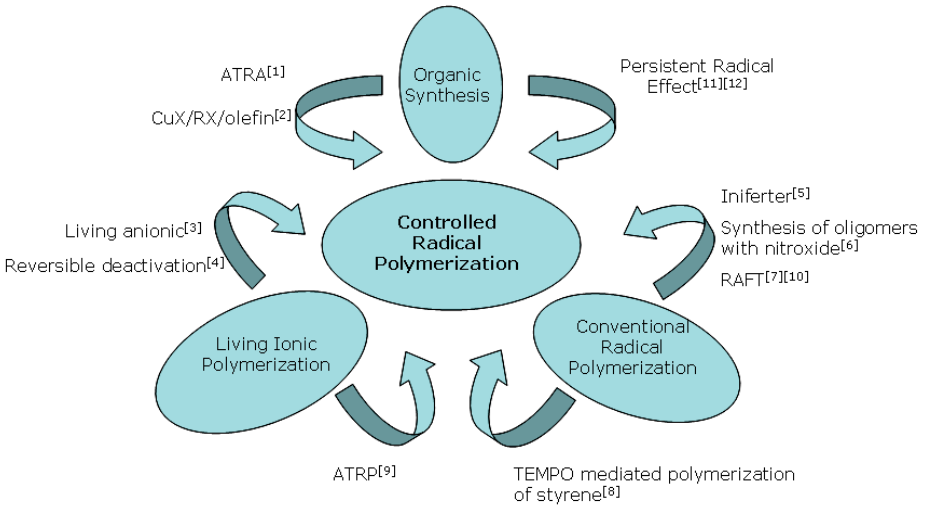

Figure 2.1 Development of CRP by integration of advances in several fields of chemistry

The first successful method to control radical addition reactions in general organic syntheses was atom transfer radical addition (ATRA) developed by Kharasch et al.[1](Scheme 2.1), where the atom (X) transfers from an organic halide (R-X) to the metal complex (Mt^n), then back to the organic radical ($RCH_2CH_2Y^*$); carbonic radical (R*) was added to alkenes (CH_2=CHY) via radical intermediates ($Mt^{n+1}X$) under photochemical conditions. This ATRA process was subsequently converted to a much more efficient metal-catalyzed reaction [2].

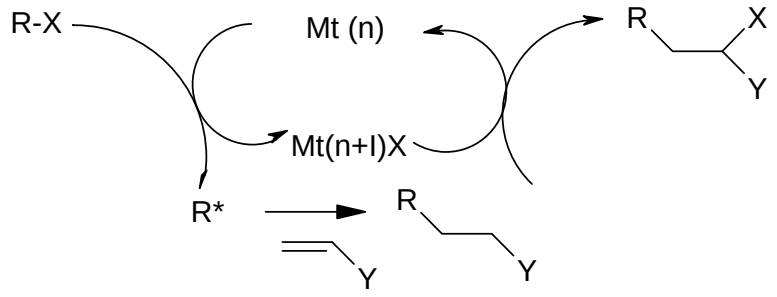

Scheme 2.1 Mechanism of atom transfer radical addition (ATRA)

The concept of "living polymerization" can be attributed to the study on anionic polymerization of non-polar monomers by Swarc et al.[3]. The elimination of transfer and termination reactions from chain growth polymerization is the core finding of this discovery. It was the first technique used to synthesize macromolecules with controlled topologies, predetermined molecular weight and nearly Poisson distribution of molecular weight. The first system in which both dormant and active species were spectroscopically observed and kinetics and thermodynamics of exchange reactions determined was cationic ring-opening polymerization of tetrahydrofuran[4]. The concept of dynamic equilibrium between dormant and active species that arose from this work has subsequently been successfully used in carbocationic polymerization (Scheme 2.2).

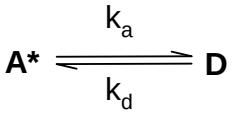

Scheme 2.2 Equilibrium between active and dormant species

Initial efforts on producing a "living" system based on free radical chemistry involved the "iniferter" concept, which takes advantage of sulfur-centered radicals[5] (Scheme 2.3).

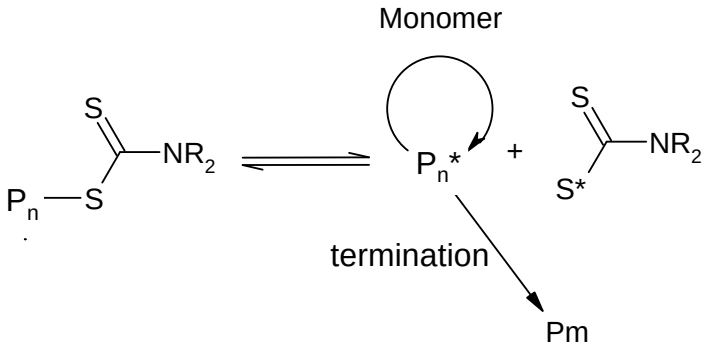

Scheme 2.3 Main mechanism for sulfur-centered radical (iniferter) mediated polymerization

The model that Otsu and Yoshida[5] proposed for this is very similar to that for modern CRP. Disulfides were proposed as photochemical initiators where cleavage can occur at the C-S bond to give a carbon-based propagating radical and the mediating thio-radical. Propagating radical can undergo reversible recombination with the primary sulfur radical to give a dormant species, thereby controlling the radical concentration and subsequently the structure of polymers. Although iniferters allowed the facile synthesis of block copolymers, they were also found to initiate new chain growth, which leads to molecular weight distributions that are as broad as those from traditional free radical processes. They could not lead to a living radical polymerization with efficient control over the polymer structure. Further development was therefore needed to produce a radical initiated polymerization with better living characteristics.

A new system for controlling radical polymerizations based on 2,2,6,6-tetramethyl-1-piper-

-idinyloxy (TEMPO) as controller appeared in the patent literature in 1986[6]. The researchers used nitroxide at temperatures above 100ºC in synthesis of oligomers (Scheme 2.4) and short-chain-length block- or graft- copolymers, and demonstrated the living nature of the polymer chain end. However, the full implications of this work were not recognized at that time.

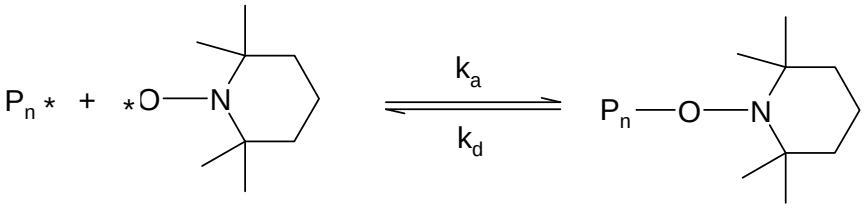

Scheme 2.4 Mechanism of TEMPO-mediated radical polymerization

Subsequently, Moad et al.[7] proposed another approach to LRP based on addition-fragmentation chemistry, which can be considered as a special case of degenerative transfer. In these systems, some understanding of LRP was reached and the mode of termination was identified.

It was not until 1993 when Georges et al.[8] published their first paper on controlling the bulk radical polymerization of styrene by using a mixture of benzoyl peroxide (BPO) and TEMPO as an initiating system (Scheme 2.5), that the wider interest in living radical polymerization was stimulated. Many publications have subsequently emerged confirming the "living" nature and demonstrating the usefulness of this approach to prepare polymers of well-defined and complex architectures, which can not be prepared using traditional methods.

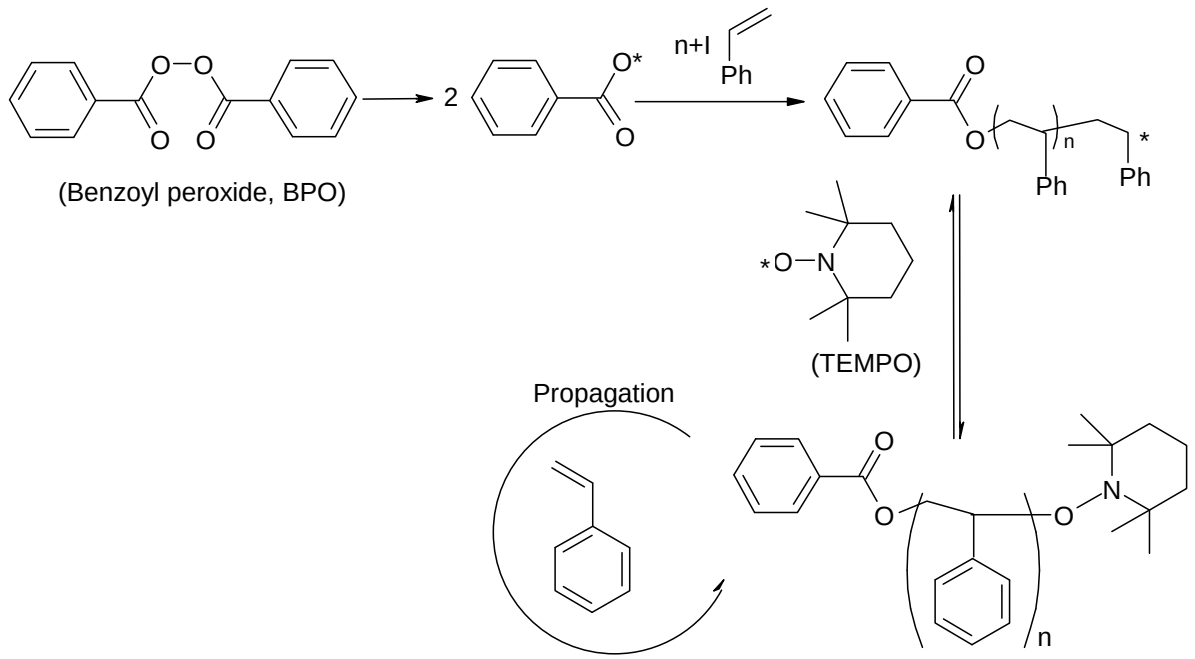

Scheme 2.5 Georges' approach to NMRP using bimolecular initiation[8]

In 1995, Wang and Matyjasewski [9] extended atom transfer radical addition (ATRA) to atom transfer radical polymerization, ATRP. The main difference between ATRA and ATRP is the fact that the addition product (RCH_2CHXY in Scheme 2.1) is able to reactivate to a radical (RCH_2CHY^*) that is able to undergo propagation reactions with available monomer. Thus, equilibrium is established between the dormant alkyl halide molecule and the active radical species (R*), the latter of which may propagate, terminate or deactivate (Scheme 2.6). Polymerizations gave polymers with very low polydispersities (down to 1.05), and predictable molecular weights based on the concentration of monomer consumed (Δ[M]) and the initial initiator concentration (i.e. degree of polymerization (DP) = $\Delta[M]/[Initiator]_0$).This provided a new and efficient way to conduct CRP.

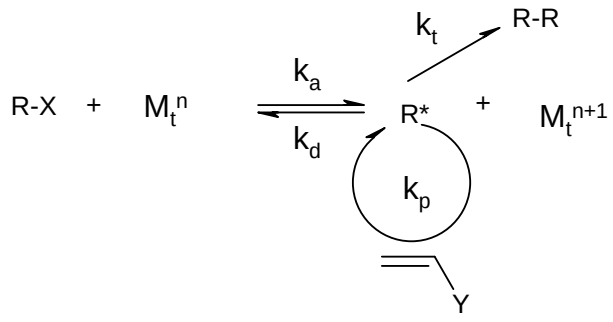

Scheme 2.6 Mechanism of atom transfer radical polymerization (ATRP)

Subsequently, Rizzardo et al.[10] reported another living free radical polymerization based on their previous study of employing addition-fragmentation chemistry for end functionalization. The mechanism involved Reversible Addition-Fragmentation (chain) Transfer (Scheme 2.7), and thus it was designated as RAFT polymerization. It also demonstrated significant living character, such as narrow polydispersity, predictable molecular weight and the ability to produce block co-polymers by further monomer addition. Compared to other processes for living/controlled free-radical polymerization, it has a major advantage that it is compatible with a wider range of monomers.

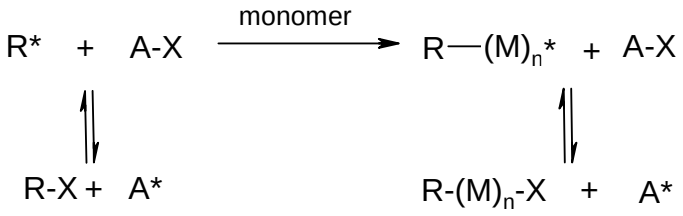

Scheme 2.7 Mechanism of reversible addition-fragmentation chain transfer polymerization

The success of polymerization using stable radical and atom transfer methods is attributed to the persistent radical effect (PRE). The model was originally developed by Fischer[11][12] in order to explain the high selectivity observed in some radical reactions. Simply stated: when a transient radical and a persistent radical are simultaneously generated, the cross reaction

between the transient and persistent radicals will be favored over self-combination of transient radicals (homo-termination). Self-combination of transient radicals leads to a build up in the concentration of the persistent species, which favors cross termination with the persistent radical over homo-termination. The homo-termination is thus self-suppressing. The effect can be generalized to a persistent species effect to embrace nitroxide-mediated radical polymerization (NMRP) and atom transfer radical polymerization (ATRP).

The development of controlled radical polymerization methods such as nitroxide-mediated radical polymerization (NMRP), atom transfer radical polymerization (ATRP) and reversible addition fragmentation transfer (RAFT) polymerization provide almost the same level of control over the microstructure as traditional ionic polymerization methods without the need of extensive purification of reagents. The combination of a living mechanism with the scope and versatility of the radical process allows a wider selection of monomers and monomer combinations that can not be made by ionic polymerization (see also section 2.1.3). These potential and subsequent applications have stimulated increasing interest in this area in the last decade.

2.1.2 Basic mechanisms and typical kinetic features of CRP

2.1.2.1 Reversible activation/deactivation in CRP

Radical polymerization includes four elementary reactions[13] (Scheme 2.8): (1) slow initiation by the homolytic cleavage of an initiator (a molecule with low thermal stability, i.e. peroxide, diazo-compound), followed by relatively fast reaction of primary radicals with monomer to generate the first growing species; (2) fast propagation by addition of monomer

to the growing species; (3) very fast termination between growing radicals; and (4) chain transfer reactions between growing radicals and monomer, solvent, chain transfer agent or initiator.

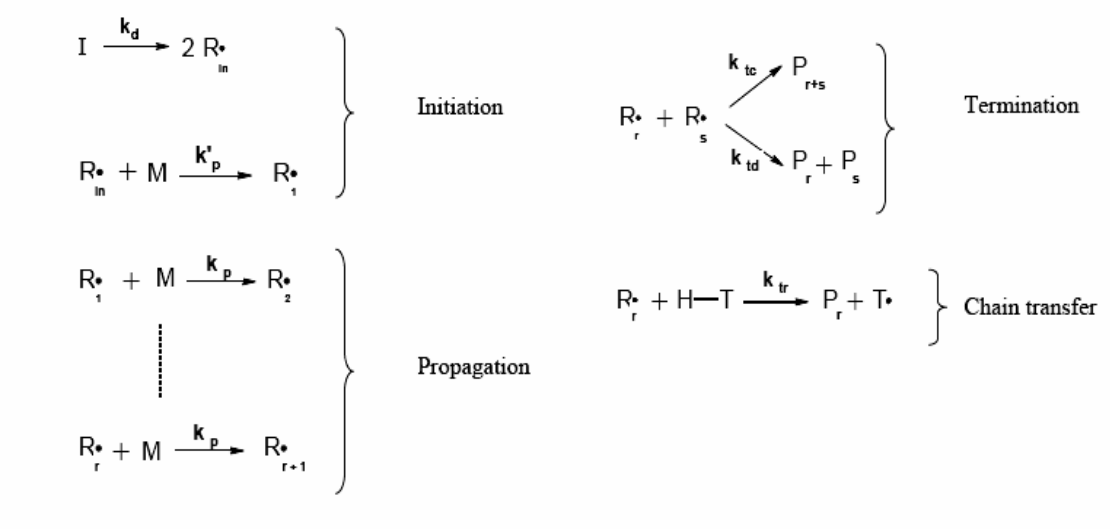

Scheme 2.8 Mechanism of conventional radical polymerization (RP)[13]

Controlled radical polymerization (CRP) distinguishes itself from conventional radical polymerization by involving a reversible activation process [14] (Scheme 2.9).

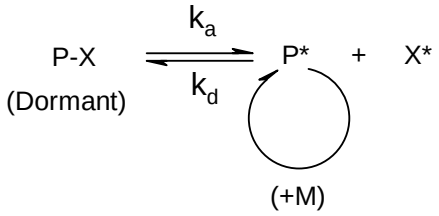

Scheme 2.9 Reversible activation process of CRP [14]

In this mechanism, an end capped (or inactive) polymer (dormant species), P-X, is homolytically unstable and undergoes thermal fragmentation to give a transient polymeric radical P*. The chains propagate by the addition of monomer to the active radical P* until it is deactivated back to P-X. K is the activation/deactivation equilibrium constant.

The reversible activation reactions in the most effective CRP methods may be classified

mechanistically into three types[14], which are: (a) dissociation-combination (DC), (b) atom transfer (AT), and (c) degenerative chain transfer (DT) (Scheme 2.10).

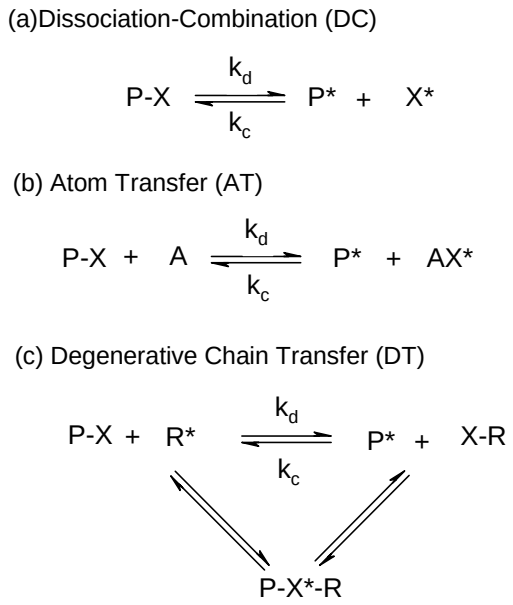

Scheme 2.10 Three main mechanisms of reversible activation[14]

In the Dissociation-Combination (DC) mechanism, P-X is thermally or photochemically dissociated into an active/propagating radical P* and a stable (persistent) radical X*. An ideal stable free radical (SFR) participates in neither self-termination nor initiation of new chains. The most widely studied and most successful class of stable radicals are nitroxides such as TEMPO.

In the Atom Transfer (AT) system, the dormant, P-X, is activated by the catalytic action of activator A, and the capping agent is transferred to form a stable species AX*. Commonly used activator A is a halide complex of a transition metal like Cu and Ru, and the capping agent is a halogen such as Cl or Br.

In the Degenerative Chain Transfer (DT) mechanism, with reversible addition-fragmentation radical (RAFT) polymerization as the best example, the dormant

chain is attacked by radical R* to form the active species P* and the dormant species R-X. The exchange reaction occurs via addition of R* to form the intermediate radical P-(X*)-R followed by fragmentation of P-(X*)-R into P* and R*.

2.1.2.2 Other elementary reactions in NMRP of styrene

Besides the reversible activation, elementary reactions in NMRP of styrene include propagation, chain transfer and termination, which can also be seen in conventional radical polymerization (Scheme 2.11 b, c, d). The rate constants of propagation and termination are assumed to be the same as in the conventional system. In addition, alkoxyamines can decompose at high temperatures through β-proton abstraction by TEMPO, forming an alkene and a hydroxylamine (Scheme 2.11e). In addition, styrene is known to undergo a thermal self-initiation at elevated temperature (T ≥ 100°)[15](Scheme 2.11a) (details see section 2.3.1).

(a) Thermal self-Initiation

$$M + M \longrightarrow D$$

$$D + M \longrightarrow D^* + M^*$$

(b) Propagation

$$P^* + M \xrightarrow{k_p} P^*$$

(c) Termination

$$P_m^* + P_n^* \xrightarrow{kt} dead.polymer$$

(d) Chain Transfer

$$P_m^* + RH \xrightarrow{k_{tr}} PH + R^*$$

(e) Decomposition of P-X

$$P - X \xrightarrow{k_{dec}} dead.polymer + XH$$

Scheme 2.11 Possible elementary reactions other than reversible activation reactions in NMRP of styrene[16]

2.1.2.3 Typical kinetic features of NMRP

CRP closely resembles conventional radical systems, yet there are some distinct features.

i) Semi-logarithmic plot of $\ln([M]_0/[M])$ vs. time is linear.

In an ideal CRP system, initiation occurs instantaneously at an early stage of polymerization, and termination is effectively minimized; a constant radical concentration is reached by balancing the rates of activation and deactivation, which demonstrates a first-order kinetic dependence of propagation rate on monomer concentration (Eq. 2.1).

$$R_p = k_p[M][P_n^*] \qquad (2.1)$$

where R_p is rate of propagation, k_p is propagation rate constant, [M] is monomer concentration, and $[P_n^*]$ is the propagating radical concentration.

A plot of $\ln([M]_0/[M])$ vs. time provides a straight line (Figure 2.2).

$$\ln\frac{[M]_0}{[M]} = k_p\left(\frac{R_i}{k_t}\right)^{1/2} t \qquad (2.2)$$

where $[M]_0$ is monomer concentration at time t = 0, and R_i is initiation rate.

If initiation is not fast enough, or termination can not be neglected, the plots will show some curvature.

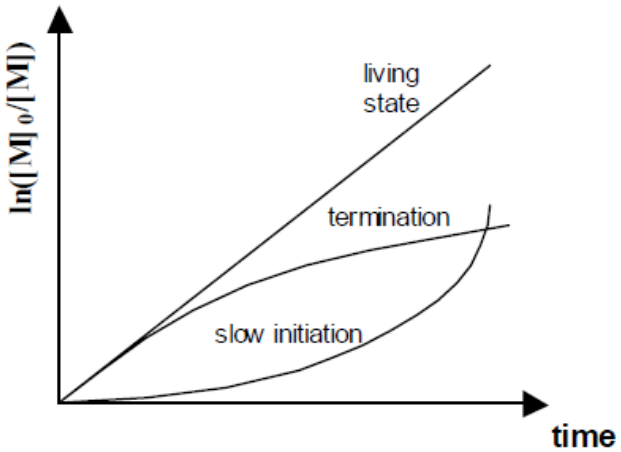

Figure 2.2 First order kinetic plot for controlled/living radical polymerization (CRP/LRP)[17]

In contrast, for conventional radical polymerization (RP) which is also described by Eq.(2.1), a steady-state is established early in the reaction by balancing continuous initiation and irreversible termination.

ii) Molecular weight increases linearly with monomer conversion (Figure 2.3).

This feature is analogous to what is seen for anionic living polymerization, which has eliminated termination. In an ideal living radical polymerization system, where initiation is faster than propagation and chain transfer side reactions and termination can be neglected, the polymer molecular weights are proportional to the ratio of monomer consumption to the concentration of initiated chains. In most cases, we assume the initiator efficiency is close to 1, so that the concentration of initiated chain can be substituted by the initial initiator concentration (Eq.2.3).

$$M_n = \frac{[M]_0 - [M]_t}{[I]_0} \times M_0 \qquad (2.3)$$

M_n is the number-average molecular weight of polymer, $[M]_0$ is monomer concentration at time t = 0, $[M]_t$ is monomer concentration at time t, $[I]_0$ is initiator concentration at time t = 0, and M_0 is the molecular weight of the monomer unit.

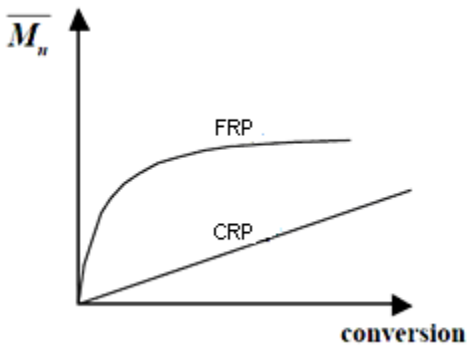

Figure 2.3 Molecular weight vs. conversion plot, comparison of CRP and RP

iii) Molecular weight distribution is narrow (Figure 2.4).

The distribution of molecular weight of polymer can be quantified by the polydispersity index (PDI), which is the ratio of weight average molecular weight to number average molecular weight (M_w/M_n). The PDI has a value always greater than 1, but as the polymer chains approach uniform chain length, the PDI approaches unit.

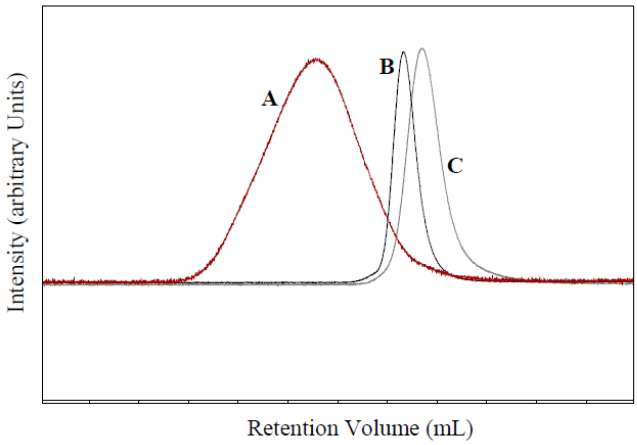

Figure 2.4 Size exclusion chromatographs of polystyrene samples. A: regular radical polymerization (PDI=2), B: anionic polymerization (PDI=1.1), C: NMRP (PDI=1.1) [17]

The narrow molecular weight distribution stems from the fact that each chain undergoes periods of growth and deactivation alternatively. The mean increase of DP in each activation/deactivation cycle (run length per activation cycle (RLPAC)) is determined by the ratio of propagation rate and deactivation rate[18],

$$RLPAC = \frac{R_p}{R_d} = \frac{k_p[M][P^*]}{k_d[X^*][P^*]} = \frac{k_p[M]}{k_d[X^*]} \qquad (2.4)$$

where k_p is propagation rate constant, k_d is deactivation rate constant, [M] is monomer residual concentration, [P*] is propagating radical concentration, and [X*]

is nitroxyl radical concentration.

It can be seen that the faster this deactivation/activation process is (Rd↑), the less propagation steps can be completed in each activation cycle (RLPAC↓), and the overall result would be that the majority of chains stay in the dormant form, and grow in a slow and incremental fashion. Since the chain growth is initiated instantaneously at the early stages of polymerization, each chain in the overall sample will grow on average for a similar period of time.

In contrast, conventional RP has a slow initiation and unavoidable termination with a rate proportional to the square of the radical concentration ($R_t \propto [P_n^*]^2$). This leads to a broad molecular weight distribution.

iv) End functionality

The participation of the reversible activation extends the average lifetime of growing chains from ≈ 1s (in RP) to more than 1h (in LRP). This combined with minimal termination, leads to the observed narrow molecular weight distribution. In addition, the nature of the mechanism also enables specific end functionalization (Figure 2.5), or addition of a second monomer to make a block copolymer, which can not be realized by conventional RP systems.

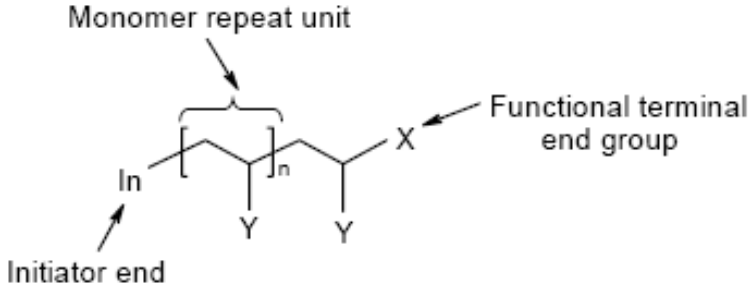

Figure 2.5 General polymer chain functionalization in controlled radical polymerizations

2.1.3 Potential applications of CRP materials

The development of CRP has allowed the preparation of polymers with novel architectures and functionality. A schematic of potential applications [19] are shown in Figure 2.6. Some examples are highlighted below.

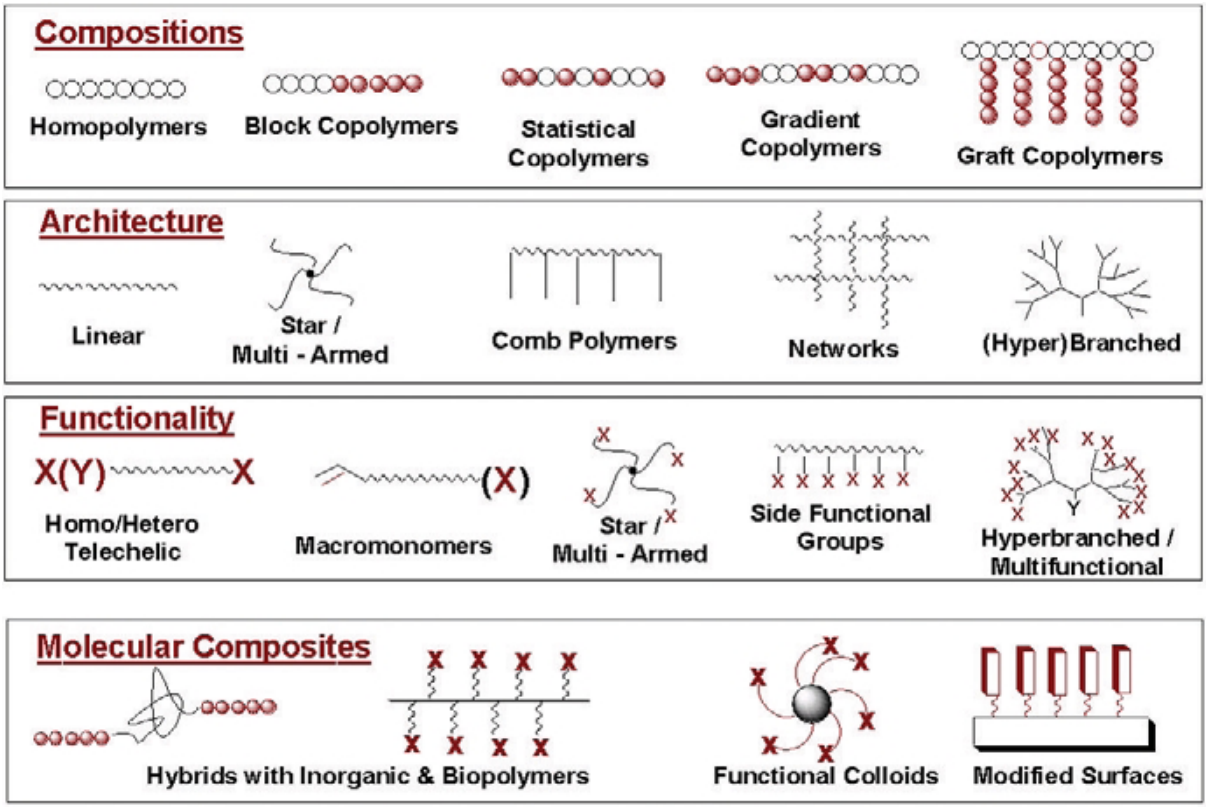

Figure 2.6 Examples of molecular structures attained through CRP [19].

Block copolymers based on acrylates and other polar monomers may find applications as polar thermoplastic elastomers[20]. Such materials can be used as adhesives and sealants, in many compounding applications, including automotive, wire and cable, footwear, medical, soft touch overmolding, cushions, squeezables etc. They can be used as thermoplastic vulcanizates, in flexographic printing, road marking, lubricants, gels, and coatings. They also can be used for much more sophisiticated applications such as specialized chromatographic packing[21] or controlled drug-release in cardiovascular stents[22].

Amphiphilic block copolymers with water soluble segments have been successfully used as very efficient surfactants[23] and also for higher end applications including pigment dispersants, additives, and components of health and beauty products[24][25]. AB and ABC triblock copolymers with precisely controlled segment lengths to self-assemble at the nanometer scale has enormous utility for applications ranging from thermoplastic elastomers, catalyst supports, organic photovoltaics, and nanoporous media [26][27]. Graft copolymers have been used as compatibilizers for polymer blends and may be used in applications intended for block copolymers[28][29]. Gradient copolymers hold great promise in applications ranging from surfactants to noise and vibration dampening materials[30].

Star and comb polymers[31] can be used as viscosity modifiers and lubricants. An ultimate example of controlled topology might be a macromolecular bottle-brush. Such polymers are lightly crosslinked and result in supersoft elastomers[32]. Thus, applications are ranging from intraocular lenses and other biomedical applications requiring a soft material that does not leach to surrounding tissue, and electronic applications requiring the protection of delicate components by a soft solid.

Molecular hybrids with a covalent attachment of well-defined functional polymer to either an inorganic component or a natural product are currently being investigated[33][34]. Such hybrids and nanocomposites may allow better dispersability of inorganic components (pigments, carbon black, carbon nanotubes, nanoparticles), and the formation of nanocomposites.

Other potential applications include microelectronics, optoelectronics, specialty membranes, sensors and components for microfluidics. Well-defined polymers prepared by CRP are very well-suited for biomedical applications such as components of tissue and bone

engineering, controlled drug release and drug targeting, antimicrobial surfaces[35], steering enzyme activity[36], and many others.

2.2 *Components of NMRP*

2.2.1 Monomers

NMRP has mainly been used for styrene polymerization and, to a lesser extent, acrylate polymerization. For styrene polymerizations carried out at temperatures greater than 100ºC, thermal initiation provides some rate enhancement and a source for controlling the excess of nitroxide that is formed as a result of radical-radical termination and the persistent radical effect. Otherwise, polymerization would come to a halt because of the inhibiting effect caused by the build up of stable free radical concentration.

NMRP with acrylates and acrylamides with TEMPO provides only very low conversions and broad dispersities. Better results were obtained with DTBN[37] (Figure 2.7). However, low conversions were still observed. The self-initiation of monomer (as seen for styrene) is absent and, as a consequence, polymerization proceeds until inhibited by the build-up of nitroxide. Molecular weight may also be limited by the occurrence of backbiting and fragmentation when high reaction temperatures are used.

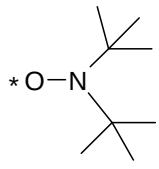

DTBN

Figure 2.7 Structure of DTBN [37]

NMRP cannot be applied to methacrylate monomers, although a small amount of the

monomers can be inserted into styrene and acrylate polymers through copolymerization[38]. This is because the disproportionation termination predominates over the coupling termination during the methacrylates polymerization at high temperature. A recent communication[39] has described a photo-living radical polymerization of MMA in the presence of 4-methoxy-TEMPO (MTEMPO). This is the first study demonstrating that nitroxide mediated radical polymerization produced PMMA with a comparatively narrow molecular weight distribution ($M_w/M_n = 1.3 \sim 1.7$).

2.2.2 Nitroxide as trapping agent

Because of relatively low cost and immediate commercial availability, TEMPO was the primary nitroxide being applied to CRP. However, as a mediating nitroxide, TEMPO has some apparent deficiencies, including the necessity to use high temperature (125-145ºC), long reaction time to high conversion (24-72h), and an incompatibility with many important monomer families other than styrenics.

In order to broaden the scope of the technique, efforts to develop new mediating nitroxides with improved performance were made. The initial efforts looked at TEMPO-based derivatives. By using 4-oxo-TEMPO[40], Keoshkerian et al. successfully controlled the polymerization of acrylates at elevated temperature (145ºC-155ºC) with relatively low polydispersity (1.40-1.67). Similarly, Matyjaszewski et al.[41] observed that the rate of polymerization of styrene had increased by using a TEMPO derivative, substituted in the 4-position with a phosphonic acid group. This prompted the development of other "TEMPO-like" nitroxides, such as di-t-butyl nitroxides. All of these approaches provide an

increased polymerization rate; yet none of them is significant enough to improve on what was observed for TEMPO and to make NMRP stand out from other living radical techniques.

The most significant breakthrough in the design of improved nitroxides was use of acyclic nitroxides, which bear no structural resemblance to TEMPO. The best example of these new materials is the phosphonate derivative, SG-1[42] (Figure 2.8) and the family of arenes, DTBN. These nitroxides have subsequently been shown to be superior to the original TEMPO derivatives. They have extended the monomer families for NMRP from styrene to acrylates, acrylamides, 1,3,-dienes, and acrylonitrile-based monomers, and they enable controlled copolymerization with a selection of monomers and functional groups.

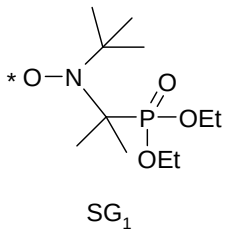

SG_1

Figure 2.8 Structure of SG-1[42]

2.3 *Initiating systems*

2.3.1 Thermal self-initiation of styrene

Styrene is known to undergo a thermal (spontaneous) self-initiation at elevated temperature ($T \geq 100^{o}$)[15]. The generally accepted mechanism of thermal self-initiation of styrene is by radical formation from unsaturated dimers according to Mayo[43]. This involves a reversible reaction between two styrene molecules to form a Diels-Alder adduct (D), followed by reaction of D with a styrene molecule to form two benzylic radicals, D* and M*, that can add monomer to initiate polymerization (Scheme 2.12). The rate of thermal initiation was

proposed to be third order with respect to monomer concentration.

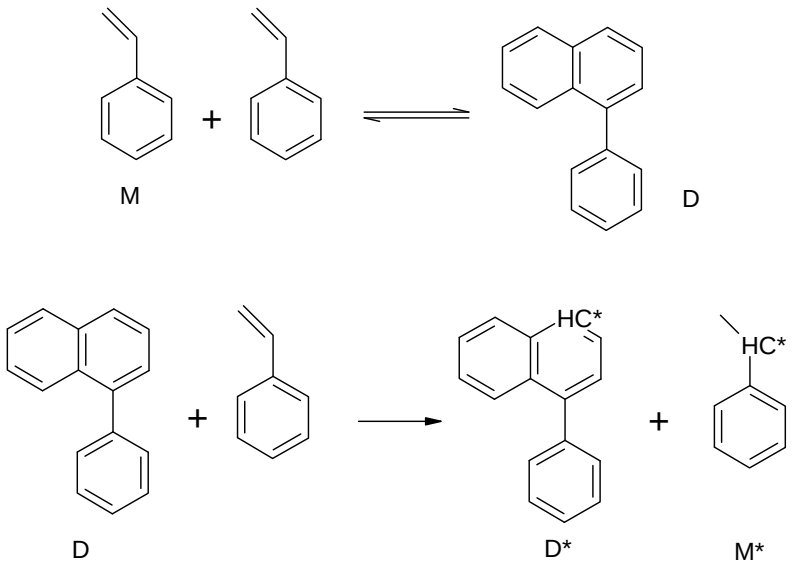

Scheme 2.12 Mechanism of self-initiation of styrene[43]

This process relies on the presence of monomer, so it will proceed until all the monomer has been consumed. The radicals generated in self-initiation will lead to termination of long/short chains, or new chain growth. The lengths of newly generated chains are varied at different reaction times: the early-born chains are long, whereas the late-born chains are short. All of these will cause a broad molecular weight distribution and subsequently deviations from controlled polymerization.

On the other hand, thermal self-initiation helps maintain a reasonable reaction rate. It continuously generates radicals to balance the built-up of nitroxyl radicals due to the termination of propagating radicals.

2.3.2 Bimolecular initiation of NMRP

Two basic strategies have been applied to initiate NMRP. The first method involves use of a conventional initiator (e.g. AIBN, BPO) in the presence of a nitroxide (Scheme 2.5). The

mixture is heated to a temperature at which initiator rapidly decomposes. The resulting initiator radicals then react with monomers to generate the initial propagating radicals, P_1*, which thus starts the chain growth. Between the propagation steps, the radicals may combine with nitroxide, X, to reversibly form an alkoxyamine so that the chain grows in a controlled fashion.

This system is called “bimolecular NMRP”. It was first successfully studied by the group of Georges[8] who described the synthesis of polystyrene (PS) and the subsequent PS-based block copolymers in the presence of TEMPO. In this reaction, a mixture of BPO, TEMPO and styrene was simply heated at 123°C. A key observation was that the molecular weight of the polymer produced increased in a linear fashion with conversion, and the polydispersity was below 1.3.

However, the yield of alkoxyamine based on the bimolecular system is not quantitative to the amount of TEMPO added. In this system, initiation consists of multiple steps, including decomposition of initiator, addition of monomer to the initiating radical and subsequent trapping of the radical intermediate with TEMPO. Various side reactions are known to accompany alkoxyamine formation. One of the important side reactions is the TEMPO promoted dissociation of BPO (Scheme 2.12), proposed by Moad et al.[44] and further clarified by Georges et al.[45] and Cunningham et al.[46]. Georges et al. suggested that up to 50% TEMPO may be lost in this reaction at 70°C, and they concluded that promoted dissociation of BPO is important at temperature lower than 80ºC[45]. Therefore, a simpler NMRP system with less initiating steps would offer better control of polymer properties.

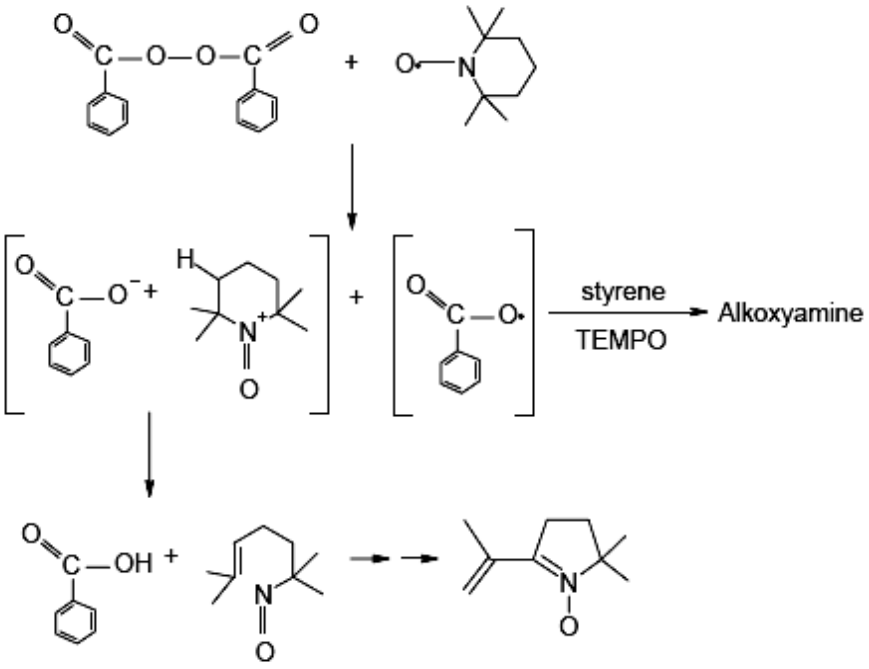

Scheme 2.13 Promoted dissociation of BPO[44]

A recent study[47] by our group has demonstrated the nature of bimolecular initiating NMRP by variation of reaction temperature and ratio of TEMPO/BPO. It has shown that experimental data and model predictions for conversion vs. time are in good agreement up to 50% conversion (Figure 2.9). Furthermore, the experimental data of molecular weight vs. conversion follow the linear trend but are higher than model predictions (Figure 2.10). These deviations were ascribed to the possible side reactions, such as the "promoted dissociation" of BPO. In addition, a study of temperature effects showed that higher temperature increases the polymerization rate. There was no significant change in the molecular weight vs. conversion plot when temperature increased; only at high conversion, Mn showed a plateau. This insignificant difference was ascribed to the most likely unchanged "run length per activation cycle (RLPAC)[18]".

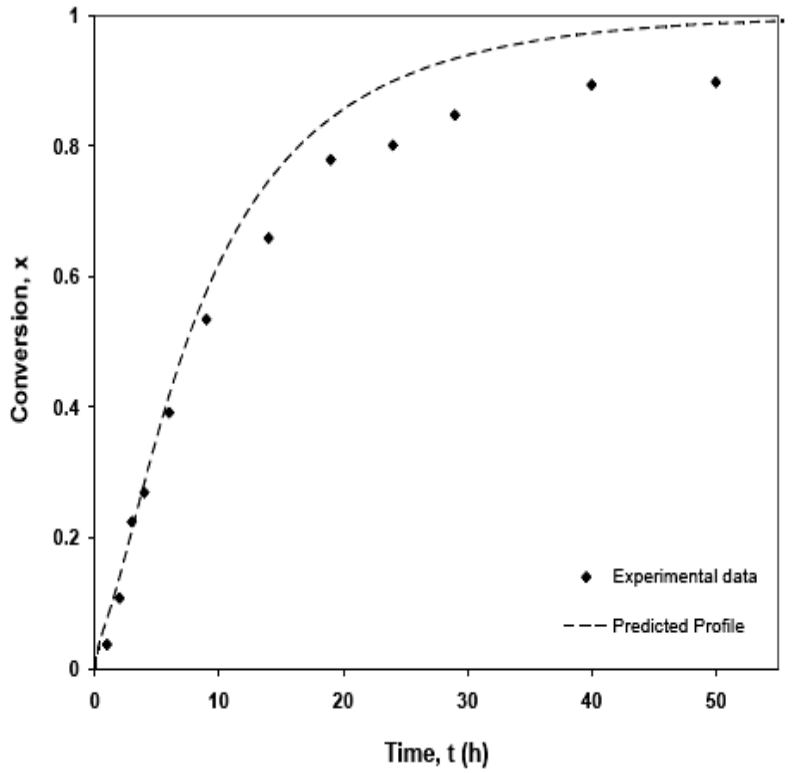

Figure 2.9 Comparison of experimental data and model predictions of conversion vs. time, at 120ºC and [TEMPO]/[BPO] = 1.1 [47]

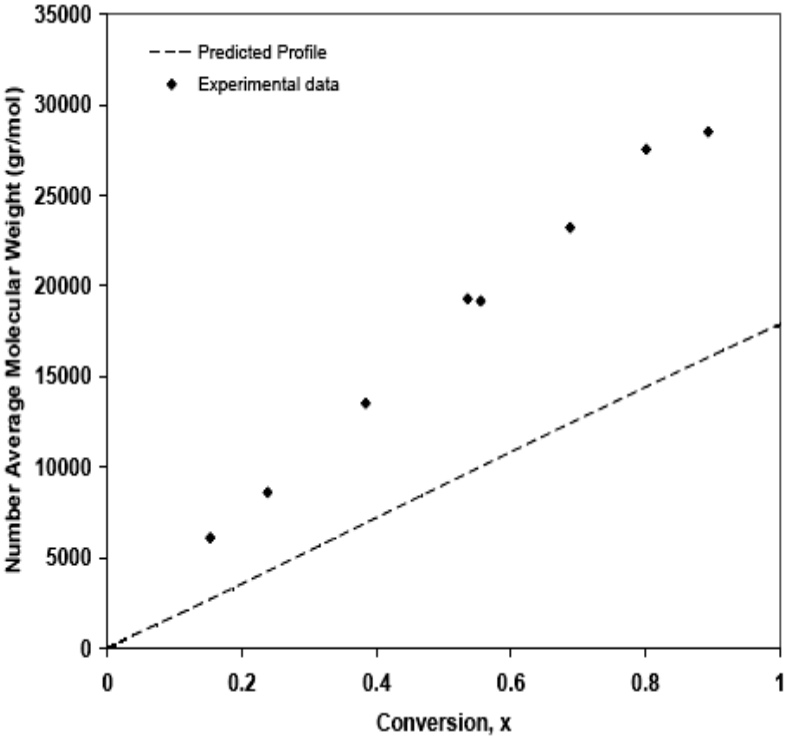

Figure 2.10 Comparison of experimental data and model predictions of molecular weight vs. conversion, at 120ºC and [TEMPO]/[BPO] = 1.1 [47]

2.3.3 Unimolecular initiator

The second approach to initiation for NMRP is possible when the initiator is a low molecular weight alkoxyamine. This approach was used in the original work of Rizzardo and Solomon [48]. Later, Hawker[49] also exploited this method and coined the term 'unimer' to describe the initiators produced. Alkoxyamine was generated by adding initiator and nitroxide in monomer and heating the mixture at 80°C. At this relatively low temperature, the small molecule alkoxyamine produced is essentially a stable compound with only a low degree of radical dissociation. Therefore it can be isolated, and then used as a unimolecular initiator, for styrene polymerization at higher temperature (125°C) (Scheme 2.13).

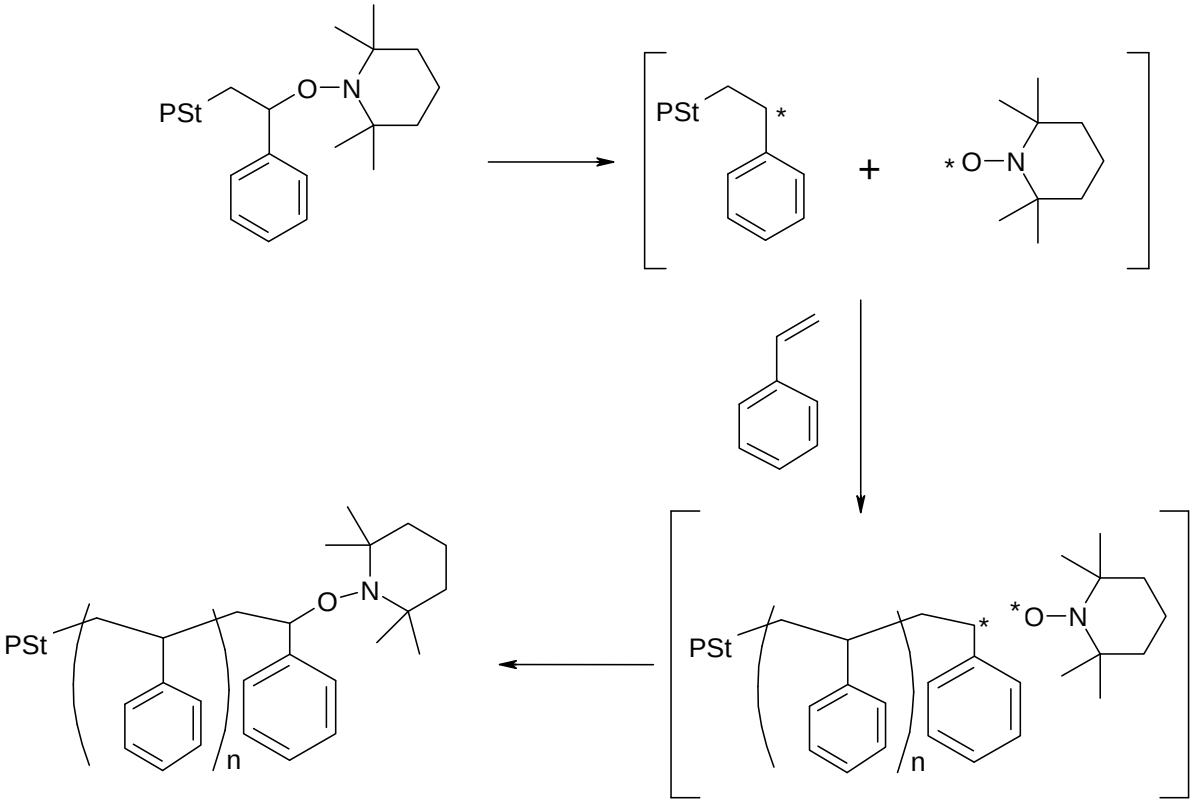

Scheme 2.14 Reactions in unimolecular NMRP[49]

2.3.3.1 Synthesis of unimolecular initiator

Although unimolecular initiators have advantages, the exploitation of them was originally limited by a lack of efficient synthetic procedures, which leads to the low yields and a wide range of by-products[50]. Several techniques have since been developed, which rely on the controlled generation of the intermediate radicals, including hydrogen abstraction from ethyl benzene with di-t-butyl peroxide[21], single electron transfer from ester enolates by treatment of lithium salts with ferrocenium ions[52], and halogen abstraction from alkyl halides by a Cu catalyst via atom transfer radical addition[53].

2.3.3.2 Kinetics of unimolecular system

It was observed by Catala et al. [54] that the polymerization rate, $R_{p,}$ of styrene polymerization in the presence of the model adduct S-DBN (S = 1-phenylethyl, and DBN = di-tert-butyl nitroxide) was independent of the adduct concentration (<30% conversion). This phenomenon was attributed to aggregation of dormant chains. Subsequently, a paper by Greszta and Matyjaszewski[55] indicated that the rate of unimolecular NMRP was equal to that of thermal self-initiation. The same researchers then extended this conclusion to other initiating systems[56]. Hence, it has been commonly accepted that the polymerization rates of unimolecular systems are independent of the concentration of alkoxyamine and remarkably close to the rate of thermal self-initiation (research was conducted at low conversion, within 15 hours).

The kinetics and mechanism of a unimolecular system were illustrated by Fukuda et al.[57]. They assumed that radical-radical termination and thermal self-initiation of styrene are

proceeding through the entire process of styrene NMRP. Termination continuously consumes growing radicals, P*. As a result, [P*] is decreasing relative to [X*]; [X*] gradually builds up, leading to an unbalance between [P*] and [X*]. On the other hand, radicals generated by self-initiation capture X*, thus preventing it from build-up. A stationary state then can be reached with the approximately constant [P*] and [X*],

$$d[P^*]/dt = d[X^*]/dt = 0 \qquad \textbf{(2.5)}$$

Controlled radical polymerization may generally be described by the following differential equations:

$$\frac{d[X^*]}{dt} = k_a[P-X] - k_d[P][X^*] \qquad \textbf{(2.6)}$$

$$\frac{d[P^*]}{dt} = k_a[P-X] - k_d[P^*][X^*] + R_i - k_t[P^*]^2 \qquad \textbf{(2.7)}$$

R_i is the rate of initiation due to an initiator and/or thermal initiation, and k_t is the termination rate constant between polymer radicals.

Substitute Eq. 2.5 into Eq. 2.6 and Eq. 2.7, we have

$$[P^*] = (\frac{R_i}{k_t})^{1/2} \qquad \textbf{(2.8)}$$

$$[P^*][X^*] = K[P-X] = KI_0 \qquad \textbf{(2.9)}$$

$$K = \frac{k_a}{k_d}. \qquad \textbf{(2.10)}$$

The (stationary) rate of polymerization is given by

$$R_p = (k_p / k_t^{1/2}) R_i^{1/2}[M] \qquad \textbf{(2.11)}$$

Thus, in the absence of a conventional initiator, thermal self-initiation is mainly responsible

for maintaining a reasonable polymerization rate, which is independent of the alkoxyamine concentration, [P-X].

This relationship applies when there is a secondary source of radical initiation. If there is neither conventional initiation nor self-initiation, there won't be enough radicals generated to balance the build up of nitroxyl radicals, thus the assumption of d[P*]/dt = d[X*]/dt = 0 can not be held. In this case, it can be shown that the polymerization rate is expressed as Eqs. 2.12 and 2.13[17].

$$R_p = k_p[P^*][M] = k_p(KI_0 / 3k_t)^{1/3} t^{(-1/3)}[M] \qquad \textbf{(2.12)}$$

$$\ln([M]_0 / [M]) = (3k_p / 2)(KI_0 / 3k_t)^{1/3} t^{(2/3)} \qquad \textbf{(2.13)}$$

Eqs. (2.12) and (2.13) indicate that in the case of no secondary initiation source (conventional and/or thermal), polymerization rate is 1/3-order dependent on initiator concentration. This conclusion was also independently drawn by Fischer using a power-law analysis[58].

The comparison of a bimolecular system ($R_i > 0$, [X*] > 0) with a unimolecular one was described by Hawker et al.[59] in an evaluation of a variety of initiating systems for nitroxide-mediated radical polymerization (NMRP) (research was conducted within the whole conversion range, up to 50 hours). Polymerization rates were observed as the same for both unimolecular and bimolecular systems even at high conversion. Interestingly, a recent study by our group[17] observed that the polymerization rate of the unimolecular system was lower than that of the corresponding bimolecular system at high conversion levels (≥ 60%) (Figure 2.11), rather than the same, which had been reported in Hawker et al.'s paper[59].

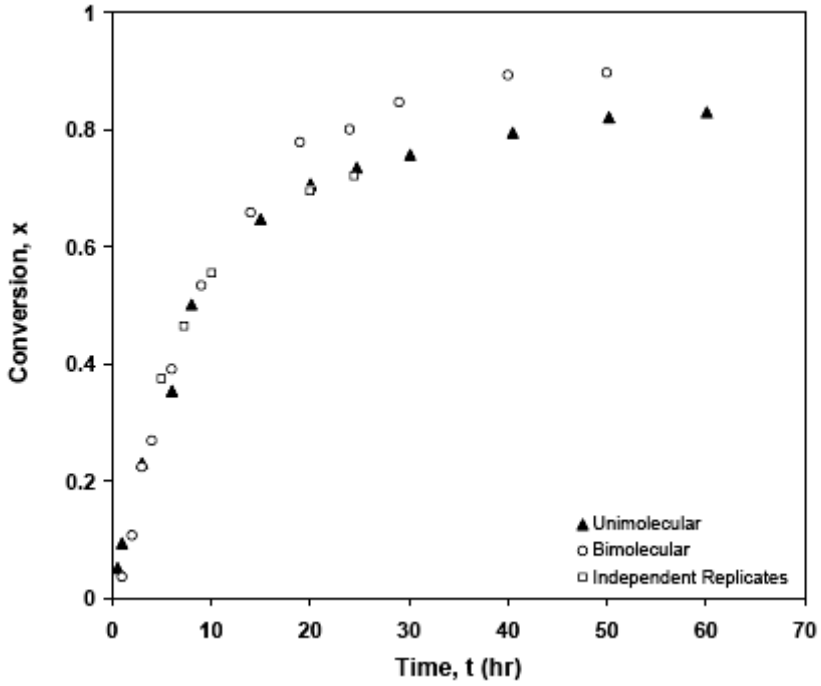

Figure 2.11 Comparison of conversion vs. time plots for the polymerization of styrene at 120ºC using the unimolecular initiator (▲) and a bimolecular system, [TEMPO]/[BPO]=1.1 (○) [17]

As the earlier study[17] has proposed, there may be two possible reasons that can account for the rate difference between unimolecular and bimolecular systems. One is because "a portion of the initial mixture volume is occupied by the unimolecular initiator so the concentration of monomer present is less (considering the same volume as in the bimolecular case)". Another assumption is that, in a bimolecular system, a large proportion of TEMPO would be lost as a consequence of side reactions, which is avoided in the unimolecular system. Hence, a unimolecular system retains a higher effective TEMPO concentration than a bimolecular system.

Nabifar[17] also observed that both molecular weight and polydispersity of the unimolecular system were lower than those of the corresponding bimolecular system (Figures 2.12, 2.13). These differences were ascribed to the significant loss of TEMPO in bimolecular system.

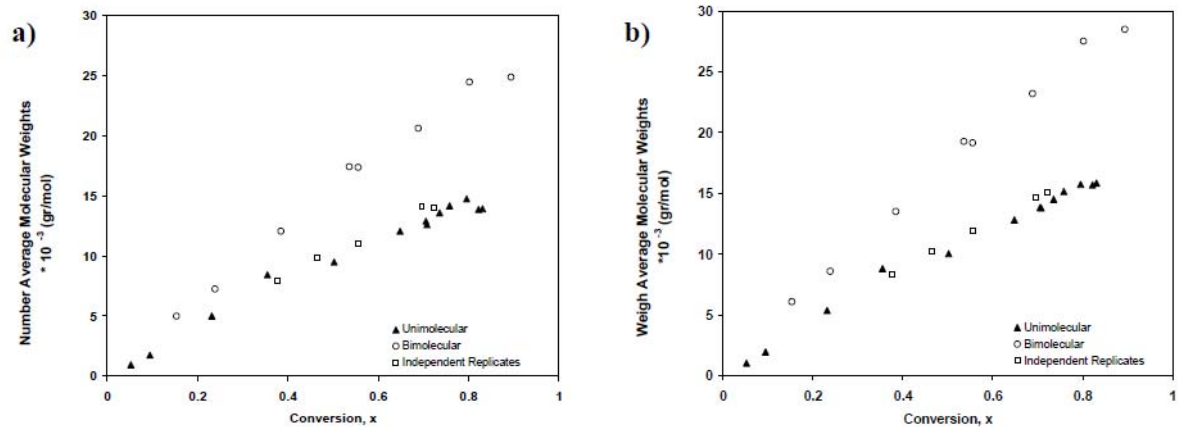

Figure 2.12 Comparison of molecular weight vs. conversion plots for the polymerization of styrene at 120ºC using the unimolecular initiator (▲) and a bimolecular system, [TEMPO]/[BPO]=1.1 (○) [17]

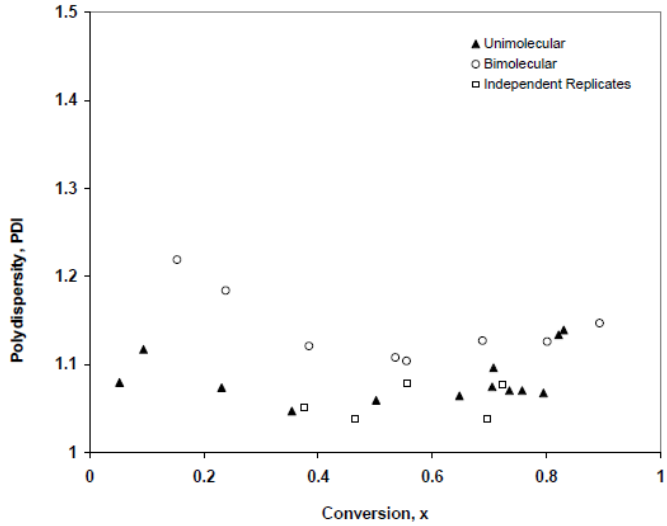

Figure 2.13 Comparison of polydispersity vs. conversion plots for the polymerization of styrene at 120ºC using the unimolecular initiator (▲) and a bimolecular system, [TEMPO]/[BPO]=1.1 (○) [17]

From this brief overview, one can appreciate that there are still some aspects worth studying with respect to a unimolecular system. For example, the loss of TEMPO due to side reactions such as promoted dissociation was considered significant at temperatures below 80ºC. However, the temperatures commonly used in NMRP are all above 100ºC. Why is the loss of TEMPO still significant when the experiments are carried out at high temperature? Furthermore, since the loss of TEMPO occurs at the initiation step, how does it relate to the

kinetic behavior at later stages of polymerization (high conversion level)? These and other related questions will be discussed in Chapter 4.

Chapter 3 Experimental Methods

3.1 *Monomer purification*

Monomer (styrene, Aldrich Canada Ltd.) was washed three times with a 10 w/v% sodium hydroxide solution, washed three times with distilled water, dried over calcium chloride and distilled under vacuum[1] just prior to use. Solvents such as ethanol, methyl chloride, and acetone used during the course of the experimentation and both BPO and TEMPO were used as received from suppliers (ATOFINA Chemicals, and Aldrich, respectively) without further purification.

3.2 *Synthesis of alkoxyamines*

3.2.1 Preparation of alkoxyamine macromolecule in ampoules

Benzoyl peroxide (0.072 mol/l) was mixed with TEMPO (0.086 mol/l)[2][3] and styrene in a flask and transferred into ampoules (capacity ~ 4 ml). The mixture in ampoules was then degassed via three freeze-vacuum-thaw cycles, sealed under vacuum, and stored in liquid nitrogen until use. Before heating, the samples in ampoules were thawed. After thawing, the samples were heated at 90°C for 1h and then at 125°C for varying times. The reaction was quenched by immersing ampoules in liquid nitrogen, and then products were precipitated from ethanol, purified by filtration and thoroughly dried. Yield was then calculated from gravimetry comparing the product mass to the initial reagent amount. Molecular weight was analyzed by size exclusion chromatography.

3.2.2 Preparation of alkoxyamine macromolecule in flask

TEMPO (0.1mol/l) was dissolved in styrene in a flask. The solution was then degassed by bubbling N_2 through it for about 1 hour and heated to 95ºC (oil bath temperature) while maintaining an N_2 atmosphere. A solution of benzoyl peroxide (molar ratio of BPO/TEMPO = 1.2) in styrene was made and degassed by bubbling N_2 through it at room temperature. The degassed BPO solution was added dropwise into the TEMPO/styrene solution over a period of 20 min, which gave a pale yellow solution. The oil bath was maintained at 95ºC for about 1h, and then the temperature was increased and maintained at 125ºC for a further 3.5 hours. The solution was concentrated by rotary evaporator, and then the residue was dissolved in the minimum amount of methylene chloride. This product was precipitated by being added dropwise into an excess ethanol (the volume ratio of product solution to ethanol was 1:10). The mixture was stirred vigorously during the precipitation. The precipitate was separated by filtration. This dissolving-precipitation-filtration was repeated several times until the product appeared ivory colored. Then the purified product was thoroughly dried in a vacuum oven at 65^{o} C. Yield was then determined gravimetrically by comparing the product mass to the initial reagent amount. Molecular weight was analyzed by size exclusion chromatography.

3.3 *Polymerization procedures*

Polymerizations were completed in borosilicate glass ampoules. Unimolecular initiator was dissolved in the distilled styrene to prepare initiator solution with the selected concentration (see sample calculation in Appendix C), and then transferred into ampoules (capacity ~ 4ml). Then the solution was degassed by three freeze-vacuum-thaw cycles, sealed off and stored in liquid nitrogen until being used. To run the polymerization, the ampoules were immersed in a

silicone oil bath at the desired reaction temperature having a temperature control of ± 0.1ºC, and taken out and quenched in liquid nitrogen at different times. Ampoules were then thawed, weighed, and opened. The contents were dissolved in methylene chloride, and precipitated using a large excess of ethanol. The mixtures were then air dried. Finally, the partially dried contents were vacuum-dried for several days at approximately 50ºC until a constant weight was reached for the amount of residue.

3.4 *Polymer characterization*

3.4.1 Gravimetry

Monomer conversion was measured gravimetrically by comparing the mass of isolated polymer to the mass of monomer feed:

$$Conversion\% = mass\ of\ polymer / mass\ of\ initial\ monomer\ feed \times 100\% \quad (3.1)$$

One thing to note is that since the unimolecular initiator took up a portion in the monomer feed and in the resulting polymer, the mass of the initiator had to be subtracted from the amount of monomer feed and from the mass of the final polymer residue.

3.4.2 Size exclusion chromatography

Size exclusion chromatography (SEC), also referred to as gel permeation chromatography (GPC), was used for determining average molecular weights and molecular weight distribution (MWD) of the polymer. As its name implies, SEC separates molecules based on their sizes. A low concentration of polymer solution passes through a column packed with

porous gel. The large molecules can not penetrate or diffuse into pores as frequently as small molecules do. As a result, large molecules are eluted faster and get out of the column earlier than the small molecules. The eluted samples can be characterized by a single concentration detector (Conventional Calibration), or series of detectors (Universal Calibration or Multiple-Detection) downstream[4].

In this study, the SEC system was maintained at 30ºC with tetrahydrofuran as the mobile phase flowing at a rate of 1.0 ml/min. The set up consisted of a Waters solvent delivery system and autosampler followed by Viscotek's quad detector equipped with a UV detector, low- and right-angle laser light scattering detectors (LALLS/RALLS), differential refractometer (RI) and viscometer in series. One PL gel 10μm guard column (50 × 7.5mm, Polymer Laboratories Ltd.) and three HR-5E columns (300 × 7.5mm, Viscotek) were used with the detectors. The laser operated at 670nm and the light-scattering intensity was measured at 7º (LALLS) and 90º (RALLS)[4]. Data analysis for results was performed using OmmiSEC version 3.0 (Viscotek)[5].

Chapter 4 Results and Discussion

4.1 *Synthesis of unimolecular initiator*

Different methods of initiator synthesis were examined. The differences between the methods were centered on type of reaction vessels used. The first method looked at carrying out synthesis in sealed glass ampoules. It provided efficiency in degassing of reaction mixtures by standard freeze-pump-thaw procedures. The second method used a standard multi-neck flask as reaction vessel. This offered ease of set up for preparation of larger quantities of initiator. Both methods were used and comparisons between them are presented in the following subsections.

4.1.1 "Ampoule method"

The objective of initiator preparation was to provide high yield of initiator that could be sufficient to use in an extended study. In addition, molecular weight (MW) of initiator was to be fairly low (~ 2000 g/mol) to ensure a low MW starting point for the planned polymerizations, so that there would be a larger proportion of free monomer in the reaction mixture. In addition, the molecular weight should be high enough so that initiator could be readily purified by precipitation from ethanol.

In order to prepare initiator with the targeted yield and molecular weight, small scale tests were first carried out with various reaction times at 125ºC and in different sizes of ampoules. Test 1 in Table 4.1 used regular-sized ampoule (capacity ≈ 4 ml). Test 2 in Table 4.1 used larger ampoules (capacity ≈ 10 ml).

Table 4.1 GPC results of preparation of unimolecular initiator

Experiment	Sample	Time (h)	Mn (g/mol)	Mw (g/mol)	Mw/Mn	Conversion (%)
Test 1 (Small ampoule)	1	2	2,094	2,637	1.26	4.40
	2	3	2,516	2,701	1.07	8.20
	3	4	3,284	3,575	1.09	12.60
	4	6	5,092	5,451	1.07	22.10
Test 2 (Big ampoule)	1	3.25	1,411	1,544	1.09	3.00
	2	3.5	1,614	1,760	1.09	3.58
	3	3.5	1,654	1,806	1.09	3.16
	4	4	1,804	1,952	1.08	5.62
	5	4	1,956	2,118	1.08	4.75

The results from the small ampoule studies indicated that the best reaction time would be about 2 h to get the desired Mn (~ 2000 g/mol). However, the yield of the product was fairly low. In order to test if the same results would be obtained using large ampoules, another study was carried out. As can be seen from the data in Table 4.1, the results were not exactly the same for corresponding reaction times in large ampoules as compared to small ampoules. Molecular weights of polymers that were produced in the large ampoules were lower than those by small ampoules at the same reaction time.

Based on these small scale tests, scaled-up preparation was carried out by using a batch of large ampoules with reaction time of 3.5 hours, which produced initiator having a molecular weight of $M_n \approx 2105$g/mol (Mw/Mn = 1.15), and yield of 7.2%.

4.1.2 “Flask method”

Although the “ampoule method” had prepared initiator with the targeted molecular weight and considerable yield, its set-up and procedures were relatively complicated. In order to simplify the set-up and procedures, a three-necked flask was used as the alternative reaction vessel. In the initial tests, a mixture of BPO, styrene and TEMPO was warmed to 90ºC. Then the reaction mixture was held at this temperature for 1 hour. After the preheating at 90ºC, the temperature was increased to 125ºC, and the reaction time was varied at that temperature for times shown in Table 4.2 (Batch#: 1-4). For the final preparations, refinements to the procedure were made as per below (Batch#: 5-7). The appropriate concentration of TEMPO was dissolved in styrene, and the solution was degassed by bubbling with N_2. This solution was then warmed to 95ºC. Separately, a solution of BPO was made in styrene, which was then degassed and added slowly to the TEMPO/styrene solution over a period of about 20 min (overall [TEMPO] = 0.10 mol/l, and [BPO]/[TEMPO] = 1.2).

Table 4.2 Summary of initiator synthesis

Batch	Conditions				Yield	MW (g/mol)	
	t (h)		[TEMPO]	[BPO]		Mn	Mw
	90ºC	125ºC	(mol/l)	(mol/l)			
1	1	4.5	0.086	0.072	18.96%	6238	6824
2	1	4	0.0859	0.072	0.60%	2260	2454
3	1	3.5	0.0861	0.072	3.57%		
4	1	4	0.086	0.072	8.04%	2626	2821
	95ºC	125ºC					
5	2	3.5	0.1	0.12	5.30%	2193	2369
6	2	3.5	0.1	0.12	7.68%	2474	2694
7	2	3.5	0.1	0.12	9.74%	2102	2347

The results show that the refined method provides relatively high yield of initiator, and a fairly low and constant molecular weight. The refined preparation avoided mixing TEMPO

and BPO at room temperature, which are known to readily react together to form nitrone plus radicals[1]; hence, the scale of losses of TEMPO and BPO in side reactions was reduced. Therefore, synthetic efficiency with respect to [TEMPO] was increased and the reaction process was better controlled.

4.2 *Comparison of bimolecular NMRP with unimolecular NMRP*

Previous studies have claimed certain advantages of unimolecular NMRP over the corresponding bimolecular NMRP, such as better control of molecular weight and lower polydispersity. Interestingly, conflicting observations related to polymerization rate have been presented by different researchers [2][3](see also section 2.3.3.2).

Two possible assumptions have been made to explain the difference of polymerization rates between the two systems[3] at high conversion. One is related to the proportion that the unimolecular initiator occupies in the initial mixture volume, which leads to a lower free monomer concentration (in the case of the same initial mixture volumes in the two systems). This assumption has some deficiencies. First, since polymerization rate is proportional to the propagating radical concentration and the free monomer concentration, this implies that the propagating radical concentrations have been the same in the two systems. The bimolecular system can be considered as a special case of the unimolecular system containing an alkoxyamine initiator. Since the conventional initiator (BPO) is used up in the first few minutes, the polymerization can progress to a large extent as in the unimolecular case if the ratio of BPO to TEMPO is kept at the appropriate level. However, the lower initial monomer concentration of a unimolecular system (at t = 0) must lead to a lower free monomer

concentration at any reaction time (t). This is so because the free monomer concentration ([M]) depends on both initial monomer concentration ($[M]_0$) and monomer conversion (p) (see Eq. 4.1).

$$[M] = [M]_0(1-p) \qquad \textbf{(4.1)}$$

It can be seen in the later discussion that the free monomer concentrations in bimolecular system are higher than those in unimolecular system at low conversion, but is similar with unimolecular system at high conversion.

Another reason that may potentially explain differences is based on the loss of TEMPO in side reactions in the bimolecular system. This may be more reasonable. The bimolecular system involves a multi-step initiation, which leads to various side reactions. Therefore, the total concentration of effective TEMPO is actually lower than that of the TEMPO initially added ($[TEMPO]_{bi} < [I]_0$). In a unimolecular system, on the other hand, preparation of alkoxyamine is stepwise, so the loss of TEMPO doesn't occur during the polymerization stage, and the total concentration of effective TEMPO is close to that of the added initiator ($[I] = [I]_0 = [TEMPO]_{uni}$). The presence of TEMPO slows down the polymerization at later stages of reaction, a bimolecular system with lower effective TEMPO concentration ($[TEMPO]_{bi} < [TEMPO]_{uni}$) would have a higher polymerization rate at high monomer conversion levels. However, several other questions remain to be answered. First, why is the loss of TEMPO still significant when the reaction undergoes at a temperature above 100ºC? This can be ascribed to the preparation and handling of samples during bimolecular initiation, where the reaction stock solutions are maintained at ambient temperature for a significant period. At low conversions, it has been shown in a number of studies[4][5][6] that rates are independent of

added alkoxyamine concentration, and are essentially equal to the rates for thermally initiated polymerization of styrene. It remains to resolve some of the issues regarding rates at high conversion levels of monomer.

To examine the aforementioned issues, a comparison of styrene polymerizations using bimolecular and unimolecular systems with conditions similar to those in Nabifar[3] was carried out. The results for conversion vs. time in both reactions are presented in Figure 4.1. It can be seen that below 70% conversion, the rates of monomer conversion were essentially the same for both unimolecular and bimolecular systems; while above 70% conversion, the polymerization rate of the bimolecular system was higher than that of the unimolecular system. These results are in agreement with the results in the earlier comparison[3], where the unimolecular system had a lower polymerization rate at high conversion.

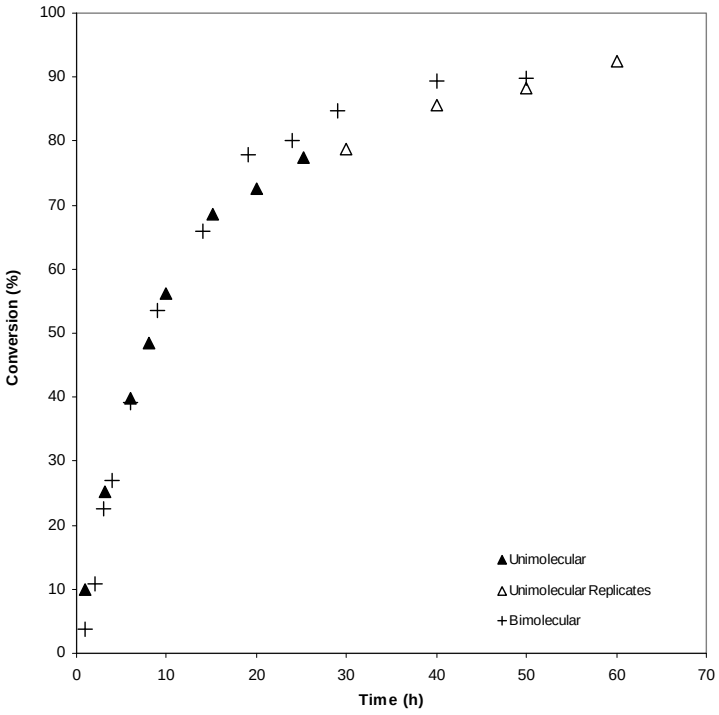

Figure 4.1 Conversion vs. time plot; comparsion of NMRP of styrene at 120°C between a unimolecular system (▲) with $[I]_0$ = 0.040 mol/l and a bimolecular system (+) with [TEMPO] = 0.040 mol/l, and [TEMPO]/BPO] = 1.1.

Based on the assumption that the free monomer concentration in a unimolecular system is lower than that in a bimolecular system, the free monomer concentrations were calculated and are shown in Figure 4.2. The free monomer concentration is obviously higher in bimolecular system than that in unimolecular system up to 60% conversion (15 h), and then above 60% conversion the differences are less pronounced. Therefore, the lower monomer concentration in unimolecular system is unlikely to account for the observed difference in the polymerization rate at high conversion levels.

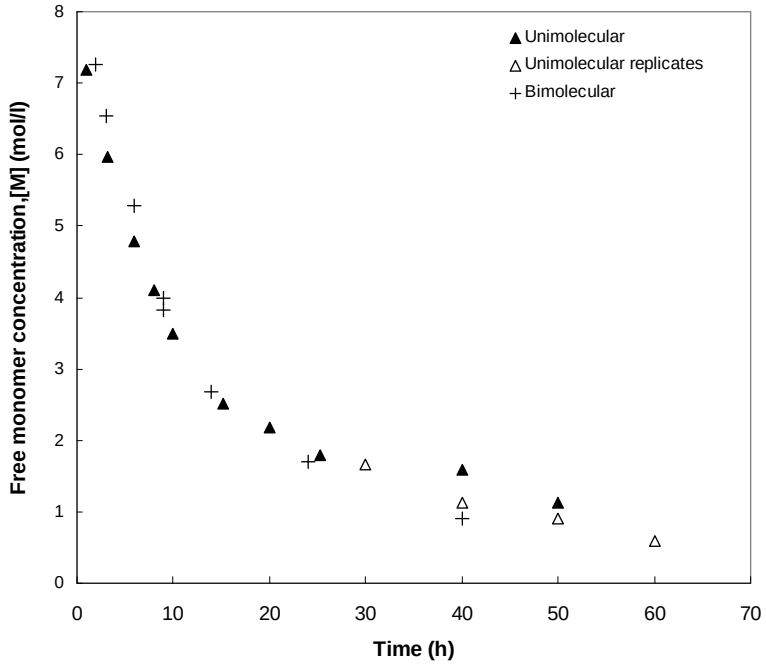

Figure 4.2 Free monomer concentration vs. time plot, comparsion of NMRP of styrene at 120°C between a unimolecular system (▲) with $[I]_0$ = 0.040 mol/l and a bimolecular system (+) with [TEMPO] = 0.040mol/l, and [TEMPO]/BPO] = 1.1.

Considering the second assumption stated above, the bimolecular system has a lower effective TEMPO concentration than a unimolecular system. At the later stages of polymerization, the monomer concentration is low. Since self-initiation of styrene is third-order dependent on monomer concentration, it is largely abated at the later stages of

reaction. This makes the situation more like the case of a unimolecular system with small amounts of self-initiation. Figure 4.3 shows the monomer conversion index, $\ln([M]_0/[M])$, for the reactions. Eq. (2.13) would not be in agreement with experimental data at high conversion for both systems since the bimolecular has a lower effective concentration of alkoxyamine. If expression 2.13 was true then the rates observed for the bimolecular should be lower than unimolecular. This is not the case and so it supports that the system is likely one where conventional (thermal) initiation is an important factor.

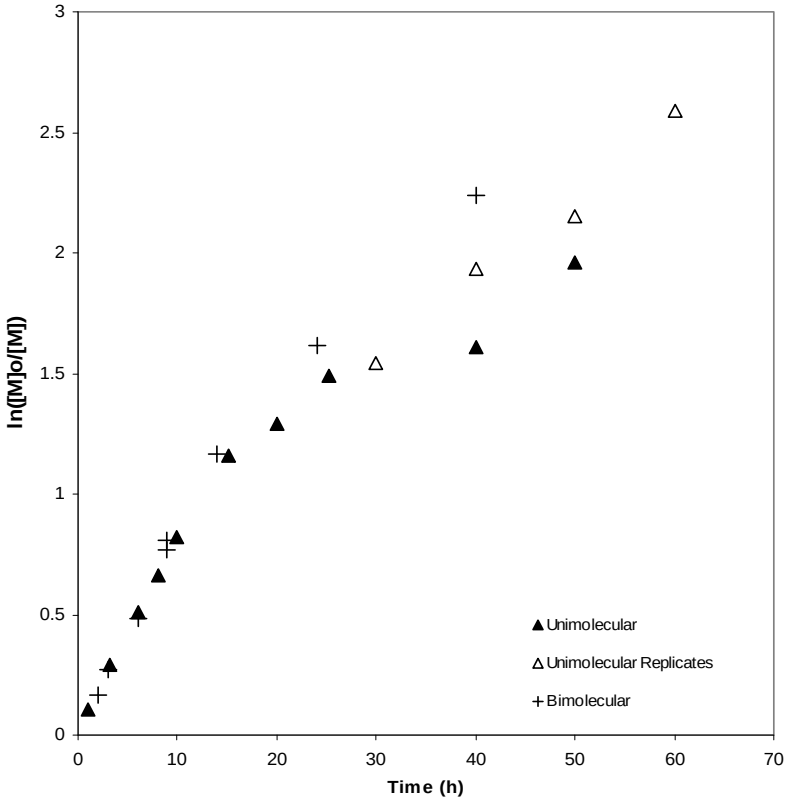

Figure 4.3 Ln($[M]_0/[M]$) vs. time plot, comparsion of NMRP of styrene at 120°C between a unimolecular system (▲) with $[I]_0$ = 0.040 mol/l and a bimolecular system (+) with [TEMPO] = 0.040mol/l, and [TEMPO]/BPO] = 1.1.

The fact that the effective nitroxide concentration is lower in bimolecular NMRP is seen in the molecular weights of the two systems. In the molecular weight vs. conversion plots of

Figure 4.4, both of the systems show linear trends, indicating that they are both controlled; the unimolecular system has a lower molecular weight for given levels of conversion.

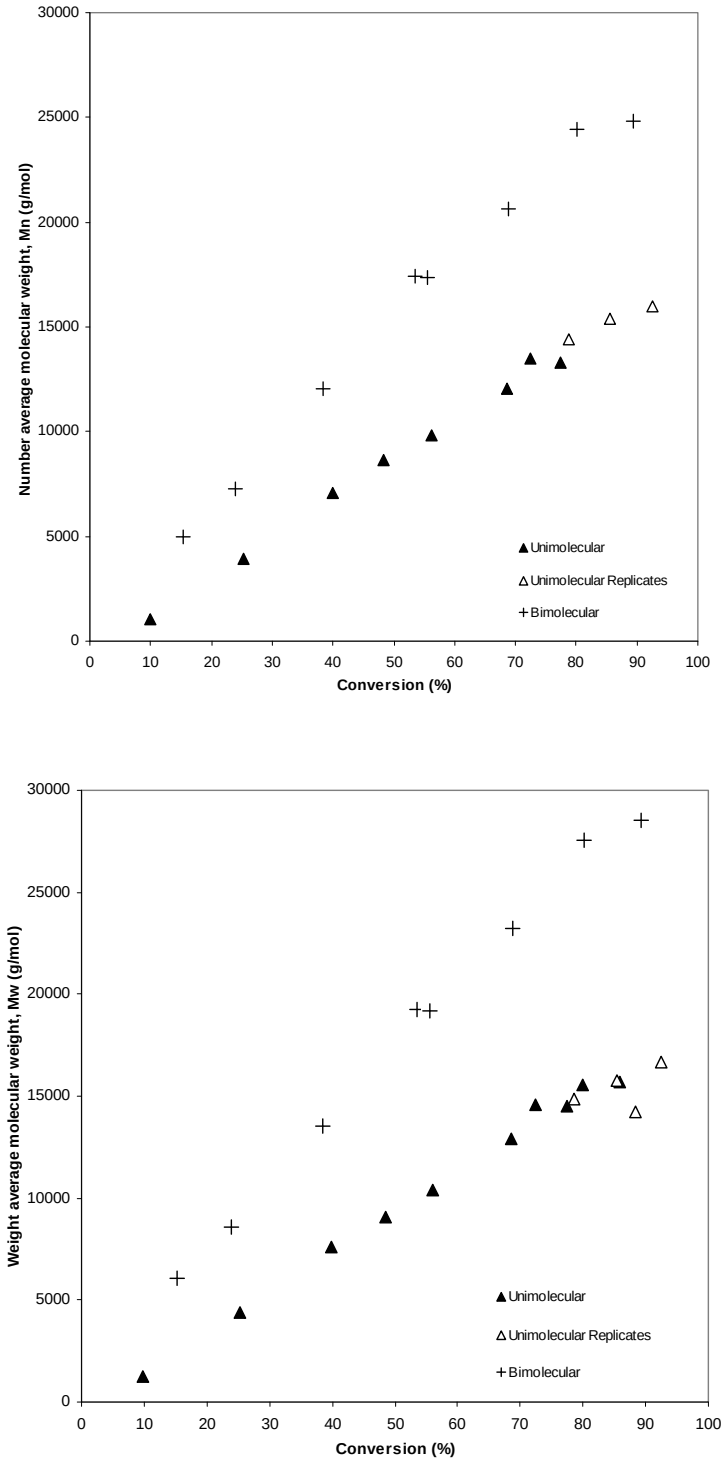

Figure 4.4 Molecular weight vs. conversion plot, comparsion of NMRP of styrene at 120°C between a unimolecular system (▲) with $[I]_0$ = 0.040 mol/l and a bimolecular system (+) with [TEMPO] = 0.040 mol/l, and [TEMPO]/BPO] = 1.1.

Figure 4.5 shows that the unimolecular system has a narrower molecular weight distribution. As mentioned in section 2.1.2.3, in an ideal living radical polymerization, the molecular weight of polymer is proportional to the ratio of molar monomer consumption and the concentration of initiated chains (Eq. 2.3). For a unimolecular system, each alkoxyamine chain end contains one TEMPO molecule, thus the total active TEMPO concentration in the reaction mixture can be considered as equal to the initial alkoxyamine concentration. The molecular weight is likely proportional to [TEMPO] (more details in section 4.4). Since the [TEMPO] concentration of a unimolecular system is intrinsically higher than that of a bimolecular system, its molecular weight would hence be lower.

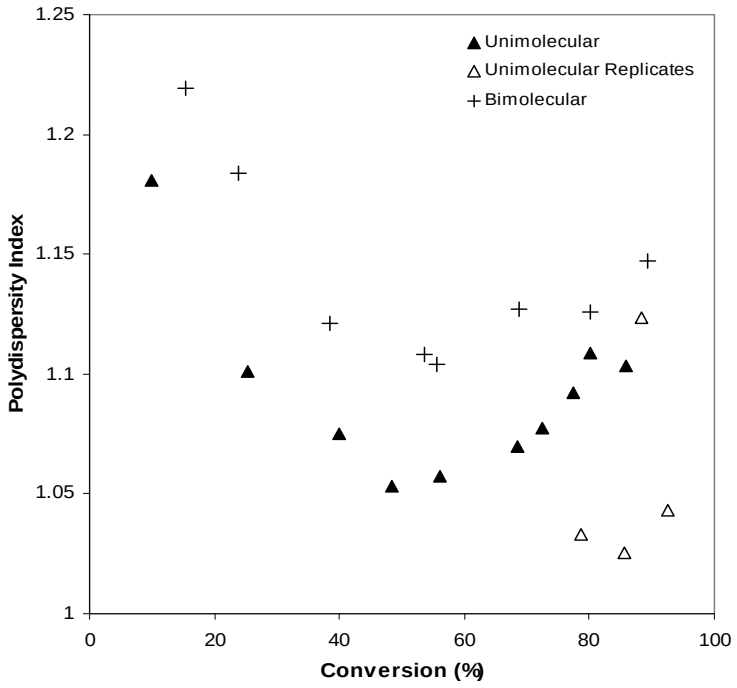

Figure 4.5 Polydispersity vs. conversion plot, comparsion of NMRP of styrene at 120°C between a unimolecular system (▲) with $[I]_0$ = 0.040 mol/l and a bimolecular system (+) with [TEMPO] = 0.040 mol/l, and [TEMPO]/BPO] = 1.1.

Given the evidence from MW trends support the theory that effective initiator (controller) concentration is lower in the bimolecular system, we can conclude that the lower rates at high

conversion levels for the unimolecular polymerization stem from the higher concentrations of nitroxide. Consider the fact that the propagation reaction competes with the associative reaction, in the control equilibrium, for reaction of radicals

$$P_n^* + [M] \xrightarrow{k_p} P_{n+1}^* \qquad \textbf{(4.2)}$$

$$P^* + NO^* \xleftrightarrow{K} P - ON \qquad \textbf{(4.3)}$$

As the polymerization proceeds, [M] decreases as does [P_n*] (because of irreversible termination). Since [P*] drops then the equilibrium will react by increasing the concentration of [NO*] in order to keep the equilibrium condition. Overall, the combination of factors will lead to a decrease in polymerization rate until essentially no measurable polymerization occurs (i.e. the RLPAC tends to be zero). If we have a higher level of [NO*] at the start of the reaction, the point at which polymerization "ceases" should probably be lower with respect to fractional conversion of monomer because the associative reaction will be even more favored relative to propagation.

4.3 *Factors affecting unimolecular NMRP*

Although there is still debate about the detailed mechanism of NMRP, the propagating species is believed to be a conventional propagating radical. Thus, radical-radical termination is not completely eliminated, though, as we shall see, with appropriate choice of reaction conditions, the significance of this process is markedly reduced in CRP. Therefore, in order to get a better understanding of how the kinetic behavior is affected by reaction variables, the present study was undertaken. In order to maximize the information content with minimum

number of experiments, and be able to draw valid conclusions from experimental work, it is crucial to have a logical experimental design. The details of experiments conducted are summarized in Table 4.3.

Table 4.3 Summary of experimental runs

		Factors			
	Exp.#	T	[I]	M_n(I)	
	1	-	-	-	
	2	+	-	-	
	3	-	+	-	
	4	+	+	-	
	5	-	-	+	
	6	+	-	+	
	7	-	+	+	
	8	+	+	+	
	9	+	0	-	
	10	-	0	-	
FACTOR LEVELS					
		-	0	+	
	T (°C)	120	130	140	
	[I] (mol/l)	0.030	0.040	0.050	
	M_n(I) (g/mol)	≈ 2000	≈ 3000	≈ 6000	
REPLICATES					
	Exp #	T	[I]	M_n(I)	Replicate of Exp#
	11	-	-	-	1
	12	+	-	-	2
	13	+	+	-	4
	14	-	0	-	10

The determination of initiator concentration levels (0.030M, 0.050M) was based on previous studies on the bimolecular NMRP of styrene. The selection of temperature levels (120-140ºC) was based on the prerequisite that TEMPO only acts efficiently as a mediator at

temperature above 115ºC (below that reactions are very slow). It should be noted also that the amount of unimolecular initiator synthesized was insufficient to complete the whole series of experiments. Therefore, slightly different initiators (in terms of their molecular weights) were used for different parts of the study. As a result of this, the effect of initiator molecular weight was considered as the third factor.

It was important to make sure that the experimental data obtained were reliable and error in each section of the experiment could be assessed. To do so, individual ampoule replicates were carried out at specific times in selected experiments. In addition, in order to check the reproducibility of data, independent replicates at specific conversion ranges were conducted. Reliability of molecular weight measurements was checked by running GPC replicates at different times. In addition, during GPC analysis, two independent injections were done for every sample (Exp 1-8). Molecular weight values plotted in the relevant figures later are averages from these two injections. Tables A.1 - Table A.14 in Appendix A cite the raw data for monomer conversion, average molecular weights and polydispersities for the study.

4.3.1 Effect of initiator concentration

Two levels of initiator concentration were selected and the effects of initiator concentration with respect to polymerization rate and molecular weight development were examined. The effect of initiator concentration on the polymerization rate (at 120ºC, initiator M_n = 2105 g/mol) is presented in Figures 4.6 and 4.7.

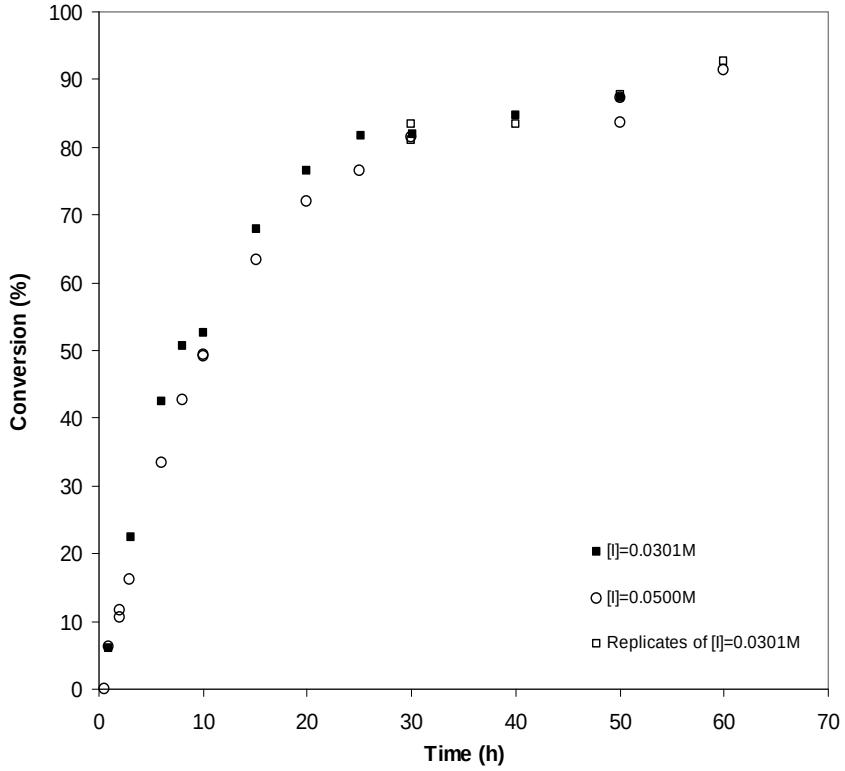

Figure 4.6 Conversion vs. time plot, effect of initiator concentration, T = 120ºC, initiator M_n = 2000 g/mol.

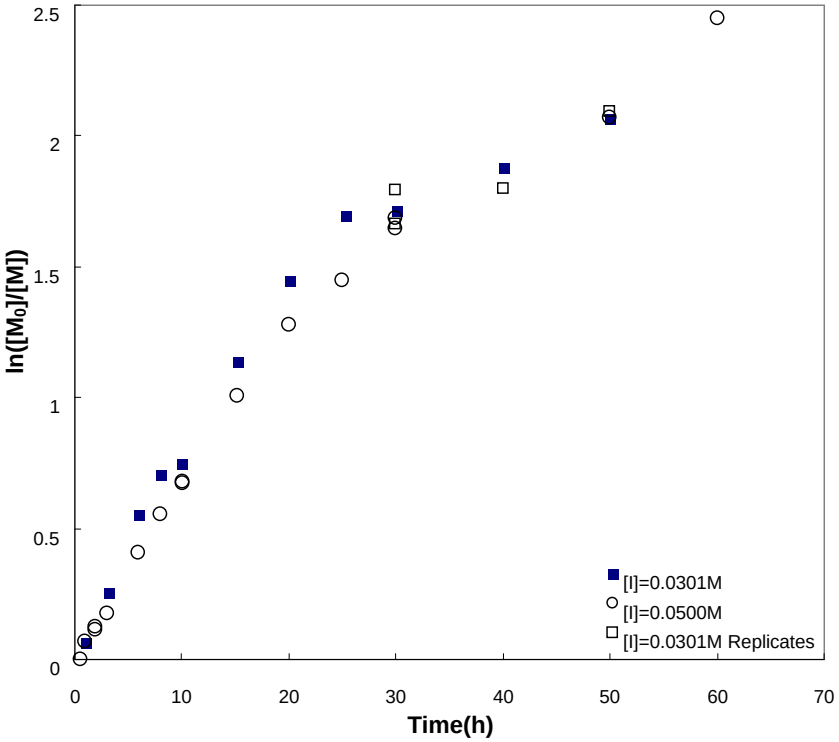

Figure 4.7 Ln($[M]_0$/[M]) vs. time plot, effect of initiator concentration, T = 120ºC, initiator M_n = 2000 g/mol.

As can be seen, below 60% conversion, conversion vs. time profiles were independent of initiator concentration. In the $\ln([M]_0/[M])$ vs. time plots of Figure 4.7, about 95.2% of the values are within 1 standard deviation of the mean, in other words, the polymerization rates using two initiator concentrations can not be distinguished. This coincided the observations in previous studies[4][5][6], which was ascribed by the stationary-state assumption ($d[P^*]/dt = d[X^*]/dt = 0$). This could also be verified, in another way, by the linear evolution of molecular weight shown in Figure 4.8, which indicated that the number of living chains is constant.

Above 60% conversion, the $\ln([M]_0/[M])$ vs. time plot of Figure 4.7 gradually lost its linear trend, and the lower initiator concentration led to a slightly higher polymerization rate; this difference virtually disappeared by 80% conversion. Possible reasons that may account for this deviation are as follows: 1) as the polymer concentration increases, the radical concentrations drop because of termination, so it would be expected that true first order kinetics would not be followed for the whole reaction. 2) as the polymer concentration increases, it is more difficult for the polymer radicals to diffuse; however, recent studies by our group have indicated that diffusion effects in NMRP systems are not very pronounced[7]. So it is unlikely that the diffusion effect is significant.

Figure 4.8 shows the average molecular weights M_n and M_w of polymer produced using different concentrations of initiator. It is evident that M_n increases linearly with conversion. This indicates that the experiment approached an ideal situation where the initiation was fast and the termination was minimized. It is noteworthy that the low initiator concentration led to a higher molecular weight of polymer. The slope of molecular weight vs. conversion plot

(degree of polymerization) for the lower initiator concentration (■) is 1.69 times larger than that for the higher initiator concentration (○). This value is close to the ratio of the $[M]_0/[I]_0$, which was equal to 1.76. This indicates that at these conditions unimolecular NMRP follows typical kinetic features of CRP, and that molecular weight is proportional to the ratio of styrene consumption to initiator concentration (further details are given section 4.4).

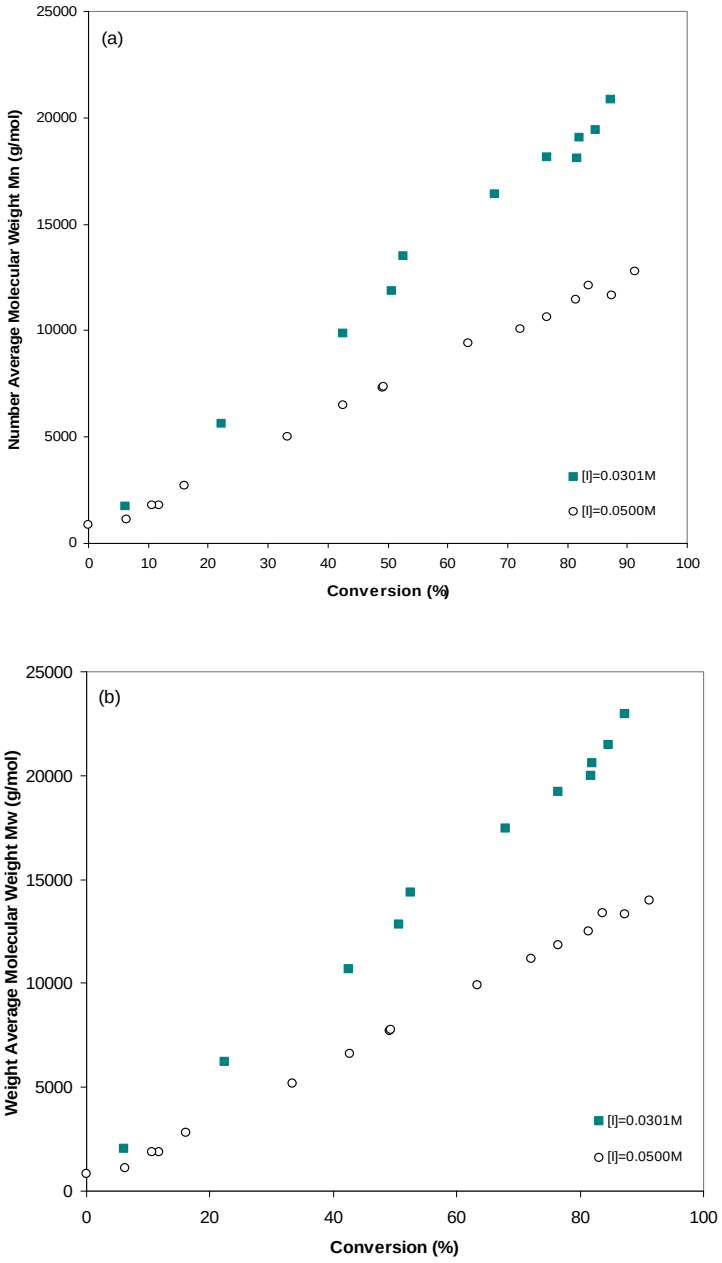

Figure 4.8 Effect of initiator concentration, (a) M_n vs. conversion; (b) M_w vs. conversion, T = 120°C, M_n(I) = 2000 g/mol.

Similar results for the effect of initiator concentration on polymerization rate and molecular weight have also been observed in the polymerizations conducted at 140ºC and when using initiator molecular weight equal to 6238 g/mol (see Appendix B, Figures 1-12). This gives consistent support for the postulate that higher nitroxyl levels will lead to some inhibition of polymerization rates at higher conversion levels

4.3.2 Effect of temperature

Radical polymerization processes are known to be sensitive to temperature, and in most cases, an increase in temperature will increase polymerization rate. Examples of this in NMRP include: a study on the role of TEMPO in polymerization of styrene by Veregin et al.[8], a recent publication by Nabifar et al.[9] studying the polymerization of styrene in the presence of BPO and TEMPO, an unimolecular NMRP of 4-vinylpridine by Fischer[10], and an unimolecular NMRP of styrene in the presence of SG-1 by Becer et al.[11]. Similar results have been obtained in our study using the unimolecular initiators. This is illustrated in Figure 4.9 which shows the effect of temperature on polymerization rate in the presence of a low-molecular-weight alkoxyamine (M_n = 2193 g/mol). As expected, at a higher temperature, the polymerization rate is significantly higher.

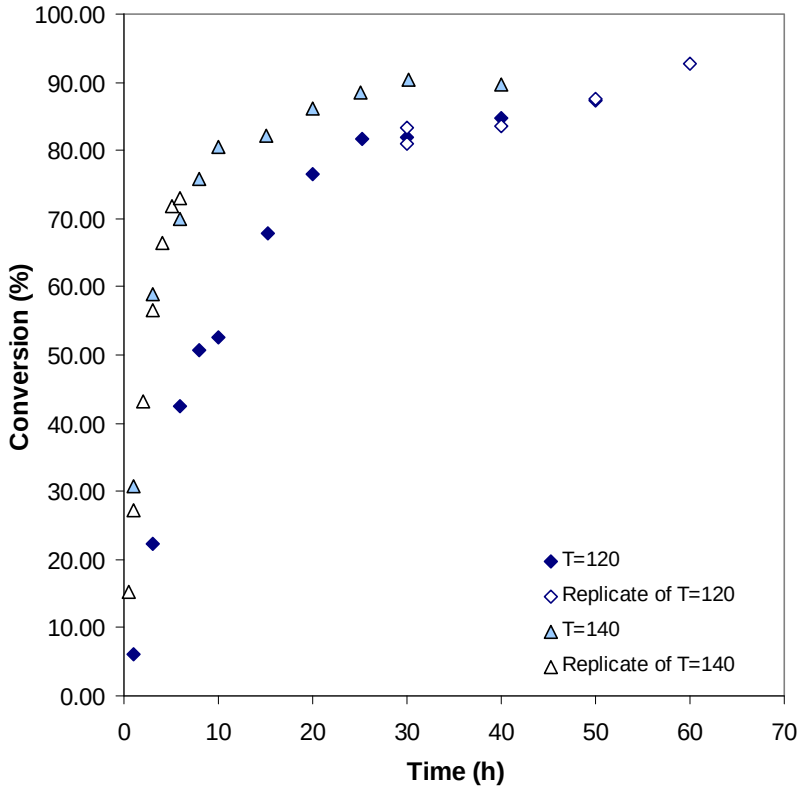

Figure 4.9 Conversion vs. time plot, effect of temperature, M_n(I) = 2193 g/mol, $[I]_0$ = 0.0301 mol/l.

However, there is no detailed discussion regarding this issue from a theoretical point of view. What follows is a discussion on this issue based on the reversible activation process (Scheme 2.10 (a)), which gives

$$[P^*][X^*] = K[P-X]_0 = KI_0 \qquad (4.4)$$

where $K = k_d/k_a$

Polymerization rate can be derived as Eq. 4.5

$$R_p = k_p[P^*][M] = (k_pK)([P-X]_0/[X^*])[M] \qquad (4.5)$$

Therefore, when the initiator concentration ($[P\text{-}X]_0$), is fixed, polymerization rate is determined by the propagation rate constant k_p, the equilibrium constant K, nitroxide radical concentration [X*], and monomer concentration [M].

Propagation is through addition of styrene monomer units to carbon-centered propagating radicals, which involves formation of C-C bonds, an exothermic process. The relationship between k_p and temperature is given by the well known Arrhenius equation,

$$k_p = A\exp(-E/RT) \qquad \textbf{(4.6)}$$

where E is the activation energy, A is the frequency factor, R is universal gas constant and T is temperature in K. In such a case, Eq. (4.6) indicates that increasing temperature will increase propagation rate ($k_p \uparrow$). In addition, dissociation of C-ON bond is an endothermic process. As a result, increase in temperature will enhance the rate of dissociation of C-ON relative to that of the associative reaction, namely, K will increase. Since k_p increases and the change in K will lead to higher [P*], the overall result of an increased temperature is to increase the polymerization rate.

For the bimolecular system, an increase of temperature was reported to have no significant effect on molecular weight except at high conversion M_n showed a plateau[9] with respect to conversion of monomer. Similar results have been observed in this thesis. As can be seen in Fig 4.10, below 60% conversion, temperature had no effect on the trends in M_n vs. conversion. Above 70% conversion, the results from the higher temperature showed a plateau in M_n values. M_w values at two temperatures remained almost the same through the whole conversion range (Figure 4.10).

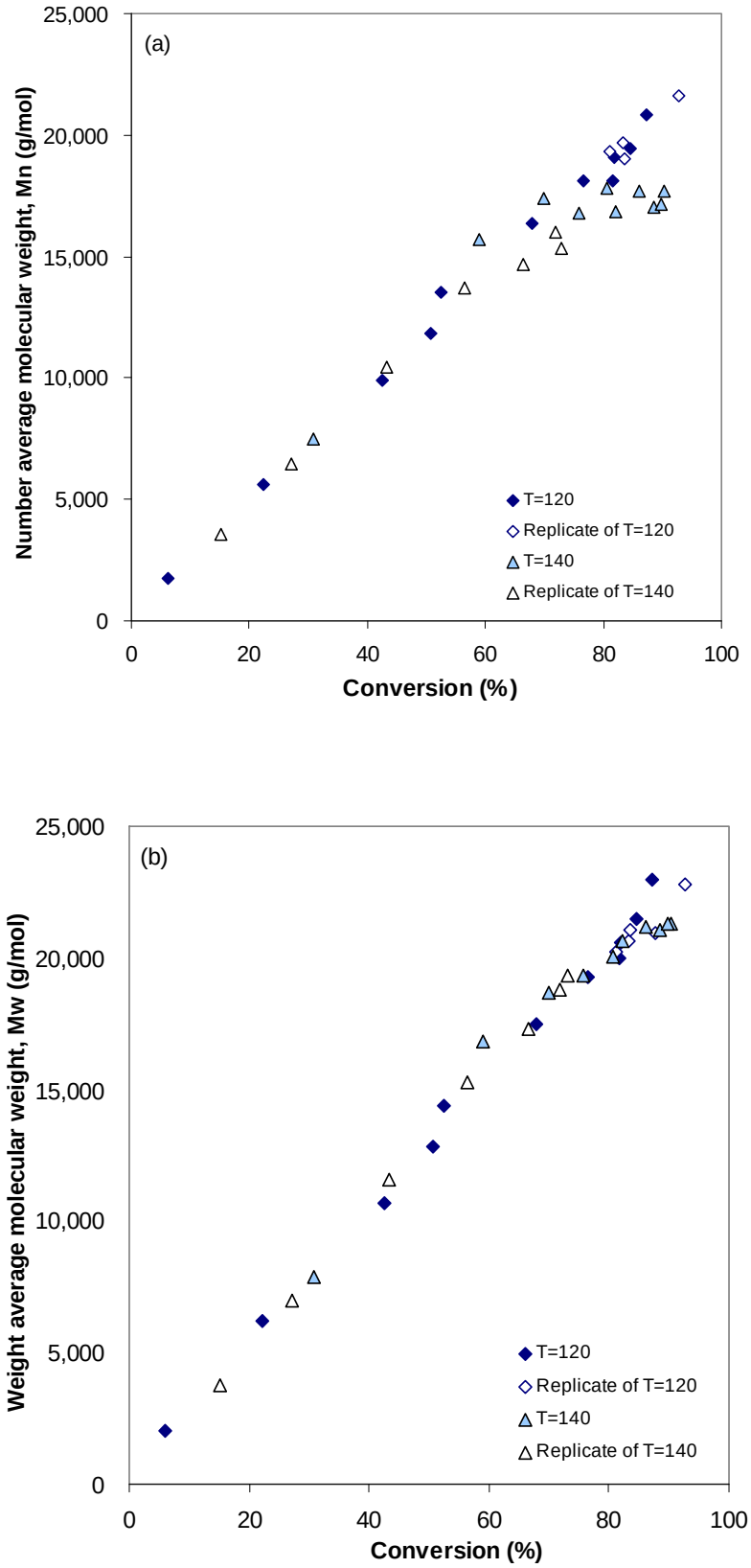

Figure 4.10 Effect of temperature, (a) M_n vs. conversion; (b) M_w vs. conversion, M_n= 2193 g/mol, $[I]_0$ = 0.0301 mol/l.

The fact that similar molecular weights are obtained at different temperature levels is now briefly discussed by relating to the concept described earlier, i.e."run length per activation cycle (RLPAC)[9][12]" (Eq. 2.4).

$$RLPAC = \frac{R_p}{R_d} = \frac{k_p[M][P^*]}{k_d[X^*][P^*]} = \frac{k_p[M]}{k_d[X^*]}$$

As previously mentioned in section 2.1.2.2, increases in molecular weight for CRP are determined by the number of initiated chains and the number of monomer units added to the propagating radicals (Eq. 2.3).

If there is no self-initiation, which may proceed through the entire course of polymerization, increase of temperature won't change the concentration of initiated chains. One of the prerequisites of an ideal living radical polymerization is that initiation is completed almost instantaneously. So the number of initiated chains is determined at the early stages of polymerization and stays constant while chain length grows in the propagation stage. Initiation is stimulated at a certain temperature. Once the temperature reaches the requirement to get over the minimum energy barrier, initiation is triggered. The rate of decomposition will be related to the temperature based on Arrhenius relationship.

An increase in temperature might be expected to have a slight effect on the number of monomer units added to the propagating radical in a given time period. As previously mentioned in section 2.1.2, the presence of a stable radical delays the propagation step by involving active radicals in the deactivation/activation cycles. Thus, the number of monomer units added to the polymer chain within a certain period depends on the rate of propagation relative to the rate of deactivation. The faster the deactivation is compared to propagation,

fewer monomer units can be added to the polymer chain. Increasing temperature not only increases the propagation rate ($k_p\uparrow$, $R_p\uparrow$), but also increases the deactivation rate ($k_d\uparrow$, $[X^*]\uparrow$, $R_d\uparrow$). As a result, the ratio of R_p/R_d won't show a significant change as long as the changes in the competing factors balance. Thus, the overall effect of temperature on molecular weight should be slight, in ideal situations, which is as observed in the experiments.

A notable plateau in M_n values with respect to monomer conversion (while M_w kept constant) was observed for higher temperature at high conversion. No study has addressed this before. A possible reason stems from the fact that self-initiation is enhanced at a higher temperature. Self-initiation is continuous through the entire course of polymerization, and the radicals generated may terminate long/short chains, or initiate new chain growth. At the later stages of polymerization, the newly initiated chains would have shorter time to grow than those initiated at the early stages of reaction, thus having a lower molecular weight. If the proportion of chains initiated from the unimolecular initiator is much higher than the amount of new chains generated by self-initiation, the molecular weight distribution (MWD) would still be narrow. If the proportion of newly initiated chains becomes higher, then MWD should be broadened. Low MW will have a significant effect on M_n but will not be so much on M_w (although the mole fraction of low MW molecules may be relatively high, their mass fraction would be low), and as a result, M_n is more sensitive to this change. Since thermal self-initiation rates are higher at a higher temperature, the proportion of thermally initiated chains will be greater at a higher temperature. The validity of this postulate was confirmed experimentally by comparing calculated data obtained from GPC results for normalized mole fraction vs. retention volume at different conversion levels at different temperatures, as

shown in Figures 4.11 and 4.12.

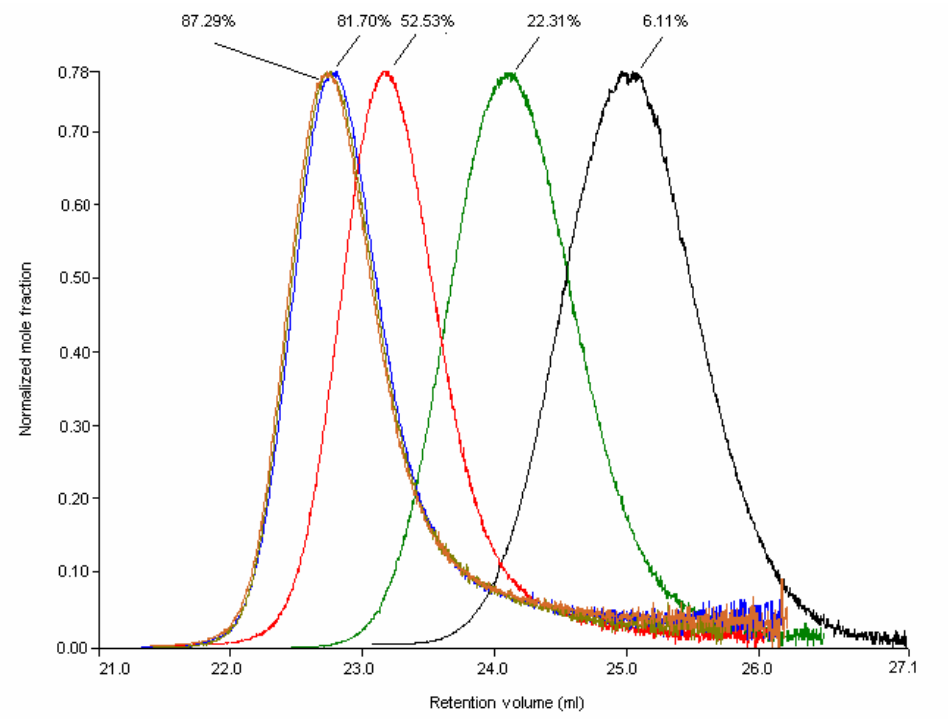

Figure 4.11 Normalized mole fraction vs. retention volume, T = 120º, Mn(I) = 2193 g/mol, [I] = 0.0301 mol/l

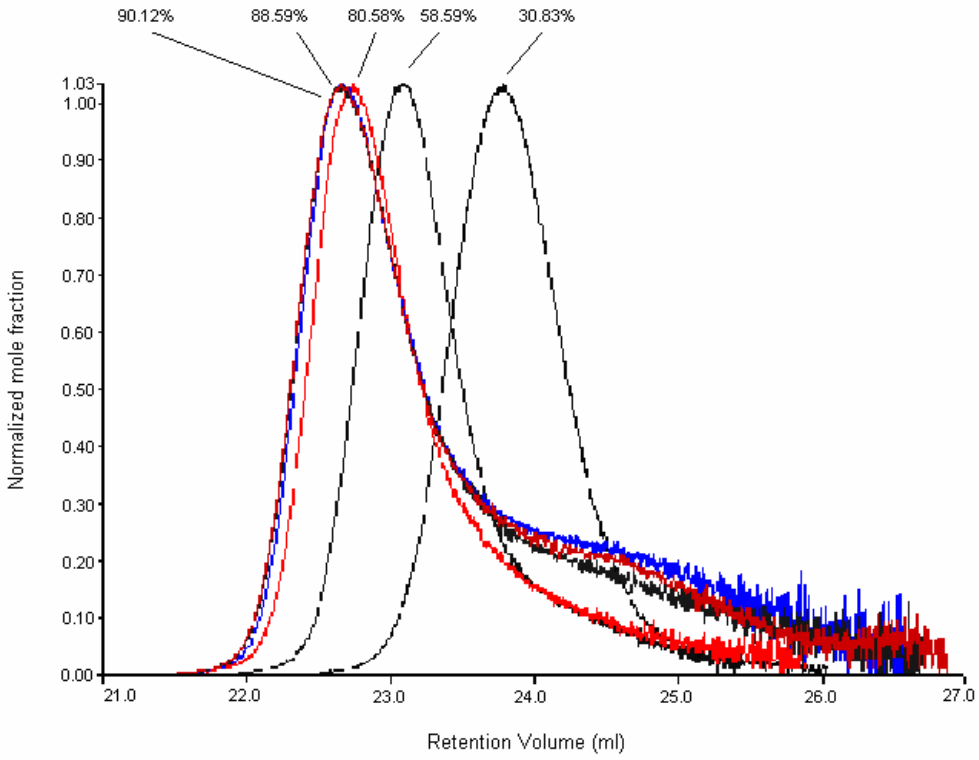

Figure 4.12 Normalized mole fraction vs. retention volume, T = 140º, M_n(I) = 2193 g/mol, [I] = 0.0301 mol/l

At both temperatures, the peaks were observed to shift to higher molecular weight (low retention volume) with increasing conversion, showing that the polymer chains are growing. The differences in the tails of the GPC traces at the two temperatures represent the reason for the differences in average MW trends. It can be seen that the mole fractions of low MW (high retention volume) are larger for the polymer made at the higher temperature, which indicates that relatively more oligomers with low molecular weight had been formed. A higher mole fraction of low MW species likely balances any increase in the peak MW causing the plateau in M_n.

Similar results have also been observed when using initiator with Mn = 6000 g/mol, and initiator concentration equal to 0.050 mol/l (see Appendix B, Figures B.17-24).

4.3.3 Effect of initiator molecular weight

As previously mentioned, it was difficult to make a large enough batch of initiator to last for the whole study. So the alkoxyamines used to conduct the polymerization studies had to be produced from different batches, leading to slightly different properties of initiator (molecular weight, polydispersity), which may have had some effect on the kinetic behavior. For example, high-molecular-weight initiator will take a larger proportion in the initial mixture volume; to prepare a mixture with the same initiator concentration, the amount of monomer initially needed would be less. Since the polymerization rate is proportional to the free monomer concentration (see Eqs. 2.11 and 2.12), which is determined by the initial monomer concentration and monomer conversion (see Eq. 4.1), the change of initial monomer concentration may lead to a difference in polymerization rates. No previous study

has discussed this issue so far, so the kinetic behavior by using initiators produced from different batches was examined and is described in this section.

An initial comparison was conducted between two batches of initiator of different molecular weight and polydispersity at the same temperature and initiator concentration (Fig 4.13).

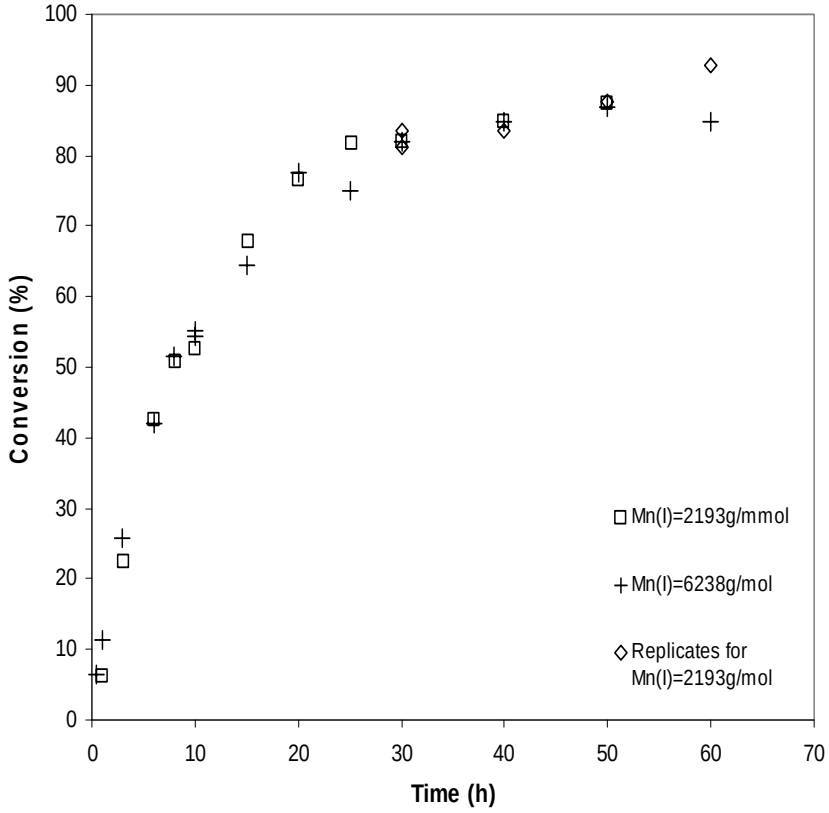

Figure 4.13 Conversion vs. time plot, effect of initiator molecular weight, T = 120°C, $[I]_0$ = 0.0301 mol/l.

It was surprising to observe that the monomer conversion rates were the same for different initiator molecular weights. As analyzed in previous sections (sections 4.2 and 4.3.1), polymerization rate is affected by the rate of thermal initiation. This implies that the slightly different thermal initiation rates caused by differences in $[M]_0$ did not have a significant effect. As discussed in section 4.3.1, the free monomer concentration is determined by the

initial monomer concentration and monomer conversion rate. If the initial monomer concentration is higher, the free monomer concentration would be higher for given conversion levels for the whole reaction. However, the results in Figure 4.14 show that at high conversion there is not a significant reduction in rate when the high molecular weight initiator was used. If the lower [M] used, when higher MW initiator was studied, was the main cause of reduced rates at high conversion then we would have expected to see a difference in conversion rates when using the different initiators. This was not observed and so would indicate that rates are more affected by the concentration of [RON] (as described in section 4.3.1)

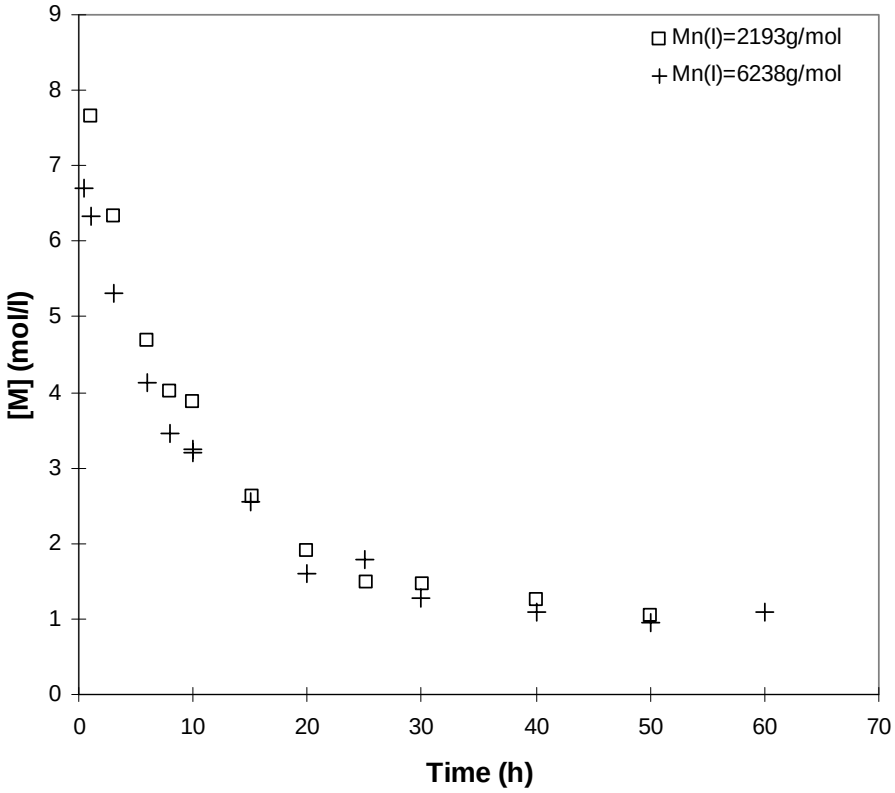

Figure 4.14 Effect of initiator molecular weight, T = 120°C, $[I]_0$ = 0.0301 mol/l. Free monomer concentration vs. time plot.

Figure 4.14 shows that the free monomer concentration values in the system with lower molecular weight initiator are higher than in the system with higher molecular weight initiator. However, this difference between the free monomer concentrations (in absolute terms) becomes smaller along with conversion. This means that the rate of monomer consumption for the system with lower $[M]_0$ (higher initiator molecular weight) decreases more slowly than that with higher $[M]_0$, so that overall result would be that the free monomer concentration values become closer.

Since the molecular weight of the resulting polymer is proportional to the concentration of monomer consumed, the initiator of high molecular weight should have a slightly lower corrected MW with respect to conversion than those observed for lower MW initiator. The experimental results of Figure 4.15 are largely in agreement with this postulate.

The differences between the free monomer concentration values can be amplified by increasing the difference between initiator molecular weights. Since it is not recommended to use initiator with molecular weight higher than 6238g/mol (to maintain the same initiator concentration, a larger amount of initiator is required if the initiator molecular weight is high), the initiator molecular weight can thus be considered to have little effect on polymerization rate and molecular weight development in the present study.

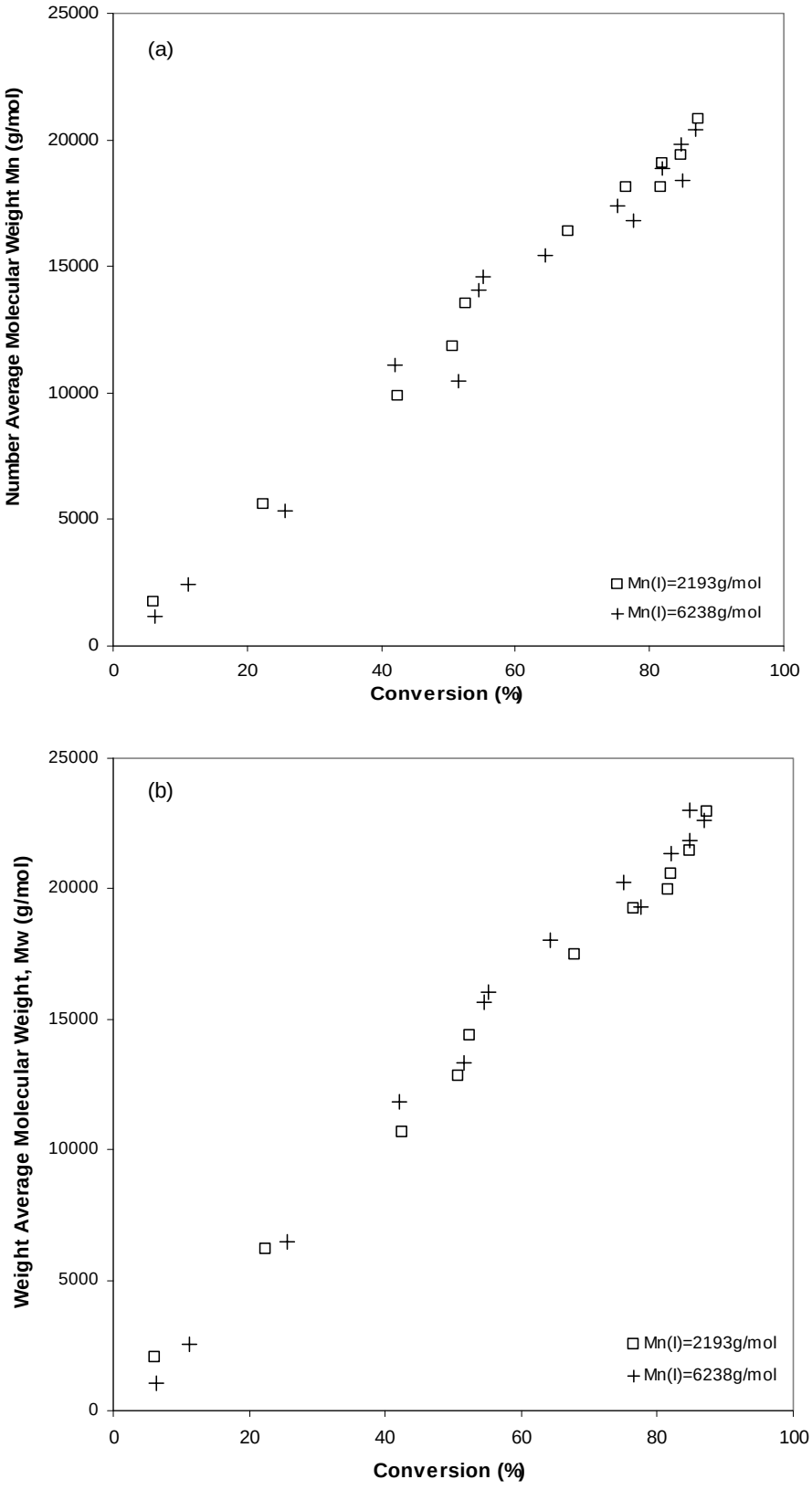

Figure 4.15 Effect of initiator molecular weight, T = 120ºC, $[I]_0$ = 0.0301 mol/l. (a) M_n vs. conversion; (b) M_w vs. conversion

4.4 *Prediction of molecular weight*

As mentioned in section 2.1.2.2, molecular weight of an ideal living radical polymerization can be determined by the ratio of monomer conversion to initiator amount (Eq. 2.3).

$$M_n = \frac{[M]_0 - [M]_t}{[I]_0} \times M_0 \qquad \textbf{(2.3)}$$

A bimolecular system may have a deviation from this rule because of several side reactions (section 2.3.1). However, since in a unimolecular system side reactions that occur in a bimolecular system are avoided, one would be able to predict molecular weight by following this simple rule. Therefore, a comparison between the experimental data of molecular weight obtained from GPC analysis and the theoretical data of molecular weight calculated by Eq.(2.3) was made.

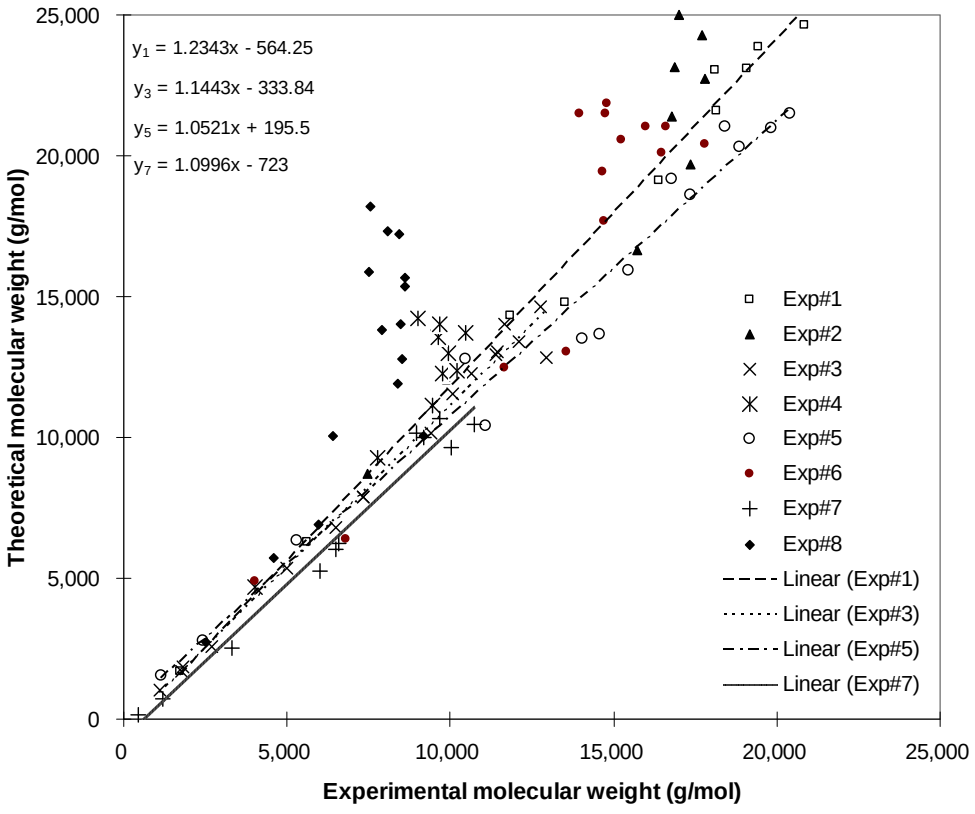

Figure 4.16 Prediction of molecular weights of polymers in unimolecular system

In section 2.3.2, such model prediction was also carried out for a bimolecular system, where the TEMPO concentration was substituted for the initiated chain number. The results showed that the experimental data were evidently higher than the theoretical data. As side reactions may lead to reduction of initiator efficiency and large loss of TEMPO, the actual initiated chain numbers are lower than the initial initiator concentration. This goes back to support one of the original postulates of our work, namely, that a unimolecular system could provide a better controlled process and better quantitative prediction for molecular weight than a bimolecular system.

For the unimolecular system, as one can see from Figure 4.16, the ratio (slope of the curves in Figure 4.16) of theoretical molecular weight to experimental molecular weight is slightly larger than 1 (see inset of figure 4.16, equations of linear fits y_1, y_3, y_5, and y_7). A likely reason for the deviation may be due to self-initiation that continuously generates new radicals during polymerization. This possibility is supported by the fact that the most significant deviations from the ideal trends are from the experiments at higher temperatures (Exp. 2, 4, 6, 8). This confirms that although high faster rates of polymerization, it will also lead to poorer control of the polymerization process.

Chapter 5 – Conclusions and Recommendations

5.1 *Conclusions*

This study has systematically assessed the kinetic behavior of a controlled radical polymerization system with a unimolecular initiator through the whole conversion range, and comparisons relative to the corresponding bimolecular system have been made.

Initially, the kinetic behavior of an unimolecular NMRP process was compared with a bimolecular system[1][2]. This was revisited under the same conditions as an earlier study[2]. The results showed good agreement with the work by Nabifar[2]. It was confirmed that polymerization rates for the two systems were largely the same in the early stages, which is as expected from standard theory explaining NMRP kinetics[3][4]. It is believed that a higher effective TEMPO concentration holds in a unimolecular system throughout the entire course of polymerization, and it leads to the early inhibition of the polymerization. Because when the radical concentrations drop, the equilibrium with respect to P* will react preferentially with NO* rather than another monomer. This ultimately leads to the slow down of polymerization.

In addition, the capabilities of molecular weight prediction for the two systems have been evaluated (Eq. 2.3). The bimolecular prediction underestimated the experimental value, while the unimolecular system gave a better estimate. The bimolecular system involves a multi-step initiation, so a significant concentration of initiator and free TEMPO is consumed in various side reactions [5][6][7]. So the stoichiometry between the growing radical, free TEMPO and BPO is not valid. In a unimolecular system, on the other hand, preparation of initiator is

stepwise; the fact that BPO reacts with TEMPO is not important since the initiator is isolated from any impurities. This method separates the preparation of initiator from polymerization, so the side reactions are no longer a factor in polymerization. Therefore, the effective free TEMPO concentration is closer to the initial initiator concentration. So the stoichiometry between the initial initiator concentration and growing radical concentration is valid, and molecular weight can be simply predicted following general CRP rules (Eq.2.3).

The effects of different reaction conditions such as initiator concentration, temperature, and initiator molecular weight on NMRP have also been considered in the thesis, both experimentally and theoretically. Initiator concentration was reported to have no effect on polymerization rate at low conversion in early studies[3][4]. This study looked at this and similar results were obtained at low conversion. Interestingly, at high conversion, polymerization rate was observed to have an inverse dependence on initiator concentration. This supports the conclusions obtained in the comparison of unimolecular and bimolecular initiations. Molecular weight measurement showed that higher initiator concentration yielded lower molecular weight polymers. This agrees with the rule for an ideal CRP system that molecular weight is inversely proportional to initiator concentration, which, again, implies that the prediction of molecular weight for a unimolecular system simply follows a general rule for CRP (Eq. 2.3).

Temperature effects were also examined for rates of polymerization and molecular weight development. In this work, increase of temperature led to an increase of the overall polymerization rate. This was ascribed to the fact that increasing temperature increases k_p and [P*](Eq. 4.6). Molecular weight appears to be independent of temperature. This may be

because the average number of monomer units added per polymer chain in each deactivation/activation cycle (RLPAC) is dependent on both propagation rate and deactivation rate; increasing temperature would increase both of these rates, so RLPAC didn't change significantly. In addition, at high conversion, M_n showed a plateau in values with respect to monomer conversion at higher temperatures. This was likely because an increase in temperature enhances the degree of self-initiation, which leads to higher proportions of new radicals. The newly initiated chains have shorter time to grow, thus giving lower molecular weight chains. Since M_n depends more on the actual number of chains, it thus shows an apparent plateau. In general, the temperature studies show that although it leads to faster polymerization rates, the control of the polymerization is poorer because of the effect that the higher levels of thermal initiation has on the polydispersity of the polymer products.

Initiators produced from different batches, with different molecular weight and polydispersity, showed no effect on polymerization rate and molecular weight. This indicates that initiator produced in different batches can be used in the same polymerization study since it won't bring significant errors to the kinetic study. The free monomer concentration in the high-molecular-weight initiator case would be lower; however, it appears this does not have a significant effect on the polymerization rates and "limiting" conversion. This suggests that the more significant factor in dictating the final conversion levels in different experiments is the concentration of initiator added.

The experimental molecular weights of the unimolecular systems under different reaction conditions have been compared to the theoretical values calculated by Eq.2.3, where molecular weight is proportional to the ratio of monomer consumption to initiator

concentration. The ratios of theoretical values to experimental data were shown to be close to 1. This demonstrates that the degree of control by unimolecular systems approaches that of an ideal CRP system. One of the important reasons for the deviation of theoretical values from experimental data may be the effect of self-initiation, which leads to a higher number of initiated chains than that generated by the original initiation, and thus a lower molecular weight. This is most noticeable for polymer produced at higher temperatures, which showed the largest deviation from ideal, especially at higher conversion. This would suggest that NMRP has a limited optimal range of temperature where one can achieve reasonable rates along with good control of MW.

5.2 Recommendation for future work

Although a considerable amount of experimental work has already been conducted on the kinetics of unimolecular NMRP, there is still a lot that can be done to improve the understanding of the polymerization system and bring it closer to industrial production.

1) The differences between bimolecular and unimolecular systems with respect to polymerization rate at high conversion have been studied. A tentative interpretation is centered on the reduction of thermal initiation. The propagating radical concentration of a bimolecular system can be proved to be intrinsically higher than that of a unimolecular system. However, the assumption for the propagating radical concentration in a bimolecular system still needs to be confirmed by experiments. This can be realized by measurement of free nitroxide concentration and calculation of polymerization rate from a conversion vs. time plot. The measurement of nitroxide concentration can be carried out

by ESR (Electronic Spin Resistance) or by fluorescence spectroscopy (if the nitroxide is fluorescent).

2) Effect of temperature is rather complex. It is not only related to the propagation rate constant (k_p), but also related to the deactivation/activation process ($K=k_d/k_a$; [X*], [M]). This can be seen in a recent simulation[8] on styrene polymerization for both bimolecular and unimolecular systems over a range of reaction conditions. The experimental data in this thesis should be compared with the newly developed model, and further explore the role of each factor contribution when temperature changes.

3) Besides initiator and temperature, there are other factors affecting the experimental results, such as those involved in GPC analysis. The measured polymer molecular weight values may vary with the different calibration methods. For example, a recent comparison between the conventional calibration and multi-detector calibration has shown that conventional calibration gave a broader MWD and notably lower values for M_n; the M_w values were almost the same for both calibration methods. This may be because conventional calibration is better for assessing concentrations and molecular weight values of low molecular weight polymers. Multi-detector techniques are dependent on primary measurement of molecular weight from light scattering. Low angle light scattering responses are very weak for low MW polymers. This leads to considerable uncertainty in the values measured for the MW of low MW fractions. Conventional calibration methods simply depend on the retention volume of a particular fraction to determine its MW and so the degree of uncertainty in measuring MW of a low MW fraction is likely less.

4) The predicted molecular weights by Eq. (2.3) are shown to be always higher than the corresponding experimental values, and this was ascribed to thermal initiation which generates extra new growing chains besides those originally initiated by alkoxyamine. Since each growing chain can be as considered containing a nitroxide end, the predicted molecular weights would be closer to the experimental values if $[I]_0$ could be replaced by the actual TEMPO concentration in Eq. (2.3). The measurement of [TEMPO] was discussed earlier. It is likely that the actual P_n-ON concentration is less than that calculated because it is unlikely that all chains in the initiator batch are capped with a nitroxyl radical. In order to get a more accurate idea for [P_n-ON], the actual concentration of TEMPO units / mass of initiator should be determined by an end group analysis method.

References

References for Chapter 2

1. Kharasch, M. S.; Jensen, E. V.; Urry, W. H., Addition of carbon tetrachloride and chloroform to olefins. Science 1945, 102 (2640), 128.

2. Asscher, M.; Vofsi, D., Chlorine-activation by redox-transfer. 3. Abnormal addition of chloroform to olefins. Journal of the Chemical Society 1963 (AUG), 3921-3927.

3. Szwarc, M.; Levy, M.; Milkovich, R., Polymerization initiated by electron transfer to monomer- A new method of formation of block polymers. Journal of the American Chemical Society 1956, 78 (11), 2656-2657.

4. Penczek, S.; Matyjaszewski, K., Ions and macroesters in living cationic polymerization of THF. Journal of Polymer Science Part C-Polymer Symposium 1976, (56), 255-269.

5. Otsu, T.; Yoshida, M., Role of initiator-transfer agent-terminator (iniferter) in radical polymerizations-polymer design by organic disulfides as iniferters. Macromolekulare Chemie-Rapid Communications 1982, 3 (2), 127-132.

6. Solomon, D.H.; Rizzardo, E.; Cacioli, P., U.S. Patent 4,581,429 (1986)

7. Moad, C. L.; Moad, G.; Rizzardo, E.; Thang, S. H., Chain transfer activity of omega-unsaturated methyl methacrylate oligomers. Macromolecules 1996, 29 (24), 7717-7726.

8. Georges, M. K.; Veregin, R. P. N.; Kazmaier, P. M.; Hamer, G. K., Narrow molecular-weight resins by a free-radical polymerization process. Macromolecules 1993, 26 (11), 2987-2988.

9. Wang, J. S.; Matyjaszewski, K., Controlled living radical polymerization – Atom transfer radical polymerization in the presence of transition-metal complexes. Journal of the American Chemical Society 1995, 117 (20), 5614-5615.

10. Rizzardo, E.; Chong, Y. K.; Evans, R. A.; Moad, G.; Thang, S. H., Control of polymer structure by chain transfer processes. Macromolecular Symposia 1996, 111, 1-11.

11. Fischer, H., The persistent radical effect in controlled radical polymerizations. Journal of Polymer Science Part A-Polymer Chemistry 1999, 37 (13), 1885-1901.

12. Fischer, H., The persistent radical effect: A principle for selective radical reactions and

living radical polymerizations. Chemical Reviews 2001, 101 (12), 3581-3610.

13. Odian, G. "Radical Chain Polymerization", In *Principles of Polymerization*; John Wiley & Sons, Inc.: Hoboken, New Jersey, 2004.

14. Matyjaszewski, K. "General Concepts and History of Living Radical Polymerization", In *Handbook of Radical Polymerization*; Matyjaszewski, K., Davis, T. P., eds. John Wiley and Sons, Inc.: Hoboken, 2002; pp 383-386.

15. Mardare, D.; Matyjaszewski, K., Thermal polymerization of styrene in the presence of stable radicals and inhibitors. Abstracts of Papers of the American Chemical Society 1994, 207, 267.

16. Fukuda, T.; Goto, A.; Ohno, K., Mechanisms and kinetics of living radical polymerizations. Macromolecular Rapid Communications 2000, 21 (4), 151-165.

17. Nabifar, A. (2007) "Investigations of kinetic aspects in nitroxide-mediated radical polymerization of styrene" M.A.Sc. Thesis, Department of Chemical Engineering, University of Waterloo, Waterloo, Canada

18. Wang, Y. X.; Hutchinson, R. A.; Cunningham, M. E., A semi-batch process for nitroxide mediated radical polymerization. Macromolecular Materials and Engineering 2005, 290 (4), 230-241.

19. Matyjaszewski, K.; Spanswick, J., Controlled/living radical polymerization. Materials Today 2005, 8(3), 26-33.

20. Matyjaszewski, K.; Shipp, D. A.; McMurtry, G. P.; Gaynor, S. G.; Pakula, T., Simple and effective one-pot synthesis of (meth)acrylic block copolymers through atom transfer radical polymerization. Journal of Polymer Science Part A-Polymer Chemistry 2000, 38 (11), 2023-2031.

21. McCarthy, P; Tsurersky N.V.; Matyjaszewski, K. Grafting chromatographic stationary phase substrates by atom transfer radical polymerization. American Chemical Society Symposium 2006, 944, 252-268.

22. Richard, R. E.; Schwarz, M.; Ranade, S.; Chan, K.; Matyjaszewski, K.; Sumerlin, B., Evaluation of acrylate-based block copolymers prepared by atom transfer radical polymerization as matrices for paclitaxel delivery from coronary stents. Abstracts of Papers of the American Chemical Society 2005, 230, 693.

23. Burguiere, C.; Pascual, S.; Coutin, B.; Polton, A.; Tardi, M.; Charleux, B.; Matyjaszewski, K.; Vairon, J. P., Amphiphilic block copolymers prepared via controlled radical polymerization as surfactants for emulsion polymerization. Macromolecular Symposia

2000, 150, 39-44.

24. Auschra, C.; Eckstein, E.; Knischka, R.; Pirrung, F.; Harbers, P., Controlled polymers for pigment dispersants. Journal of European Coatings 2004, 26, 31–32.

25. Auschra, C.; Eckstein, E.; Knischka, R.; Pirrung, F.; Harbers, P., Tailor-made additives controlled polymer structures enhance performance. Journal of European Coatings 2005, 156, 8, 62–63.

26. Lindner, S.M.; Thelakkat, M., Nanostructures of n-type organic semiconductor in a p-type matrix via self-assembly of block copolymers. Macromolecules 2004, 37, 8832–8835.

27. Jabbar, R.; Graffe, A.; Lessard, B.; Maric, M., Nitroxide-mediated synthesis of styrenic-based segmented and tapered block copolymers using poly(lactide)-functionalized TEMPO macromediators. Journal of Applied Polymer Science 2008, 109 (5), 3185-3195.

28. Matsugi, T.; Kojoh, S.; Kawahara, N.; Matsuo, S.; Kaneko, H.; Kashiwa, N., Synthesis and morphology polyethylene-block-poly(methyl metallocene methacrylate) catalysis through the combination of living radical polymerization. Journal of Polymer Science Part A-Polymer Chemistry 2003, 41 (24), 3965-3973.

29. Mohajery, S.; Rahmani, S.; Entezami, A. A., Synthesis of functional polyethylene graft copolymers by nitroxide-mediated living radical polymerization. Polymers for Advanced Technologies 2008, 19 (11), 1528-1535.

30. Matyjaszewski, K.; Ziegler, M. J.; Arehart, S. V.; Greszta, D.; Pakula, T., Gradient copolymers by atom transfer radical copolymerization. Journal of Physical Organic Chemistry 2000, 13 (12), 775-786.

31. Lessard, B.; Maric, M., Nitroxide-Mediated Synthesis of Poly(poly(ethylene glycol) acrylate) (PPEGA) Comb-Like Homopolymers and Block Copolymers. Macromolecules 2008, 41 (21), 7870-7880.

32. Pakula, T.; Zhang, Y.; Matyjaszewski, K.; Lee, H.I.; Boerner, H,; Qin, S.H.; Berry, G.C., Molecular brushes as super-soft elastomers. Polymer 2006, 47 (20), 7198-7206.

33. Lewis, G. T.; Cohen, Y., Controlled Nitroxide-Mediated Styrene Surface Graft Polymerization with Atmospheric Plasma Surface Activation. Langmuir 2008, 24 (22), 13102-13112.

34. Zhao, B.; Brittain, W. J., Polymer brushes: surface-immobilized macromolecules. Progress in Polymer Science 2000, 25 (5), 677-710.

35. Lee, S. B.; Russell, A. J.; Matyjaszewski, K., ATRP synthesis of amphiphilic random, gradient, and block copolymers of 2-(dimethylamino)ethyl methacrylate and n-butyl methacrylate in aqueous media. Biomacromolecules 2003, 4 (5), 1386-1393.

36. Heredia, K. L.; Bontempo, D.; Ly, T.; Byers, J. T.; Halstenberg, S.; Maynard, H. D., In situ preparation of protein - "Smart" polymer conjugates with retention of bioactivity. Journal of the American Chemical Society 2005, 127 (48), 16955-16960.

37. Goto, A.; Fukuda, T., Kinetic study on nitroxide-mediated free radical polymerization of tert-butyl acrylate. Macromolecules 1999, 32 (3), 618-623.

38. Harth, E.; Fan, W. H.; van Horn, B.; Hawker, C. J.; Waymouth, R., New routes to functionalized polymers: Elucidation of a novel strategy for chain end functionalization and the development of improved third generation nitroxides. Abstracts of Papers of the American Chemical Society 2001, 221, U363-U363.

39. Yoshida, E., Photo-living radical polymerization of methyl methacrylate by a nitroxide mediator. Colloid and Polymer Science 2008, 286 (14-15), 1663-1666.

40. Keoshkerian, B.; Georges, M.; Quinlan, M.; Veregin, R.; Goodbrand, B., Polyacrylates and polydienes to high conversion by a stable free radical polymerization process: Use of reducing agents. Macromolecules 1998, 31 (21), 7559-7561.

41. Matyjaszewski, K.; Gaynor, S. G.; Greszta, D.; Mardare, D.; Shigemoto, T.; Wang, J. S. In unimolecular and bimolecular exchange-reactions in controlled radical polymerization. Macromolecular Symposia1995; 95, 217-231.

42. Benoit, D.; Grimaldi, S.; Robin, S.; Finet, J. P.; Tordo, P.; Gnanou, Y., Kinetics and mechanism of controlled free-radical polymerization of styrene and n-butyl acrylate in the presence of an acyclic beta-phosphonylated nitroxide. Journal of the American Chemical Society 2000, 122 (25), 5929-5939.

43. Mayo, F. R., Dimerization of styrene. Journal of the American Chemical Society 1968, 90 (5), 1289-1295.

44. Moad, G.; Rizzardo, E.; Solomon, D. H., The reaction of acyl peroxides with 2,2,6,6-tetramethylpiperidinyl-1-oxy. Tetrahedron Letters 1981, 22 (12), 1165-1168.

45. Georges, M. K.; Hamer, G.; Szkurhan, A. R.; Kazemedah, A.; Li, J., Stable free radical polymerization process - Initiation mechanisms with benzoyl peroxide and various nitroxides. Abstracts of Papers of the American Chemical Society 2002, 224, 625.

46. Cunningham, M. F.; Ng, D. C. T.; Milton, S. G.; Keoshkerian, B., Low temperature TEMPO-mediated styrene polymerization in miniemulsion. Journal of Polymer Science

Part A-Polymer Chemistry 2006, 44 (1), 232-242.

47. Nabifar, A.; McManus, N. T.; Vivaldo-Lima, E.; Lona, L. M. F.; Penlidis, A., A replicated investigation of nitroxide-mediated radical polymerization of styrene over a range of reaction conditions. Canadian Journal of Chemical Engineering 2008, 86 (5), 879-892.

48. Rizzardo, E.; Solomon, D. H., New method for investigating the mechanism of initiation of radical polymerization. Polymer Bulletin 1979, 1 (8), 529-534.

49. Hawker, C. J., Molecular-weight control by a living free-radical polymerization process. Journal of the American Chemical Society 1994, 116 (24), 11185-11186.

50. Zink, M. O.; Kramer, A.; Nesvadba, P., New alkoxyamines from the addition of free radicals to nitrones or nitroso compounds as initiators for living free radical polymerization. Macromolecules 2000, 33 (21), 8106-8108.

51. Li, I. Q.; Howell, B. A.; Dineen, M. T.; Kastl, P. E.; Lyons, J. W.; Meunier, D. M.; Smith, P. B.; Priddy, D. B., Block copolymer preparation using sequential normal/living radical polymerization techniques. Macromolecules 1997, 30 (18), 5195-5199.

52. Jahn, U.; Hartmann, P., Electron transfer-induced sequential transformations of malonates by the ferrocenium ion. Chemical Communications 1998, 2, 209-210.

53. Matyjaszewski, K.; Woodworth, B. E.; Zhang, X.; Gaynor, S. G.; Metzner, Z., Simple and efficient synthesis of various alkoxyamines for stable free radical polymerization. Macromolecules 1998, 31 (17), 5955-5957.

54. Catala, J. M.; Bubel, F.; Hammouch, S. O., Living radical polymerization – kinetic results. Macromolecules 1995, 28 (24), 8441-8443.

55. Greszta, D.; Matyjaszewski, K., Living radical polymerization: Kinetic results - Comments. Macromolecules 1996, 29 (15), 5239-5240.

56. Greszta, D.; Matyjaszewski, K., Mechanism of controlled/"living" radical polymerization of styrene in the presence of nitroxyl radicals. Kinetics and simulations. Macromolecules 1996, 29 (24), 7661-7670.

57. Fukuda, T.; Terauchi, T.; Goto, A.; Ohno, K.; Tsujii, Y.; Miyamoto, T.; Kobatake, S.; Yamada, B., Mechanisms and kinetics of nitroxide-controlled free radical polymerization. Macromolecules 1996, 29 (20), 6393-6398.

58. Fischer, H., The persistent radical effect in "living" radical polymerization. Macromolecules 1997, 30 (19), 5666-5672.

59. Hawker, C. J.; Barclay, G. G.; Orellana, A.; Dao, J.; Devonport, W., Initiating systems for nitroxide-mediated "living" free radical polymerizations: Synthesis and evaluation. Macromolecules 1996, 29 (16), 5245-5254.

References for Chapter 3

1. McIsaac, S. L.; Dube, M. A.; Gao, J.; Penlidis, A. Experimental procedures for ampoule polymerization. (1993) Internal Report, Department of Chemical Engineering, University of Waterloo, Waterloo, Canada.

2. Fukuda, T.; Terauchi, T.; Goto, A.; Ohno, K.; Tsujii, Y.; Miyamoto, T.; Kobatake, S.; Yamada, B., Mechanisms and kinetics of nitroxide-controlled free radical polymerization. Macromolecules 1996, 29 (20), 6393-6398.

3. Hawker, C. J.; Barclay, G. G.; Orellana, A.; Dao, J.; Devonport, W., Initiating systems for nitroxide-mediated "living" free radical polymerizations: Synthesis and evaluation. Macromolecules 1996, 29 (16), 5245-5254.

4. Mori, S.; Barth, H.G. Size Exclusion Chromatography, Springer: New York, 1999.

5. Scorah, M. J., McManus, N. T., Penlidis, A. (2004) GPC operating manual. Internal Report, Department of Chemical Engineering, University of Waterloo, Waterloo, Canada.

References for Chapter 4

1. Moad, G.; Rizzardo, E.; Solomon, D. H., The reaction of acyl peroxides with 2.2.6.6.-tetramethylpiperidinyl-1-oxy. Tetrahedron Letters 1981, 22 (12), 1165-1168.

2. Hawker, C. J.; Barclay, G. G.; Orellana, A.; Dao, J.; Devonport, W., Initiating systems for nitroxide-mediated "living" free radical polymerizations: Synthesis and evaluation. Macromolecules 1996, 29 (16), 5245-5254.

3. Nabifar, A. (2007) "Investigations of kinetic aspects in nitroxide-mediated radical polymerization of styrene" M.A.Sc Thesis, Department of Chemical Engineering, University of Waterloo, Waterloo, Canada

4. Catala, J. M.; Bubel, F.; Hammouch, S. O., Living radical polymerization – kinetic results. Macromolecules 1995, 28 (24), 8441-8443.

5. Greszta, D.; Matyjaszewski, K., Mechanism of controlled/"living" radical polymerization of styrene in the presence of nitroxyl radicals. Kinetics and simulations. Macromolecules

1996, 29 (24), 7661-7670.

6. Fukuda, T.; Terauchi, T.; Goto, A.; Ohno, K.; Tsujii, Y.; Miyamoto, T.; Kobatake, S.; Yamada, B., Mechanisms and kinetics of nitroxide-controlled free radical polymerization. Macromolecules 1996, 29 (20), 6393-6398.

7. Roa-Luna, M.; Diaz-Barber, M. P.; Vivaldo-Lima E., Assessing the importance of diffusion-controlled effects on polymerization rate and molecular weight development in nitroxide-mediated radical polymerization of styrene. Journal of Macromolecular Science Part A – Pure and Applied Chemistry 2007, 44(2), 193-203.

8. Veregin, R. P. N.; Odell, P. G.; Michalak, L. M.; Georges, M. K., The pivotal role of excess nitroxide radical in living free radical polymerizations with narrow polydispersity. Macromolecules 1996, 29 (8), 2746-2754.

9. Nabifar, A.; McManus, N. T.; Vivaldo-Lima, E.; Lona, L. M. F.; Penlidis, A., A replicated investigation of nitroxide-mediated radical polymerization of styrene over a range of reaction conditions. Canadian Journal of Chemical Engineering 2008, 86 (5), 879-892.

10. Fischer, H., The persistent radical effect in controlled radical polymerizations. Journal of Polymer Science Part A-Polymer Chemistry 1999, 37 (13), 1885-1901.

11. Becer, C. R.; Paulus, R. M.; Hoogenboom, R.; Schubert, U. S., Optimization of the nitroxide mediated radical polymerization conditions for styrene and tert-butyl acrylate in an automated parallel synthesizer. Journal of Polymer Science Part A-Polymer Chemistry 2006, 44 (21), 6202-6213.

12. Wang, Y.; Hutchinson, R. A.; Cunningham, M. F., A semi-batch process for nitroxide mediated radical polymerization. Macromolecular Materials and Engineering 2005, 290, 230-241.

References for Chapter 5

1. Hawker, C. J.; Barclay, G. G.; Orellana, A.; Dao, J.; Devonport, W., Initiating systems for nitroxide-mediated "living" free radical polymerizations: Synthesis and evaluation. Macromolecules 1996, 29 (16), 5245-5254.

2. Nabifar, A., Investigations of kinetic aspects in nitroxide-mediated radical polymerization of styrene. Master Thesis 2007, Department of Chemical Engineering, University of Waterloo, Waterloo, Canada

3. Greszta, D.; Matyjaszewski, K., Mechanism of controlled/"living" radical polymerization

of styrene in the presence of nitroxyl radicals. Kinetics and simulations. Macromolecules 1996, 29 (24), 7661-7670.

4. Fukuda, T.; Goto, A.; Ohno, K., Mechanisms and kinetics of living radical polymerizations. Macromolecular Rapid Communications 2000, 21 (4), 151-165.

5. Moad, G.; Rizzardo, E.; Solomon, D. H., The reaction of acyl peroxides with 2,2,6,6-tetramethylpiperidinyl-1-oxy. Tetrahedron Letters 1981, 22 (12), 1165-1168.

6. Georges, M. K.; Hamer, G.; Szkurhan, A. R.; Kazemedah, A.; Li, J., Stable free radical polymerization process - Initiation mechanisms with benzoyl peroxide and various nitroxides. Abstracts of Papers of the American Chemical Society 2002, 224, 625.

7. Cunningham, M. F.; Ng, D. C. T.; Milton, S. G.; Keoshkerian, B., Low temperature TEMPO-mediated styrene polymerization in miniemulsion. Journal of Polymer Science Part A-Polymer Chemistry 2006, 44 (1), 232-242.

8. Belincanta-Ximenes, J.; Mesa, P. V. R.; Lona, L. M. F.; Vivaldo-Lima, E.; McManus, N. T.; Penlidis, A., Simulation of styrene polymerization by monomolecular and bimolecular nitroxide-mediated radical processes over a range of reaction conditions. Macromolecular Theory and Simulations 2007, 16 (2), 194-208.

Appendices

Appendix A – Tables of Raw Data

Table A. 1 Raw data for Exp. 1

Sample	Time(h)	Conversion (%)	Mn	Mw	Mw/Mn
1	1.00	6.11	3,922	4,423	1.13
2	3.13	22.31	7,801	8,585	1.10
3	6.00	42.52	12,070	13,047	1.08
4	8.05	50.72	14,052	15,222	1.08
5	10.00	52.53	15,706	16,747	1.07
6	15.18	67.87	18,582	19,826	1.07
7	20.00	76.55	20,338	21,613	1.06
8	25.22	81.70	20,301	22,357	1.10
9	30.07	81.96	21,262	22,944	1.08
10	40.00	84.68	21,608	23,840	1.10
11	50.00	87.29	23,028	25,349	1.10

Table A. 2 Raw data for Exp. 2

	Time(h)	Conversion (%)	Mn	Mw	Mw/Mn
1	1.00	30.83	9,680	10,267	1.06
2	3.00	58.98	17,921	19,218	1.07
3	6.00	69.85	19,566	21,039	1.08
4	8.00	75.76	18,980	21,684	1.14
5	10.00	80.58	19,992	22,423	1.12
6	15.00	82.12	19,063	23,019	1.21
7	20.00	86.13	19,891	23,530	1.25
8	25.00	88.59	19,209	23,436	1.23
9	30.25	90.38	19,905	23,684	1.19
10	40.00	89.71	19,371	23,652	1.22
11	50.00	90.12	18,690	17,871	0.96

Table A. 3 Raw data for Exp. 3

	Time(h)	Conversion (%)	Mn	Mw	Mw / Mn
1	0.50	0.04	3,320	3,529	1.06
2	1.00	6.35	3,593	3,810	1.06
3	2.00	11.74	4,273	4,574	1.07
4	2.00	10.59	4,243	4,545	1.07
5	3.00	16.12	5,168	5,486	1.06
6	6.00	33.30	7,467	7,878	1.06
7	8.03	42.62	8,956	9,321	1.04
8	10.10	49.07	9,801	10,376	1.06
9	10.10	49.29	9,816	10,470	1.07
10	15.13	63.37	11,867	12,597	1.06
11	20.00	72.07	12,541	13,863	1.11
12	25.00	76.55	13,111	14,546	1.11
13	30.00	81.41	13,922	15,194	1.09
14	30.00	80.77	13,854	15,163	1.09
15	40.00	80.16	15,428	16,115	1.04
16	50.00	83.64	14,582	16,094	1.10
17	50.00	87.37	14,154	16,002	1.13
18	60.00	91.35	15,255	16,685	1.09

Table A. 4 Raw data for Exp. 4

	Time(h)	Conversion (%)	Mn	Mw	Mw/Mn
1	1.00	28.91	6,211	7,892	1.27
2	3.02	57.21	9,962	11,176	1.12
3	6.02	68.53	11,646	12,696	1.09
4	8.00	75.47	11,968	13,330	1.11
5	10.00	76.39	12,407	13,634	1.10
6	15.02	79.96	12,149	13,762	1.13
7	20.00	83.39	11,821	14,088	1.19
8	25.00	32.67	11,669	14,023	1.20
8'	25.00	84.39	12,674	14,300	1.13
9	30.25	50.74	11,736	14,033	1.20
10	40.00	86.53	11,884	14,236	1.20
11	50.02	87.78	11,223	14,176	1.26

Table A. 5 Raw data for Exp. 5

	Time(h)	Conversion (%)	Mn	Mw	Mw / Mn
1	0.5	6.34	7,406	7,852	1.06
2	1	11.24	8,653	9,382	1.08
3	3	25.65	11,552	13,316	1.15
4	6	42.10	17,315	18,661	1.08
5	8	51.55	16,714	20,173	1.21
6	10	54.46	20,277	22,504	1.11
7	10	55.19	20,831	22,866	1.10
8	15	64.35	21,679	24,882	1.15
9	20	77.49	23,025	26,142	1.14
10	25	75.12	23,614	27,061	1.15
11	30	82.00	25,115	28,196	1.12
12	40	84.82	24,638	28,672	1.16
13	50	86.84	26,624	29,468	1.11
14	60	84.78	26,072	29,811	1.14

Table A. 6 Raw data for Exp. 6

	Time(h)	Conversion (%)	Mn	Mw	Mw/Mn
1	0.5	19.81	10,249	11,506	1.12
2	1	25.84	13,057	14,666	1.12
3	2	50.34	17,898	19,986	1.12
4	3	52.68	19,798	22,516	1.14
5	6	71.49	20,935	25,758	1.23
6	8	78.51	20,903	26,794	1.28
7	10	81.27	22,721	27,304	1.20
8	15	83.05	21,487	27,909	1.30
9	15	82.51	24,047	28,383	1.18
10	20	84.94	22,825	28,094	1.23
11	25	85.06	22,244	28,181	1.27
12	30	86.95	20,980	28,428	1.36
13	40	76.21	22,166	28,294	1.28
14	50	85.39	17,802	28,097	1.58
15	50	88.27	21,016	28,374	1.35
16	60	86.75	20,214	28,220	1.40

Table A. 7 Raw data for Exp. 7

	Time(h)	Conversion%	Mn	Mw	Mw/Mn
1	0.50	1.04	6,672	7,004	1.05
2	1.00	5.76	7,421	7,841	1.06
3	3.00	19.78	9,552	10,087	1.06
4	6.00	41.27	12,248	12,993	1.06
5	8.00	47.46	12,733	13,701	1.08
6	10.00	48.84	12,804	14,149	1.11
7	15.00	65.03	13,327	15,271	1.15
8	21.33	70.62	13,002	15,115	1.16
9	25.00	79.79	15,184	16,976	1.12
10	25.00	75.65	16,272	17,319	1.06
11	30.00	78.45	15,422	17,348	1.12
12	40.00	83.96	16,547	17,880	1.08
13	50.02	83.86	15,899	17,997	1.13
14	50.02	81.90	16,990	18,266	1.08

Table A. 8 Raw data for Exp. 8

Sample	Time(h)	Conversion%	Mn	Mw	Mw/Mn
1	0.50	14.13	2,521	2,471	0.98
2	1.03	29.43	4,584	4,647	1.01
3	2.00	35.68	5,952	6,566	1.10
4	3.00	51.67	6,401	7,459	1.17
5	6.00	61.33	8,383	9,449	1.13
6	8.00	71.11	7,892	9,746	1.23
7	10.00	72.12	8,470	10,095	1.19
8	15.03	65.76	8,515	10,524	1.24
9	15.03	51.68	9,183	10,816	1.18
10	20.00	93.71	7,545	10,504	1.39
11	25.00	79.15	8,618	10,906	1.27
12	30.00	80.75	8,626	10,870	1.26
13	40.00	88.73	8,424	10,859	1.29
14	50.00	81.59	7,488	10,949	1.46
15	60.03	89.06	8,070	11,296	1.40

Table A. 9 Raw data for Exp. 9

Sample	Time (h)	Conversion (%)	Mn	Mw	Mw/Mn
1	0.5	14.39	5,547	6,000	1.08
2	1	24.34	8,057	8,585	1.07
3	3	50.04	13,183	14,811	1.12
4	6	73.19	15,629	18,283	1.17
5	8	77.77	16,498	19,323	1.17
6	10	78.98	16,784	19,886	1.18
7	20	82.72	17,492	20,937	1.20
8	25	82.45	17,046	19,601	1.15
9	40	91.25	16,627	20,397	1.23
10	50	92.12	18,347	21,719	1.18
11	60	90.14	17,529	21,241	1.21
12	70.01	93.49	16,431	20,896	1.27
13	80	85.59	15,285	20,925	1.37

Table A. 10 Raw data for Exp 10

Sample	Time(h)	Conversion (%)	Mn	Mw	Mw/Mn
1	1.00	9.88	3,228	3,591	1.11
2	3.13	25.19	6,156	6,733	1.09
3	6.00	39.85	9,242	9,947	1.08
4	8.05	48.41	10,831	11,464	1.06
5	10.00	56.12	12,035	12,775	1.06
6	15.18	68.56	14,235	15,252	1.07
7	20.00	72.52	15,713	16,935	1.08
8	25.22	77.48	15,475	16,875	1.09
9	30.07	91.05	16,046	16,809	1.05
10	40.00	80.04	16,197	17,896	1.10
11	50.00	85.89	16,426	18,077	1.10

Table A. 11 Raw data for Exp 1’

	Time(h)	Conversion (%)	Mn	Mw	Mw / Mn
1	30.02	81.07	21,770	22,943	1.05
1'	30.02	83.39	22,163	23,324	1.05
2	40.00	83.49	21,475	23,773	1.11
3	50.00	87.65	19,718	23,660	1.2
4	60.00	92.75	24,104	25,470	1.06

Table A. 12 Raw data for Exp 2'

	Time(h)	Conversion (%)	Mn	Mw	Mw / Mn
1	0.50	15.23	6,017	6,479	1.08
2	1.00	27.15	8,908	9,663	1.09
3	2.00	43.23	12,947	14,298	1.10
4	3.02	56.50	16,201	17,942	1.11
5	4.03	66.45	17,133	20,002	1.17
6	5.02	71.93	18,486	21,496	1.16
7	6.00	72.99	17,821	22,007	1.24
8	6.00	73.35	11,058	13,605	1.23

Table A. 13 Raw data for Exp 4'

	Time(h)	Conversion (%)	Mn	Mw	Mw / Mn
1	0.50	14.53	4,351	4,682	1.08
2	1.02	22.90	5,891	6,302	1.07
3	2.00	42.12	8,250	8,929	1.08
4	3.02	54.88	11,238	11,827	1.05
5	4.05	63.13	7,134	11,556	1.62
6	5.02	69.53	11,301	12,995	1.15
7	6.00	73.35	11,058	13,605	1.23

Table A. 14 Raw data for Exp 10'

	Time(h)	Conversion (%)	Mn	Mw	Mw / Mn
1	30.02	78.70	16,862	17,562	1.04
2	40.00	85.53	17,851	18,461	1.03
3	50.02	88.34	15,653	18,197	1.16
4	60.00	92.52	18,463	19,371	1.05

Appendix B – Complementary Figures

Table B. 1 Summary of figures

Effect	Mn(I)	T (°C)	Exp			Figure #
[I]	2000	120	1(1')	10(10')	3	
		140	2(2')	9	4(4')	Figures B.1-B.4
	6000	120	5	7		Figures B.5-B.8
		140	6	8		Figures B.9-B.12
		[I]				
T	2000	0.030	1(1')	2(2')		
		0.050	3	4(4')		Figures B.13-B16
	6000	0.030	5	6		Figures B.17-B.20
		0.050	7	8		Figures B.21-B.24
	T	[I]				
Mn(I)	120	0.030	1(1')	5		
		0.050	3	7		Figures B.25-B.28
	140	0.030	2(2')	6		Figures B.29-B.33
		0.050	4(4')	8		Figures B.34-B.37

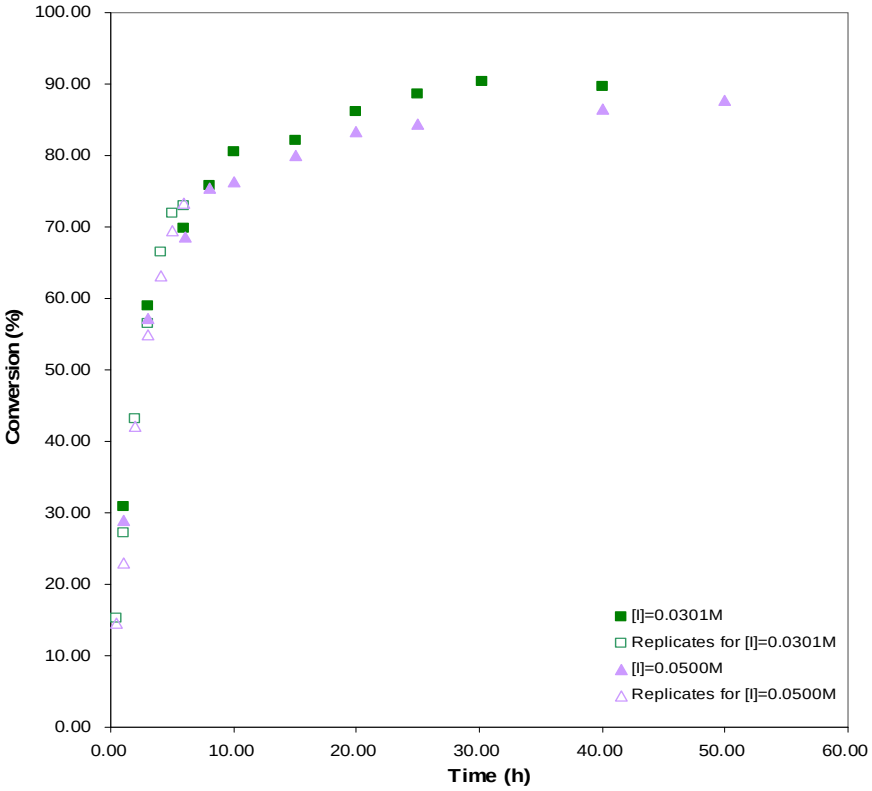

Figure B.1 Conversion vs. time plot, effect of initiator concentration, T=140º, M_n(I) = 2193 g/mol.

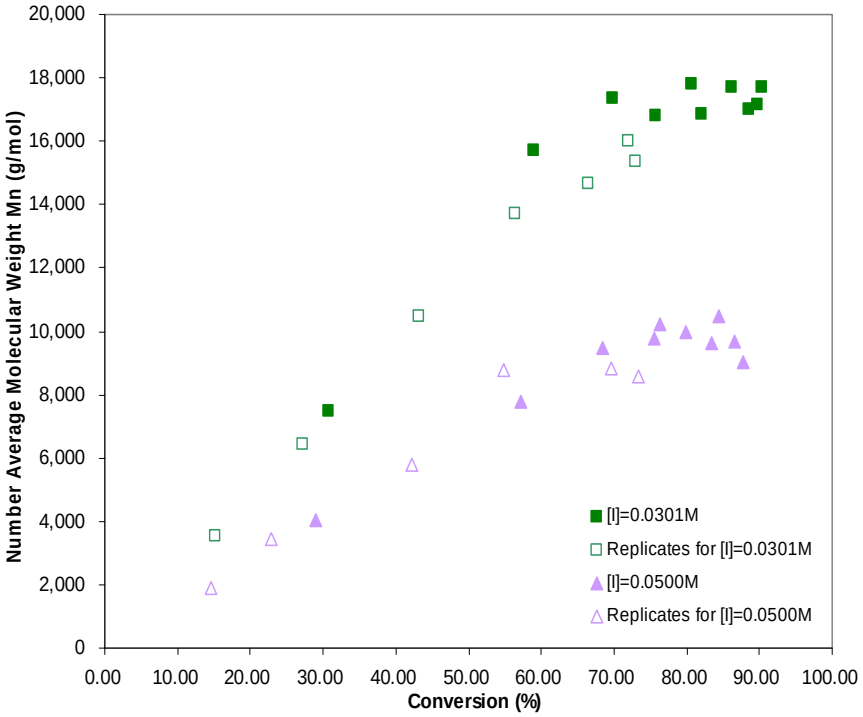

Figure B.2 M_n vs. conversion plot, effect of initiator concentration, T=140º, M_n(I) = 2193 g/mol.

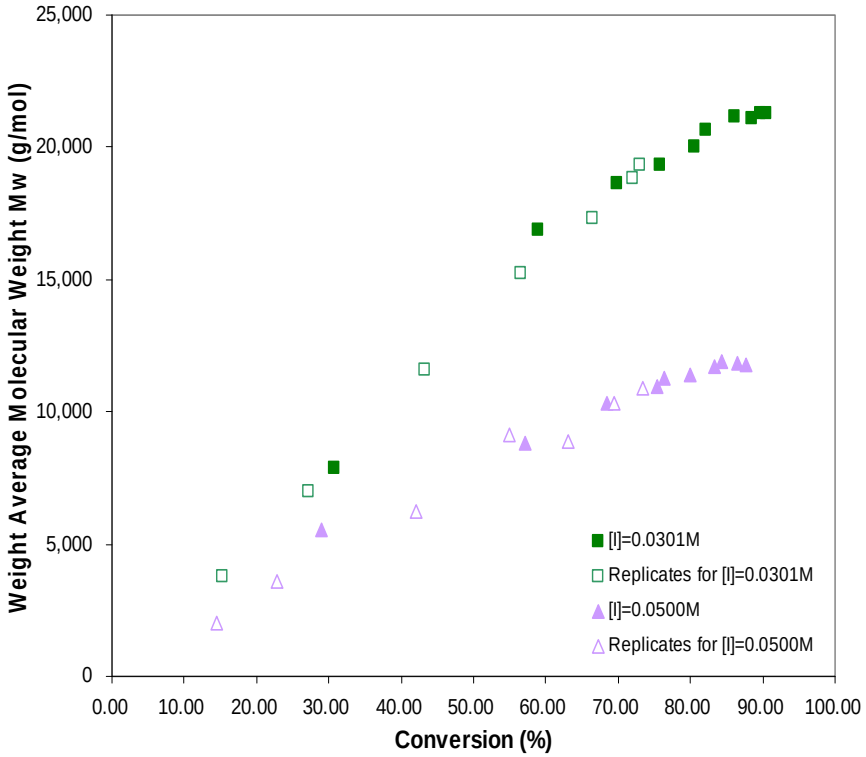

Figure B.3 M_w vs. conversion plot, effect of initiator concentration, T=140°, M_n(I) = 2193 g/mol.

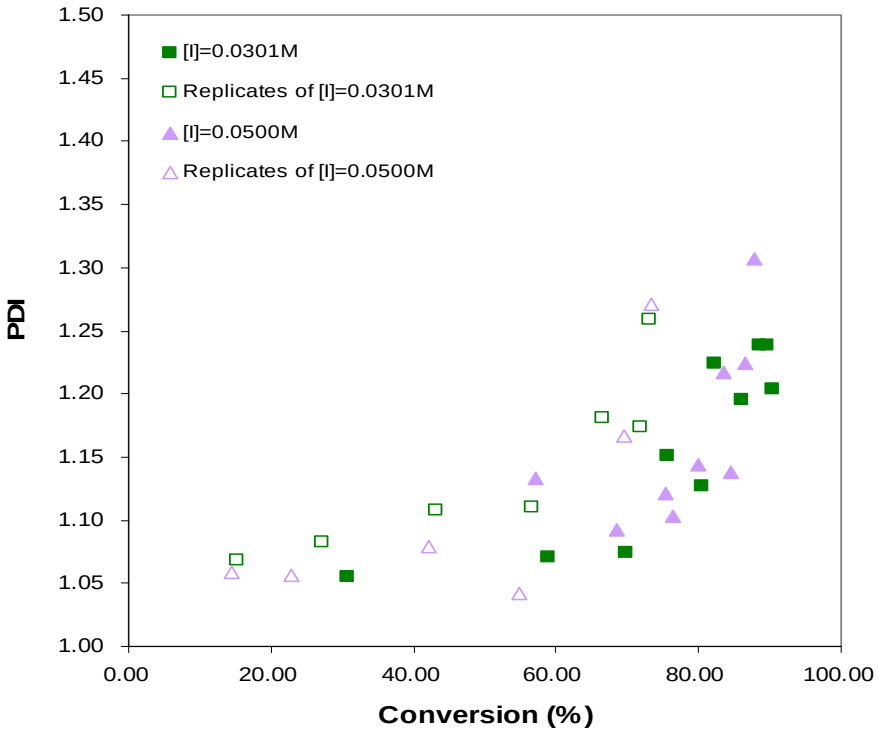

Figure B.4 PDI vs. conversion plot, effect of initiator concentration, T=140°, M_n(I) = 2193 g/mol.

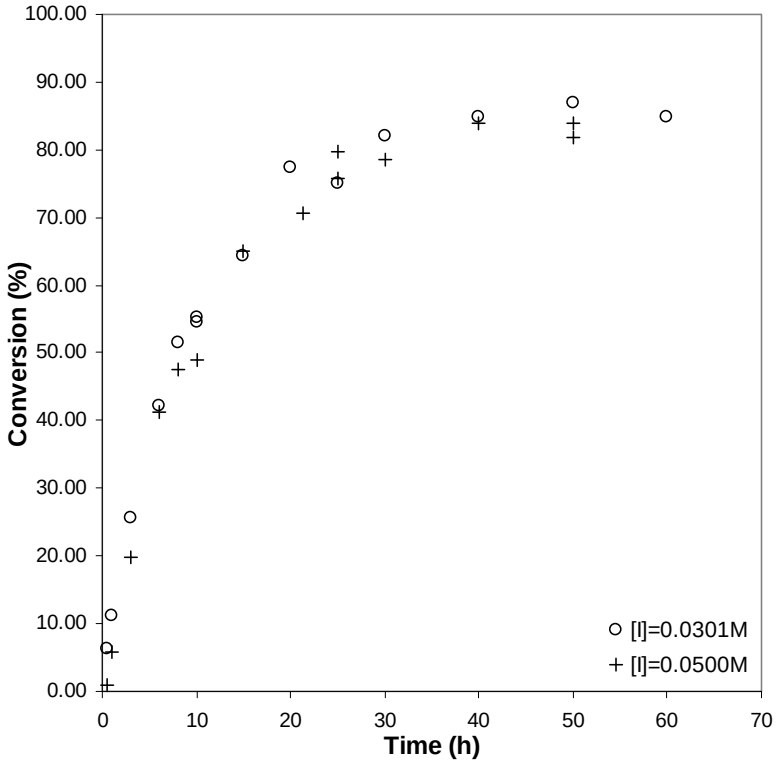

Figure B.5 Conversion vs. time plot, effect of initiator concentration, T=120º, M_n(I) = 6238 g/mol.

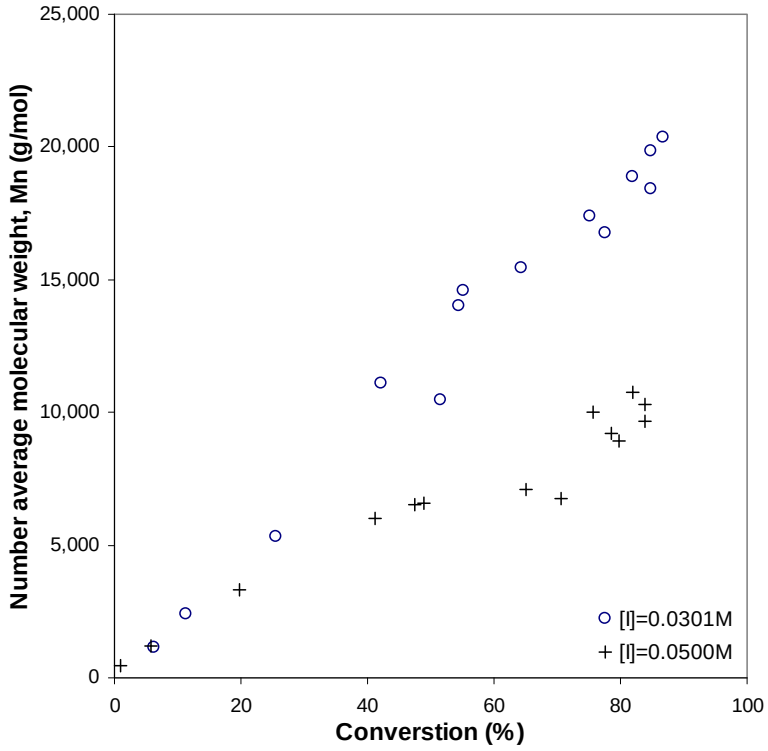

Figure B.6 M_n vs. conversion plot, effect of initiator concentration, T=120º, M_n(I) = 6238 g/mol.

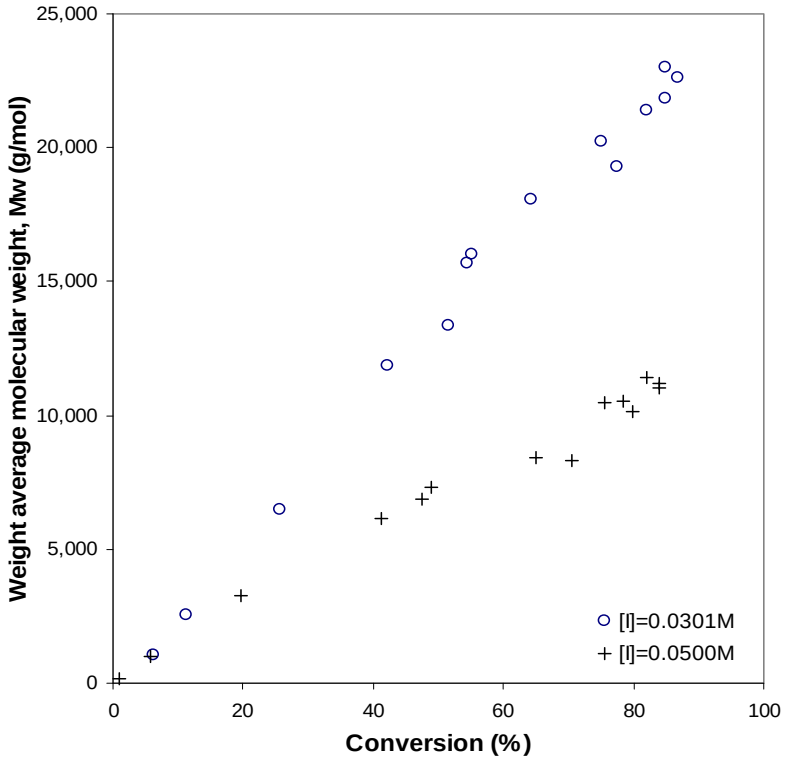

Figure B. 7 M_w vs. conversion plot, effect of initiator concentration, T=120º, M_n(I) = 6238 g/mol.

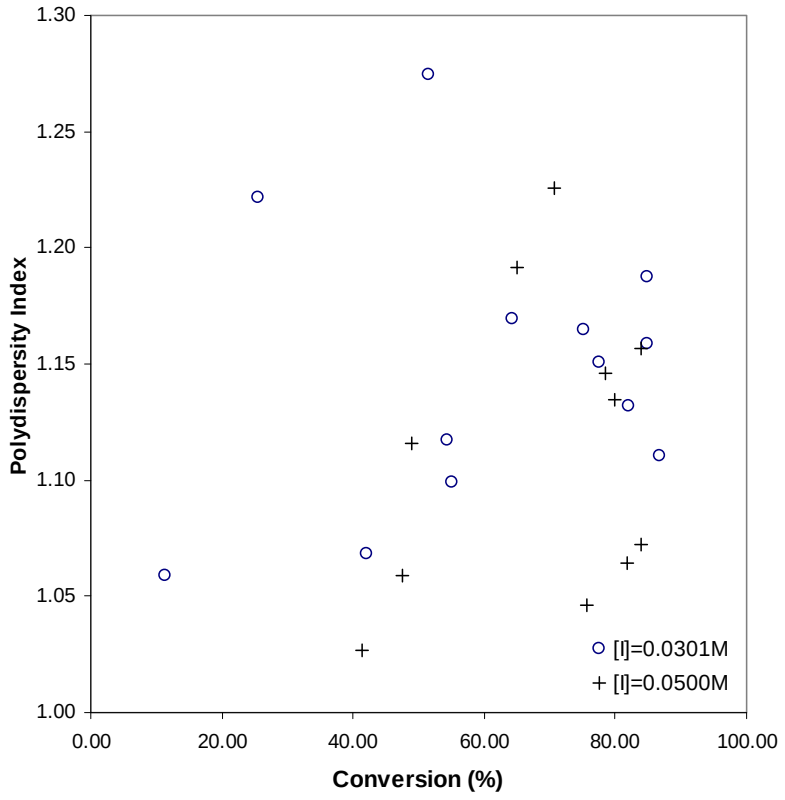

Figure B.8 Polydispersity vs. conversion plot, effect of initiator concentration, T=120º, M_n(I)= 6238g/mol.

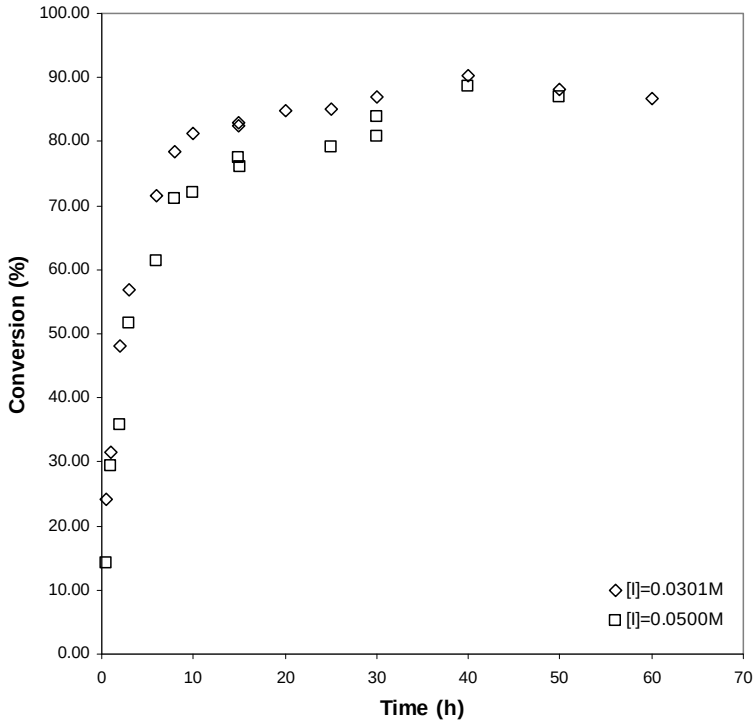

Figure B. 9 Conversion vs. time plot, effect of initiator concentration, T = 140°C, M_n(I) = 6238 g/mol

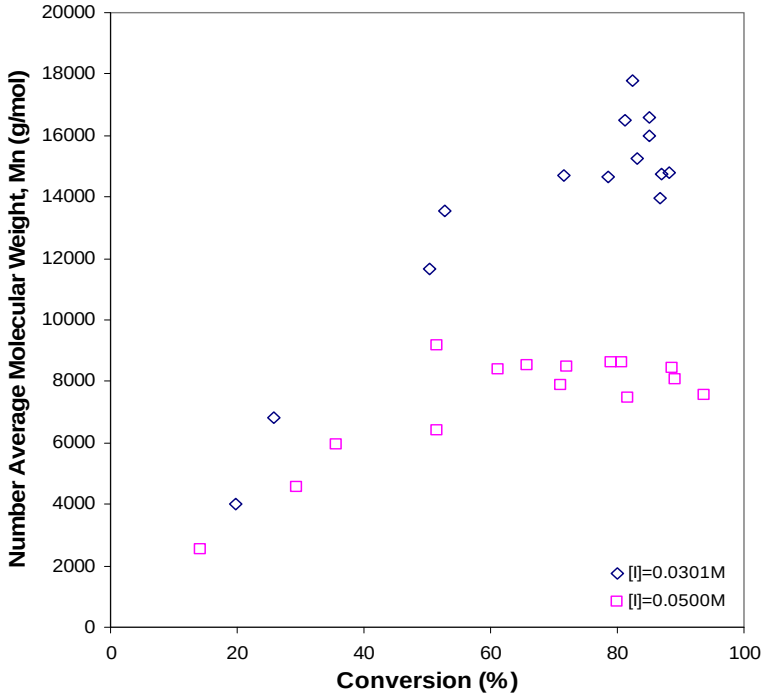

Figure B. 10 M_n vs. conversion plot, effect of initiator concentration, T = 140°C, M_n(I) = 6238 g/mol

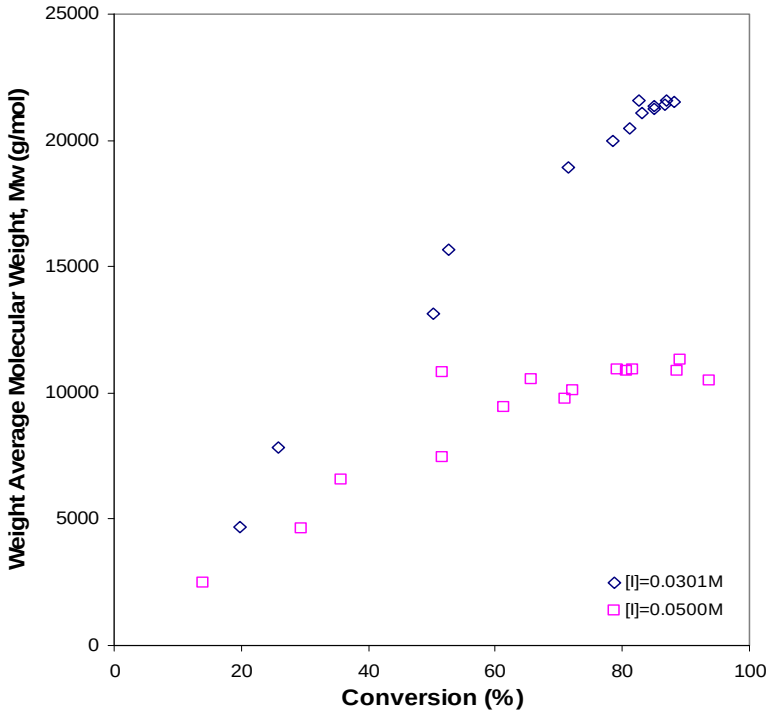

Figure B. 11 M_w vs. conversion plot, effect of initiator concentration, T = 140°C, M_n(I) = 6238 g/mol

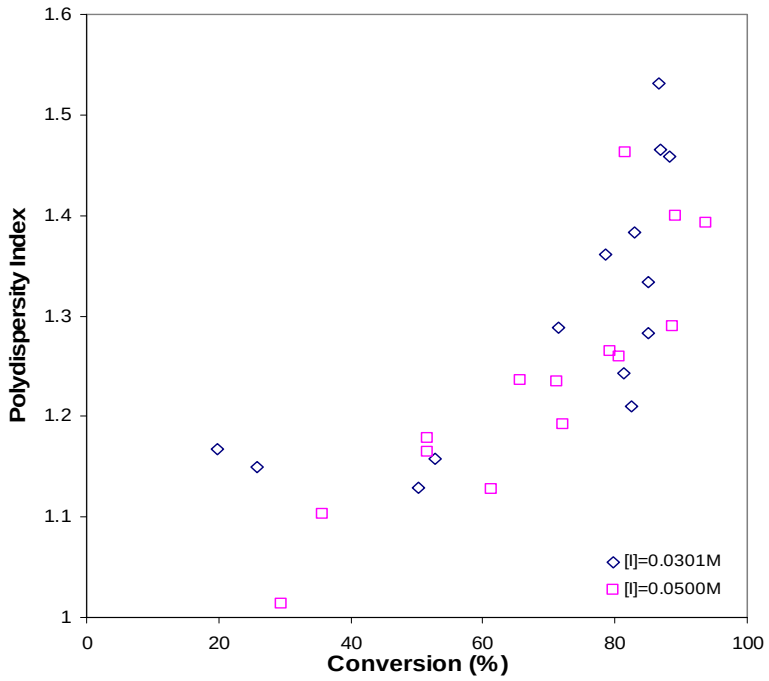

Figure B. 12 Polydispersity vs. conversion plot, effect of initiator concentration, T = 140°C, M_n(I) = 6238 g/mol

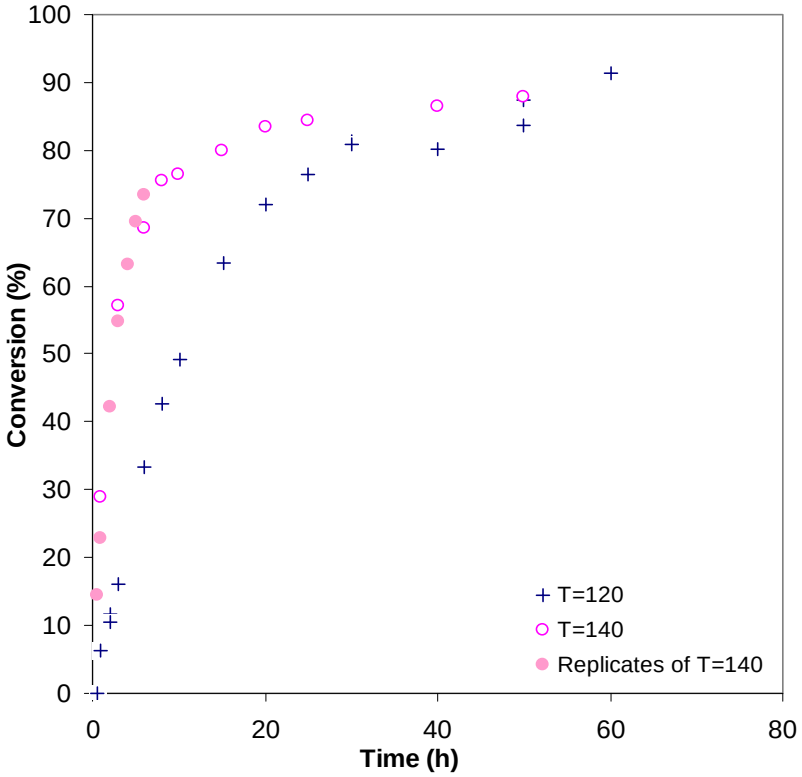

Figure B. 13 Conversion vs. time plot, effect of temperature, [I] = 0.0500 mol/l, M_n(I) = 2193 g/mol.

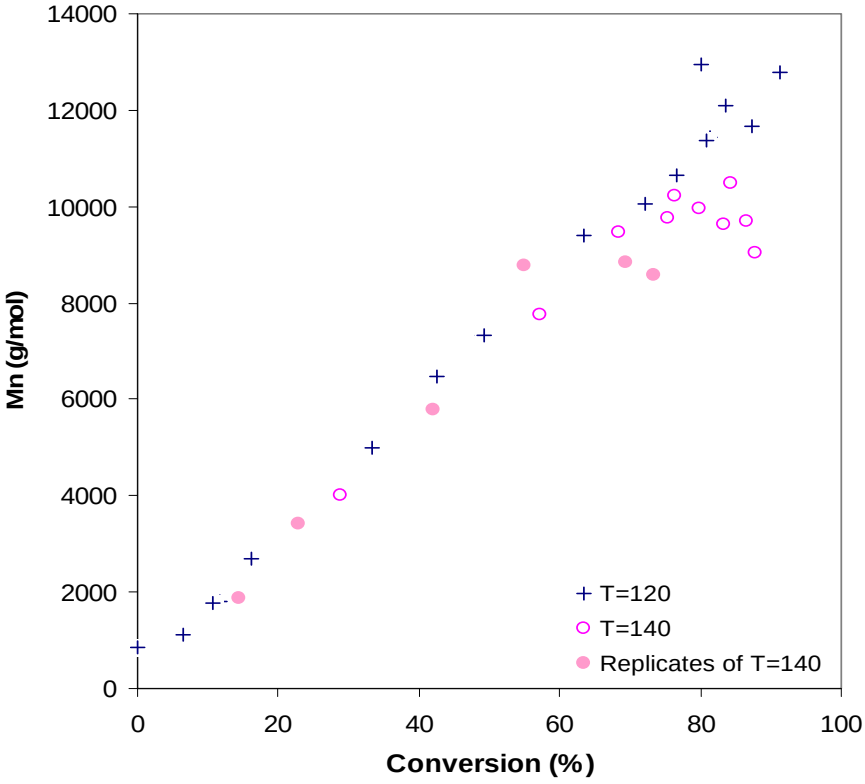

Figure B. 14 M_n vs. conversion plot, effect of temperature, [I] = 0.0500 mol/l, M_n(I) = 2193 g/mol .

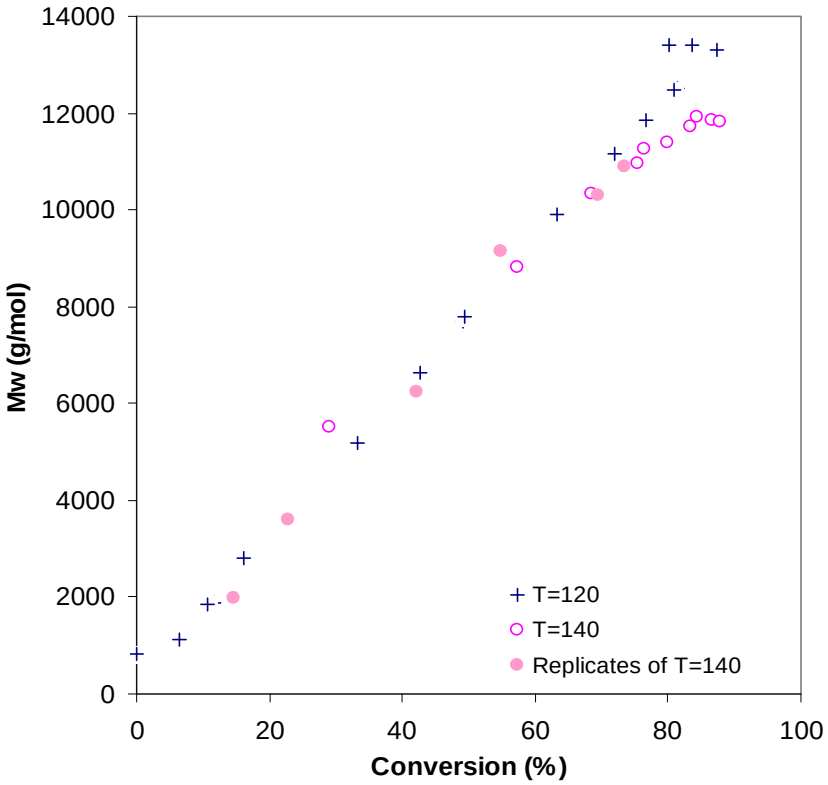

Figure B. 15 M_w vs. conversion plot, effect of temperature, [I] = 0.0500 mol/l, M_n(I) = 2193 g/mol.

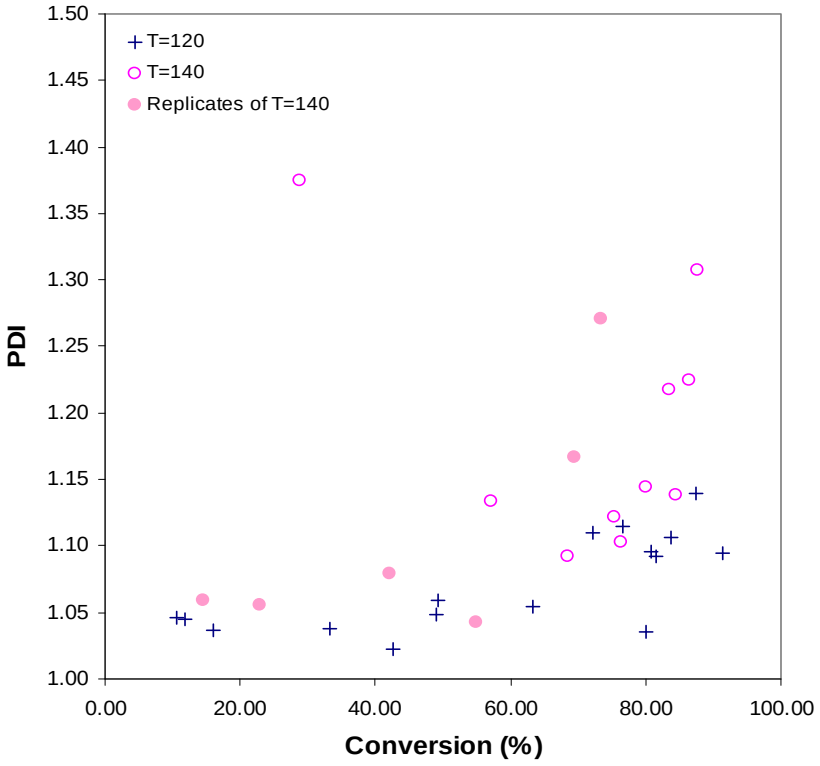

Figure B. 16 Polydispersity vs. conversion plot, effect of temperature, T = 120°, M_n(I) = 6238 g/mol.

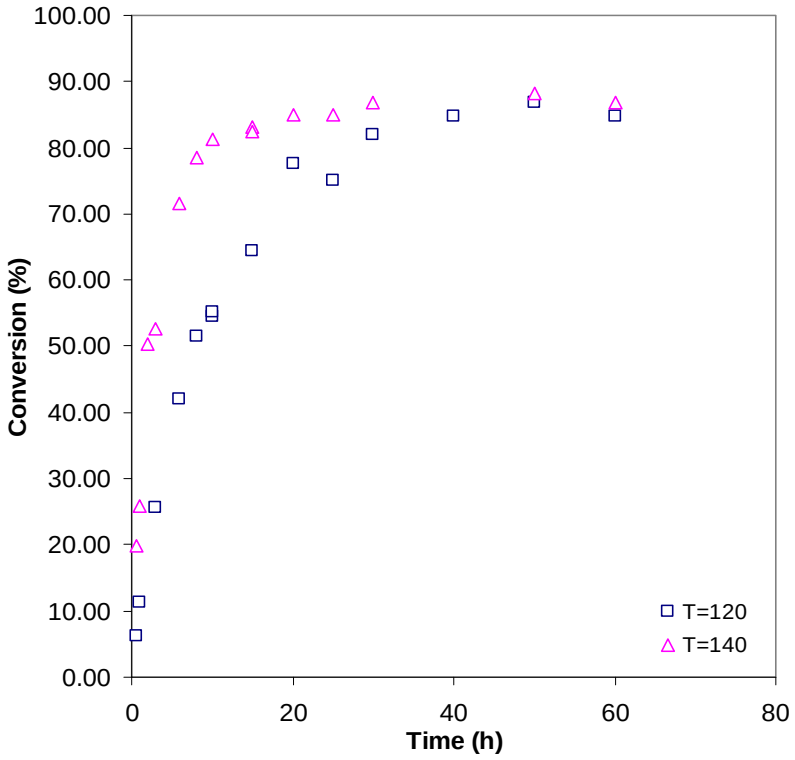

Figure B. 17 Conversion vs. time plot, effect of temperature. [I] = 0.0301mol/l, Mn(I) = 6238 g/mol.

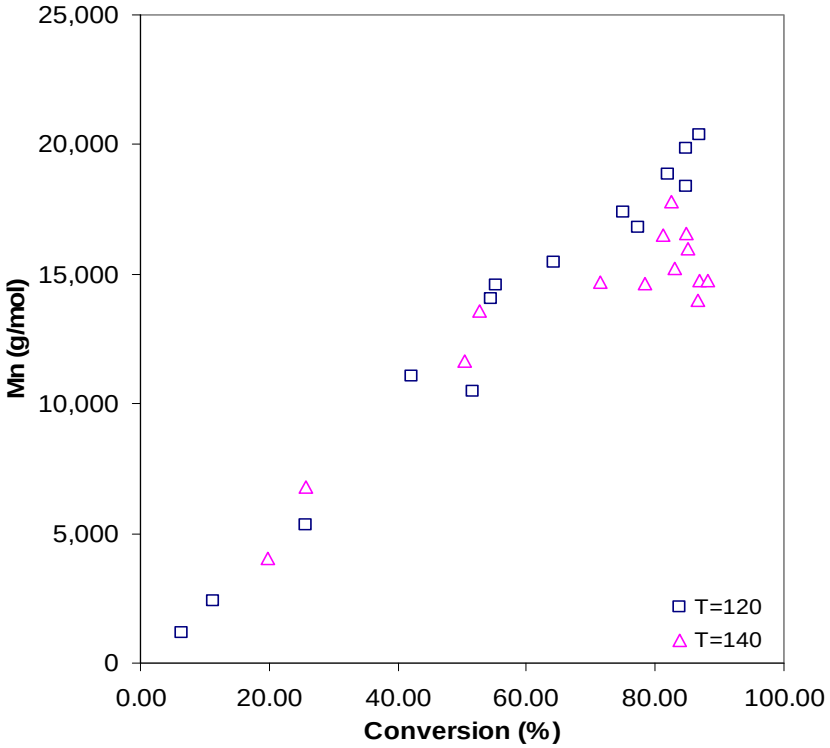

Figure B. 18 M_n vs. conversion plot, effect of temperature, [I] = 0.0301 mol/l, M_n(I) = 6238 g/mol .

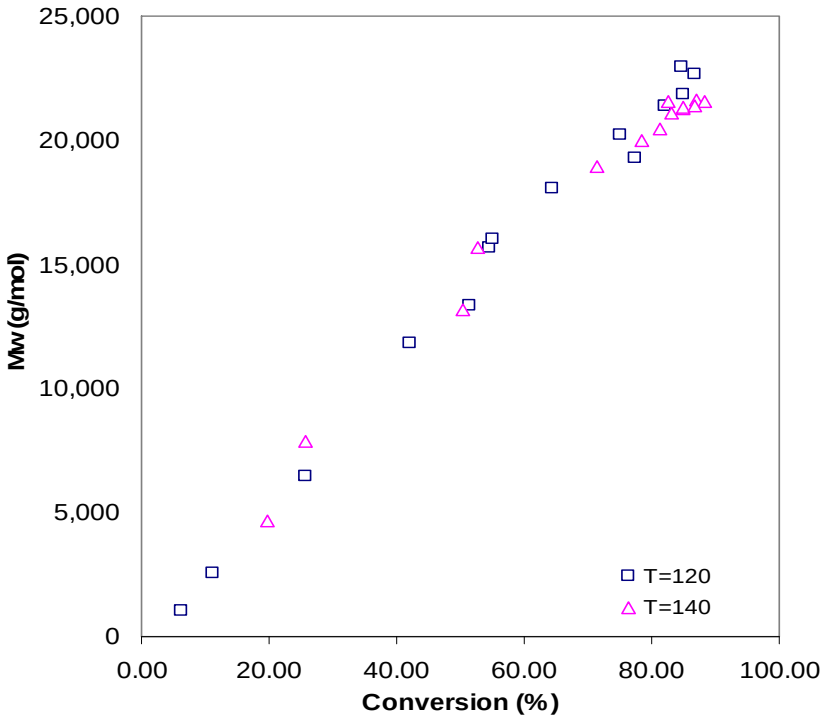

Figure B. 19 M_w vs. conversion plot, effect of temperature, [I] = 0.0301 mol/l, M_n(I) = 6238 g/mol.

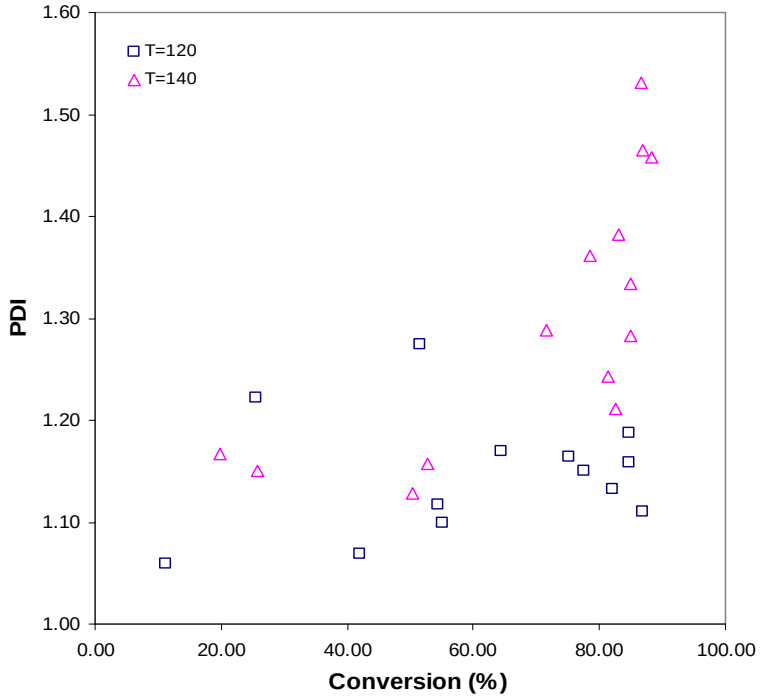

Figure B. 20 Polydispersity vs. conversion plot, effect of temperature, [I] = 0.0301 mol/l, M_n(I) = 6238 g/mol.

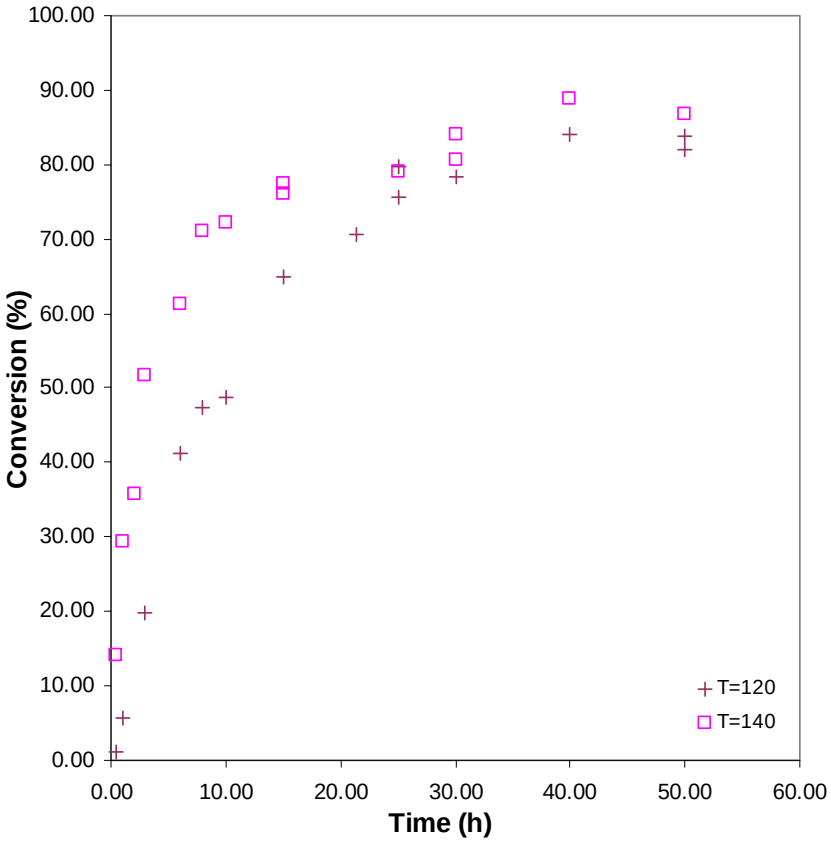

Figure B. 21 Conversion vs. time plot, effect of temperature, [I] = 0.0500 mol/l, M_n(I) = 6238 g/mol

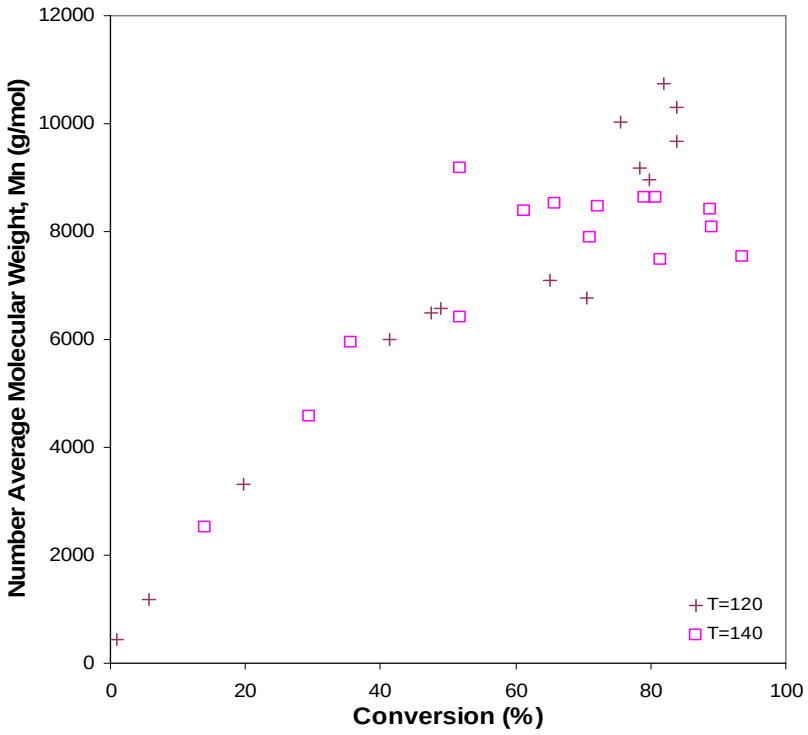

Figure B. 22 M_n vs. conversion plot, effect of temperature, [I] = 0.0500 mol/l, M_n(I) = 6238 g/mol

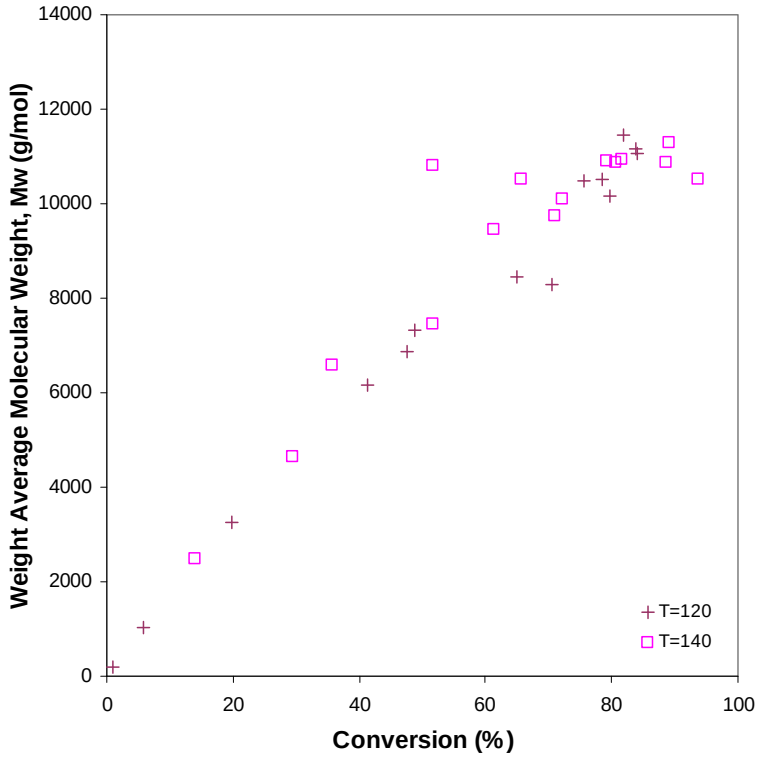

Figure B. 23 M_w vs. conversion plot. Effect of temperature. [I]=0.0500M, M_n(I)=6238g/mol

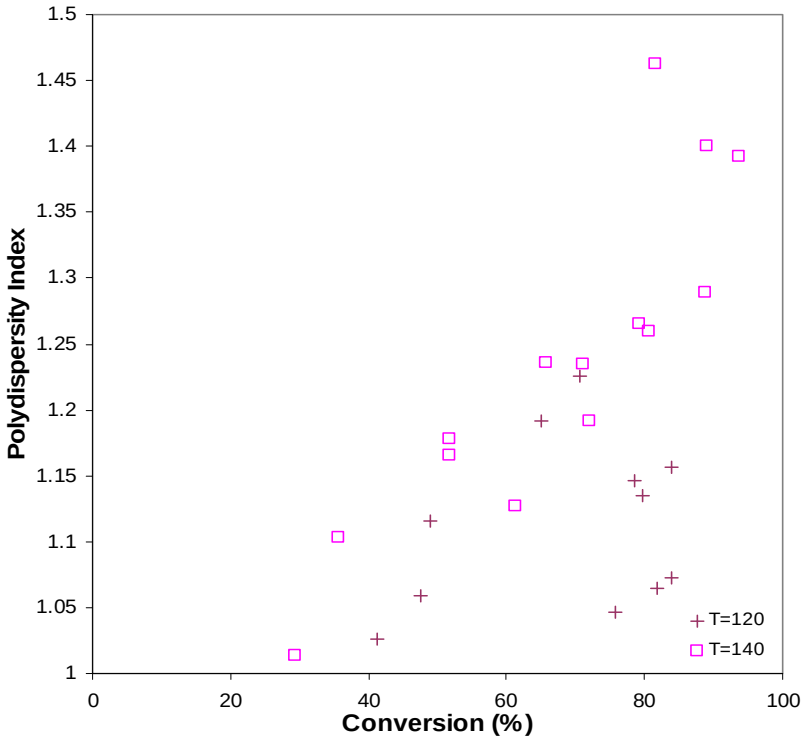

Figure B. 24 PDI vs. conversion plot. Effect of temperature. [I]=0.0500M, M_n(I)=6238g/mol

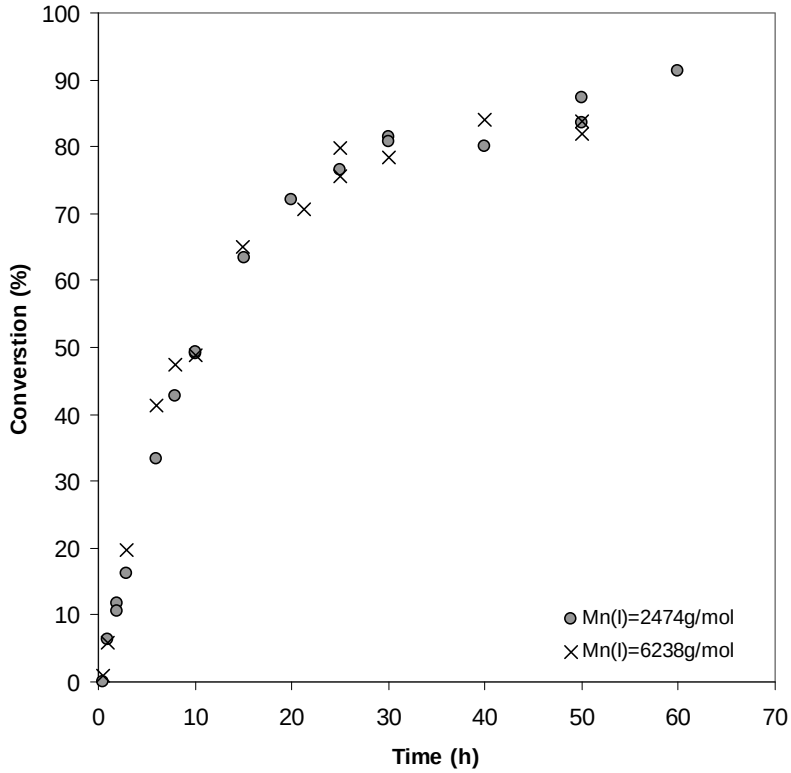

Figure B. 25 Conversion vs. time plot, effect of initiator molecular weight, [I] = 0.0500 mol/l, T = 120ºC.

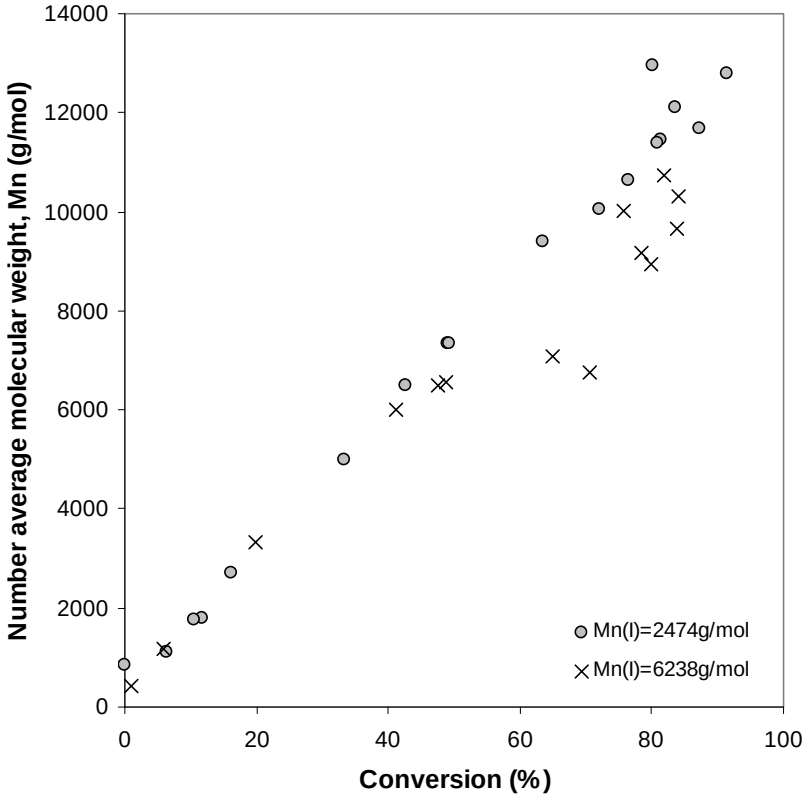

Figure B. 26 M_n vs. conversion plot, effect of initiator molecular weight, [I] = 0.0500 mol/l, T = 120ºC .

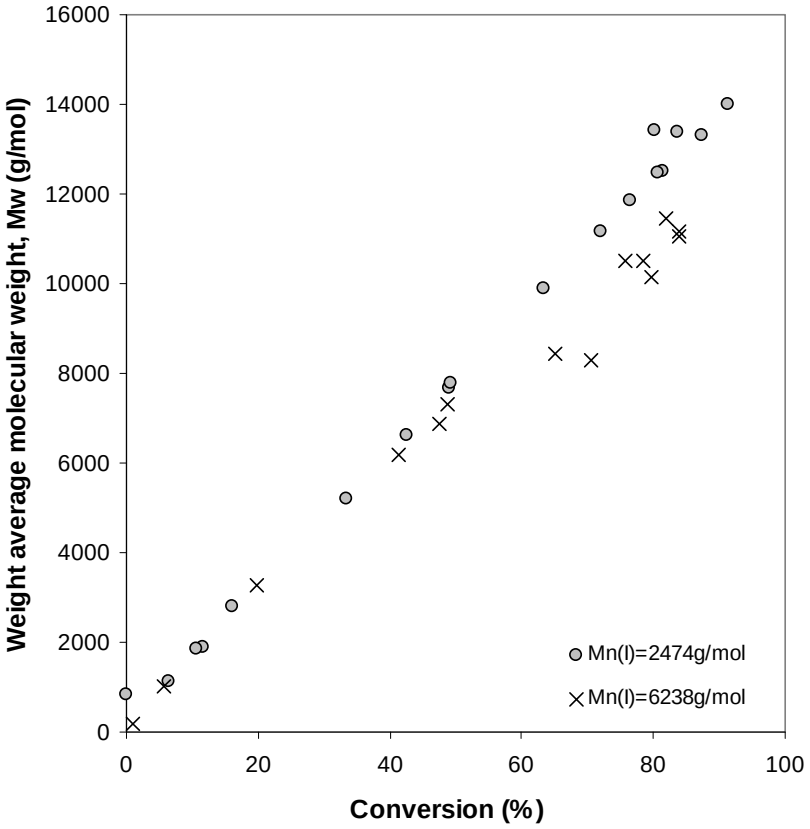

Figure B. 27 M_w vs. conversion plot, effect of initiator molecular weight, [I] = 0.0500 mol/l, T = 120ºC.

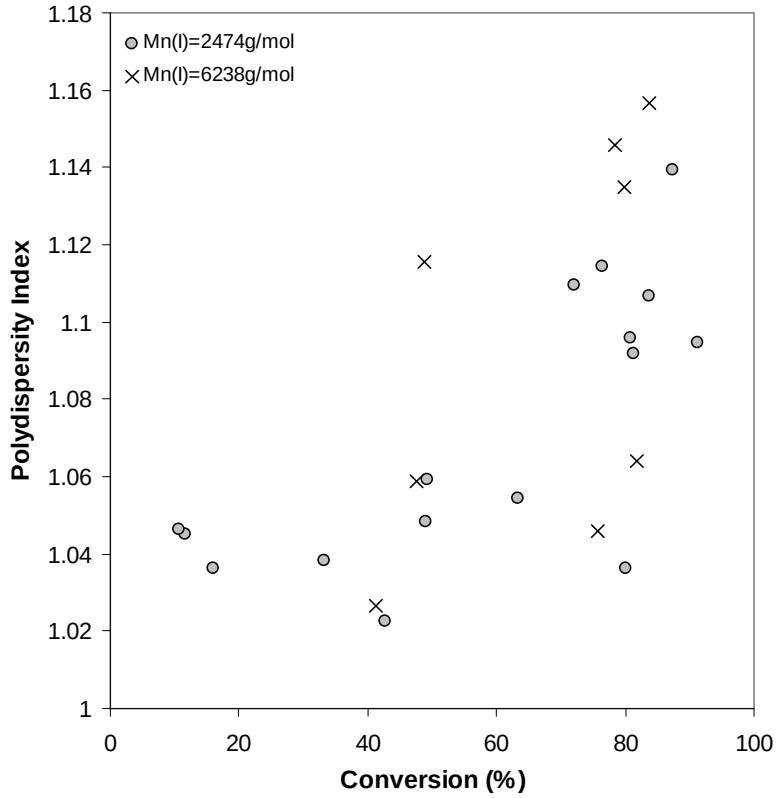

Figure B. 28 Polydispersity vs. conversion plot, effect of molecular weight, [I] = 0.0500 mol/l, T = 120ºC.

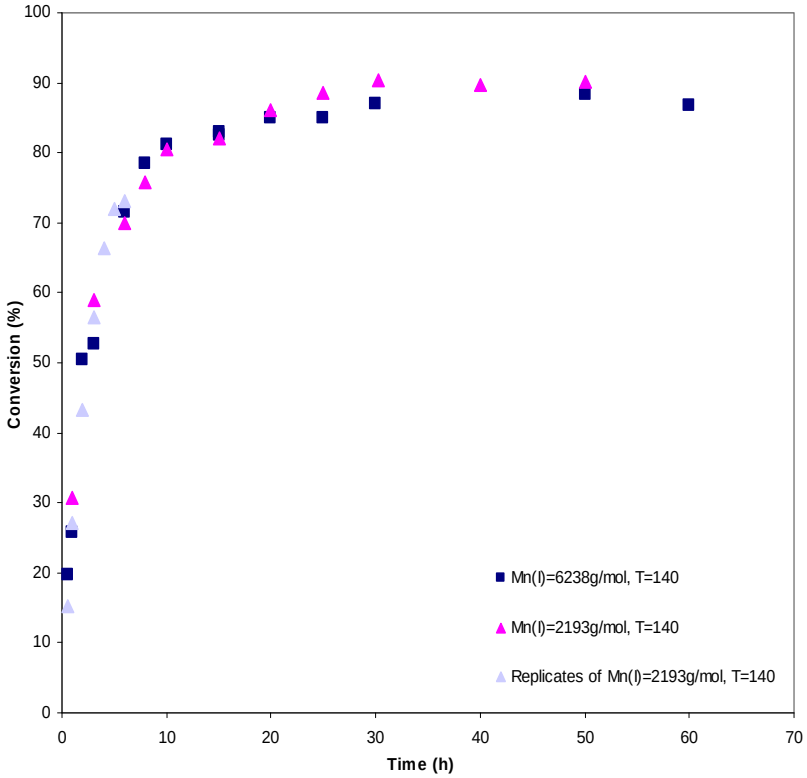

Figure B. 29 Conversion vs. time plot, effect of initiator molecular weight, [I] = 0.0301 mol/l, T = 140ºC.

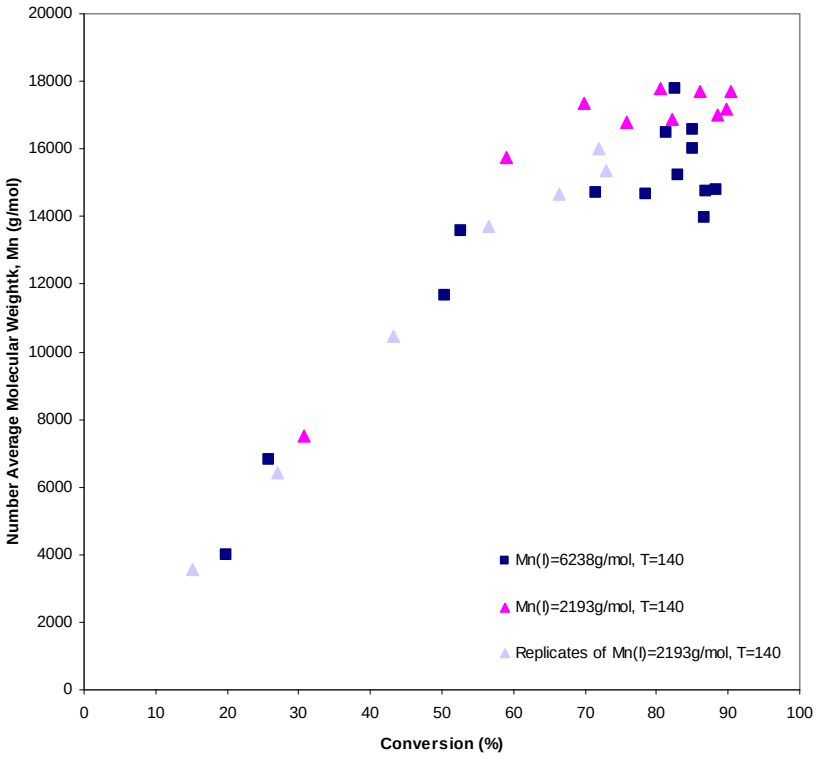

Figure B. 30 M_n vs. conversion plot, effect of initiator molecular weight, [I] = 0.0301 mol/l, T = 140ºC.

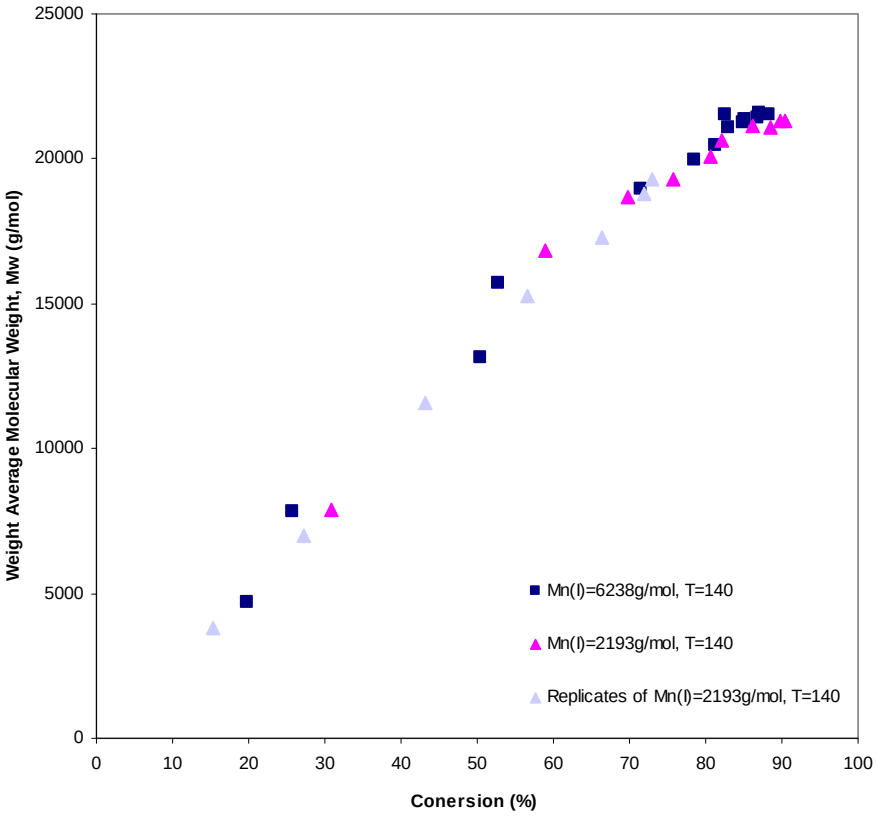

Figure B. 31 M_w vs. conversion plot, effect of initiator molecular weight, [I] = 0.0301 mol/l, T = 140°C.

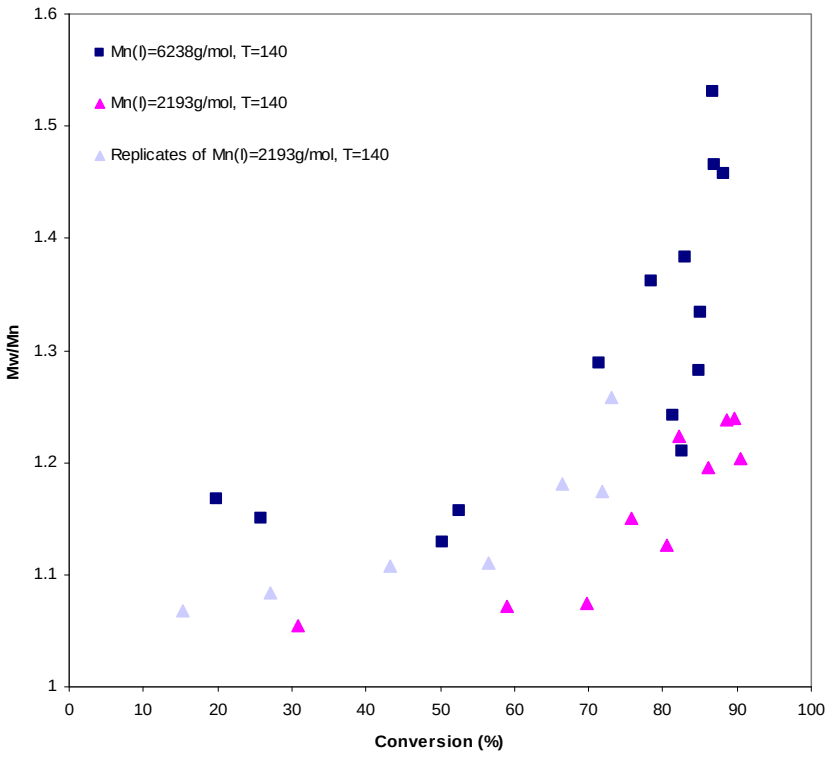

Figure B. 32 Polydispersity vs. conversion plot, effect of initiator molecular weight, [I] = 0.0301 mol/l, T = 140°C.

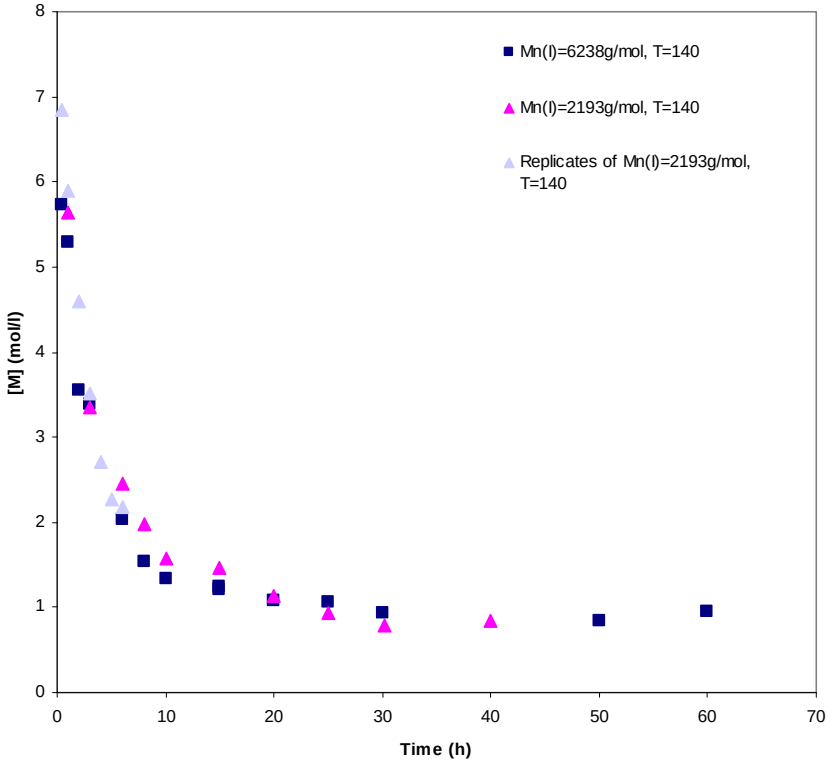

Figure B. 33 [M] vs. time plot, effect of initiator molecular weight, [I] = 0.0301 mol/l, T = 140°C

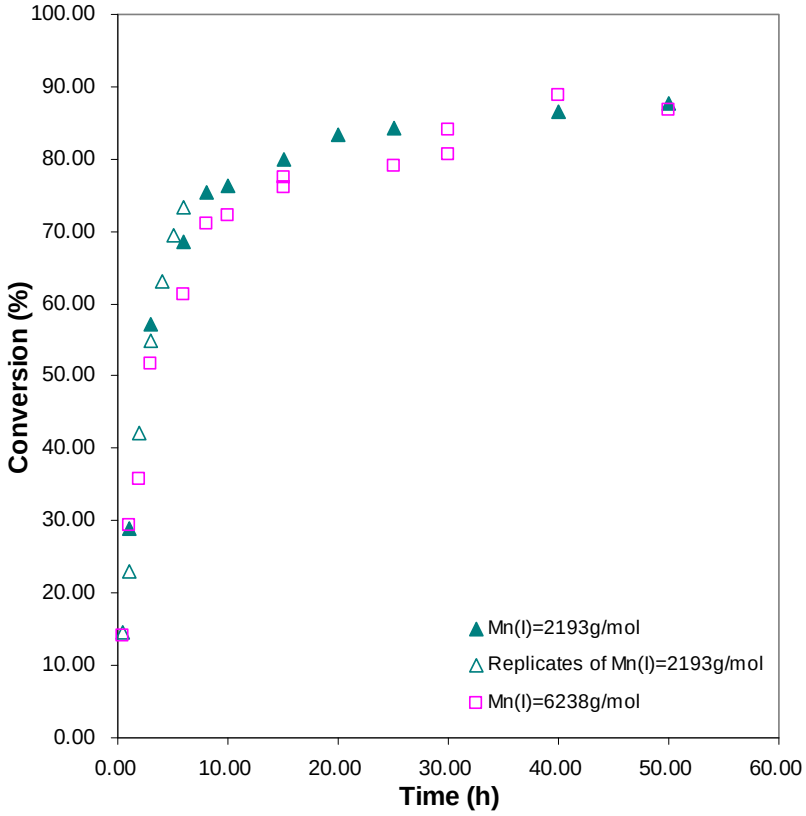

Figure B. 34 Conversion vs. time plot, effect of initiator molecular weight, [I] = 0.0500 mol/l, T = 140°C.

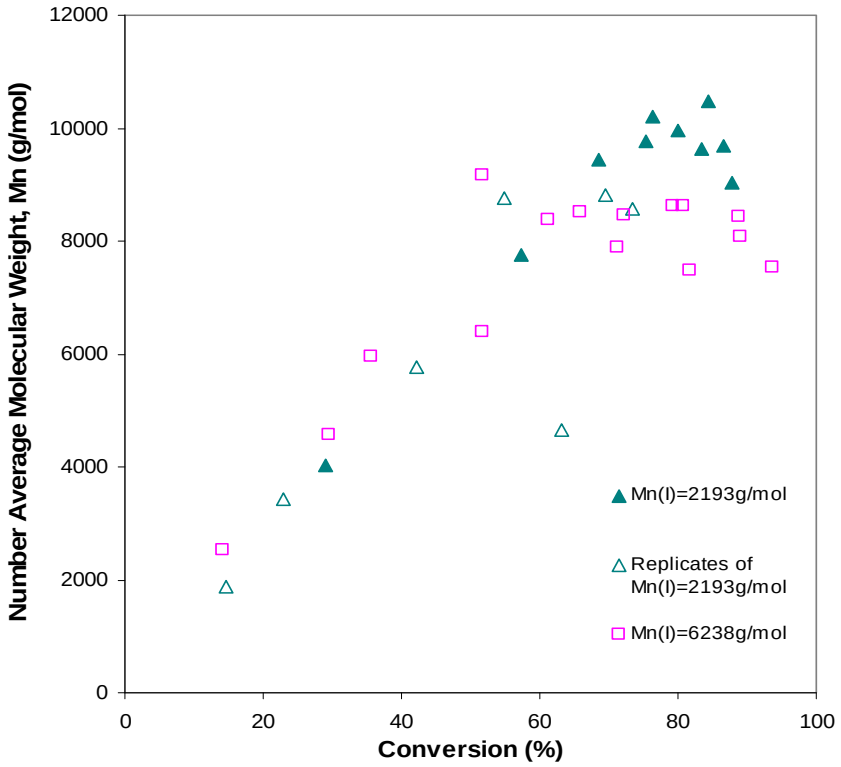

Figure B. 35 M_n vs. conversion plot, effect of initiator molecular weight, [I] = 0.0500 mol/l, T = 140°C.

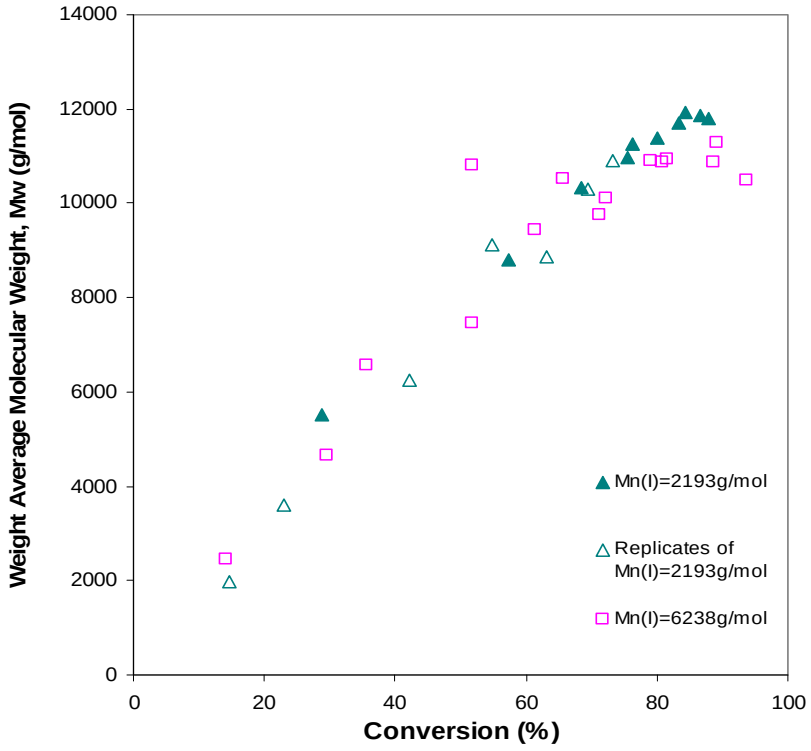

Figure B. 36 M_w vs. conversion plot, effect of initiator molecular weight, [I] = 0.0500 mol/l, T = 140°C.

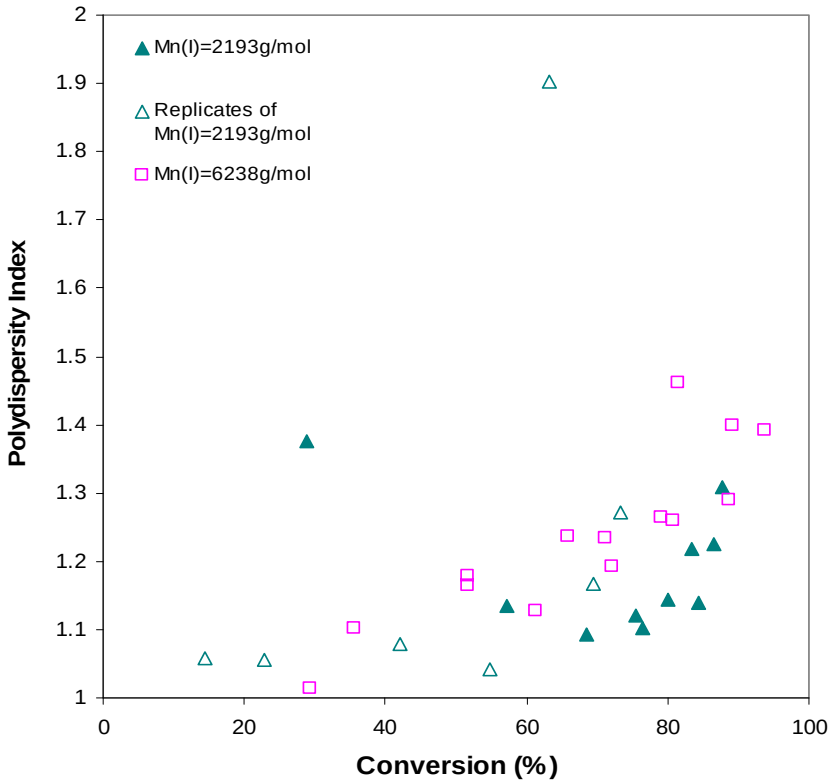

Figure B. 37 PDI vs. conversion plot, effect of initiator molecular weight, [I] = 0.0500 mol/l, T = 140°C.

Appendix C – Sample Calculation of Initiator Concentration

If the required volume of initial mixture is 1 L, the mass of initiator needed should be:

m_i = [Initiator] × V_{mix} × M_i = [Initiator] × (V_i + V_{sty}) × M_i

where m_i is the mass of initiator added to the initial mixture;

[Initiator] is the expected initiator concentration (i.e. 0.0500 mol·L^{-1});

M_i is the molar mass of initiator (~ 2200 g·mol^{-1});

V_{mix}, $V_{sty,}$ V_i are the volume of initial mixture, styrene and initiator, respectively.

Thus,

m_i = 0.0500 mol·L^{-1} × 1 L × 2200 g·mol^{-1} = 110 g

Then the relevant mass of styrene can be obtained from

$m_{sty} = V_{sty} \times \rho_{sty} = (1000\ mL - V_i) \times \rho_{sty} = (1000\ mL - m_i / \rho_i) \times \rho_{sty}$

where ρ_i is the density of polystyrene at 20°C, which is equal to 1.05 g·mL^{-1};

ρ_{sty} is the density of styrene at 20°C, which is equal to 0.906 g·mL^{-1};

Thus,

m_{sty} = (1000 mL – 110 g / 1.05 g·mL^{-1}) × 0.906 g·mL^{-1} = 811.0857 g

The mass ratio of styrene to initiator should be

R = m_i / m_{sty} = 811.0857 g / 110 g = 7.3735

Since the actual volume of initial mixture is based on the number of samples:

$V_{mix} = V_{sty} + V_i = N_{sample} \times 1.5$ ml/sample

where N_{sample} is the number of samples required

If we required 15 samples, then

$V_{mix} = 15 \times 1.5$ ml/sample = 22.5 ml

The mass of initiator should be

$m_i = [\text{Initiator}] \times V_{mix} \times M_i$

$= 0.0500 \text{ mol}\cdot\text{L}^{-1} \times 22.5 \text{ mL} \times 10^{-3} \text{ L}\cdot\text{mL}^{-1} \times 2200 \text{ g}\cdot\text{mol}^{-1}$

$= 2.475$ g

And the mass of monomer should be

$m_{sty} = mi \times R = 2.475 \text{ g} \times 7.3735 = 18.2494$ g